CHARACTERIZATION OF HUMAN TEAR PROTEOME IN DRY EYE SYNDROME

Dissertation

Zur Erlangung des Grades

Doktor der Naturwissenschaften

Am Fachbereich Biologie

Der Johannes Gutenberg-Universität Mainz

NATARAJAN PERUMAL

geb. am 08.03.1980 in India

Mainz, 2015

Tag der mündlichen Prüfung: 08. June. 2016

DECLARATION

I declare that this thesis is my original work except for quotations and citations which have been duly acknowledged. I also declare that it has not been previously, and is not concurrently, submitted for any other degree at Johannes Gutenberg-Universität Mainz or at any other institution.

_____

NATARAJAN PERUMAL

Date:

TABLE OF CONTENTS

LIST OF FIGURES

LIST OF TABLES

LIST OF ABBREVIATIONS

%	percentage
(v/v)	volume per volume
(w/v)	weight per volume
<	less than
>	more than
°C	degree Celsius
µg	microgram
µl	microliter
1DE	one-dimensional electrophoresis
2DE	two-dimensional electrophoresis
ACN	acetonitrile
AGC	automatic gain control
AIMS	accurate inclusion mass screening
Bis	N,N'-methylenebisacrylamide
CHAPS	3-[(3-cholamidopropyl)dimethyla-mino]-1-propanesulfonate
CHCA	α-cyano-4- hydroxy cinnamic acid
CID	collision-induced dissociation
CTRL	healthy subjects
Da	dalton (molecular mass)
DES	dry eye syndrome
DES_SS	dry eye patients with primary Sjogren syndrome
DEWS	dry eye workshop
DRY_CL	contact lens-related dry eye
DRY_RA	dry eye associated with rheumatoid arthritis
DRY_SJS	dry eye associated with Stevens–Johnson syndrome
DRYaq	aqueous-deficient DES
DRYaqlip	combination of the DRYaq and DRYlip
DRYlip	lipid-deficient DES
DTT	dithiothreitol
ESI	electrospray ionization
FDR	false discovery rate
g	gram
GOBP	gene ontology biological process
GOCC	gene ontology cellular components
GOMF	gene ontology molecular functions
iBAQ	intensity-based absolute quantification
IEF	isoelectric focusing
IPG	immobilised pH gradient
iTRAQ	isobaric tags for relative and absolute quantitation
kDa	kilodalton (molecular mass)
LC	liquid chromatography
LFQ	label-free quantitative
LIPCOF	lid-parallel conjunctival folds
LTQ	linear quadrupole ion trap
M	molar
m/z	mass to charge ratio
MALDI	matrix-assisted laser desorption/ionization
MDE	mildly symptomatic aqueous deficiency
MES	2-(N-morpholino)ethanesulfonic acid

mg	milligram
MIAPE	minimum information about a proteomics experiment
min	minute
ml	milliliter
Mr	relative molecular mass (dimensionless)
MS	mass spectrometry
MS/MS	tandem mass spectrometry
MSDE	symptomatic aqueous deficiency
MXDE	combination of the MDE and MSDE
NH_4HCO_3	ammonium bicarbonate
n.a	non-significant
OSDI	ocular surface disease index
PAGE	polyacrylamide gel electrophoresis
PBS	phosphate-buffered saline
pI	isoelectric point
ppm	parts per million
PTM	post-translational modification
RP	reversed phase
S/N	signal-to-noise ratio
SD	standard definition
SDS	sodium dodecyl sulfate
SELDI	surface-enhanced laser desorption ionization
SS	Sjogren syndrome
SCX	strong-cation-exchange
TBUT	tear film break-up time
TFA	trifluoroacetic acid
TFOS	Tear film and ocular surface
TOF	time of flight
Tris	tris(hydroxymethyl) aminomethane
V	Volt

1 INTRODUCTION

1.1 Dry eye syndrome (DES)

The Tear Film and Ocular Surface (TFOS) Dry Eye Workshop (DEWS) in 2007 defined DES as follows: “Dry eye is a multifactorial disease of the tears and ocular surface that results in symptoms of discomfort, visual disturbance and tear film instability with potential damage to the ocular surface. It is accompanied by increased osmolarity of the tear film and inflammation of the ocular surface” **[1]**. The study of DES has become a subject of much interest due to the high rate of occurrence in different ethnic groups, gender (preponderance in women), age (> 50 years old) and other ocular surface-affecting systemic diseases (especially Sjögren's syndrome, diabetes mellitus, pterygium and allergy) **[2-8].** In recent years, assessment studies in several Western and Asian countries reported a high global prevalence of this pathology, ranging from 2 % to over 50 % of the world population. **[9-19].** Apart from afflicting one out of every two elderly in some populations, this condition also poses a substantial economic burden on the health system **[18, 20, 21]**. Yu *et al* reported an annual financial burden of 55.4 billion dollars in 2008 for DES in the United States **[20]**.

1.2 DES subgroups

The DEWS report advanced the notion that there are numerous risk factors for the development of the DES disease, as summarized in **Figure 1.1 [1, 22, 23]**. Despite the extensive study of DES over the years, the underlying etiology of this pathology remains elusive. This disease is generally categorized into two major categories: aqueous-deficient DES (DRYaq) and lipid-deficient DES (DRYlip). The pathophysiology of both conditions is complex and thought to signify the interaction of multiple mechanisms underlying an individual patient’s development and progression of disease, namely, ageing, androgen deficiency, contact lens wear, refractive surgery or an autoimmune disease. However, the ultimate common clinical expression of DES is a dysfunctional tear film that is unstable and hyperosmolar in nature **[24-26].** These two defining characteristics of the disease contribute to activation of an inflammatory cascade, with release of inflammatory mediators into the tears, which in turn can damage the ocular surface epithelium **[27].** Studies had demonstrated that several pro-inflammatory cascades are activated by tear hyperosmolarity and there is an increase in apoptotic cell death in the ocular surface of DES patients **[28-30].** It is important to highlight that reflex stimulation of the lacrimal gland is a compensatory mechanism activated to lower tear osmolarity and can operate transiently and asymmetrically between

eyes. On the other hand, chronic reflex tearing can cause an overexpression of autoantigens in the lacrimal glands and neurogenic inflammation within the gland that ultimately compromise aqueous tear production **[31].** These factors cultivate a vicious cycle of mutually re-enforcing events, which increase inflammation, tear film hyperosmolarity and instability, besides aggravate the disease. Increased tear osmolarity is conjectured to be the central pathogenic mechanism leading to ocular surface damage in DES **[1]**.

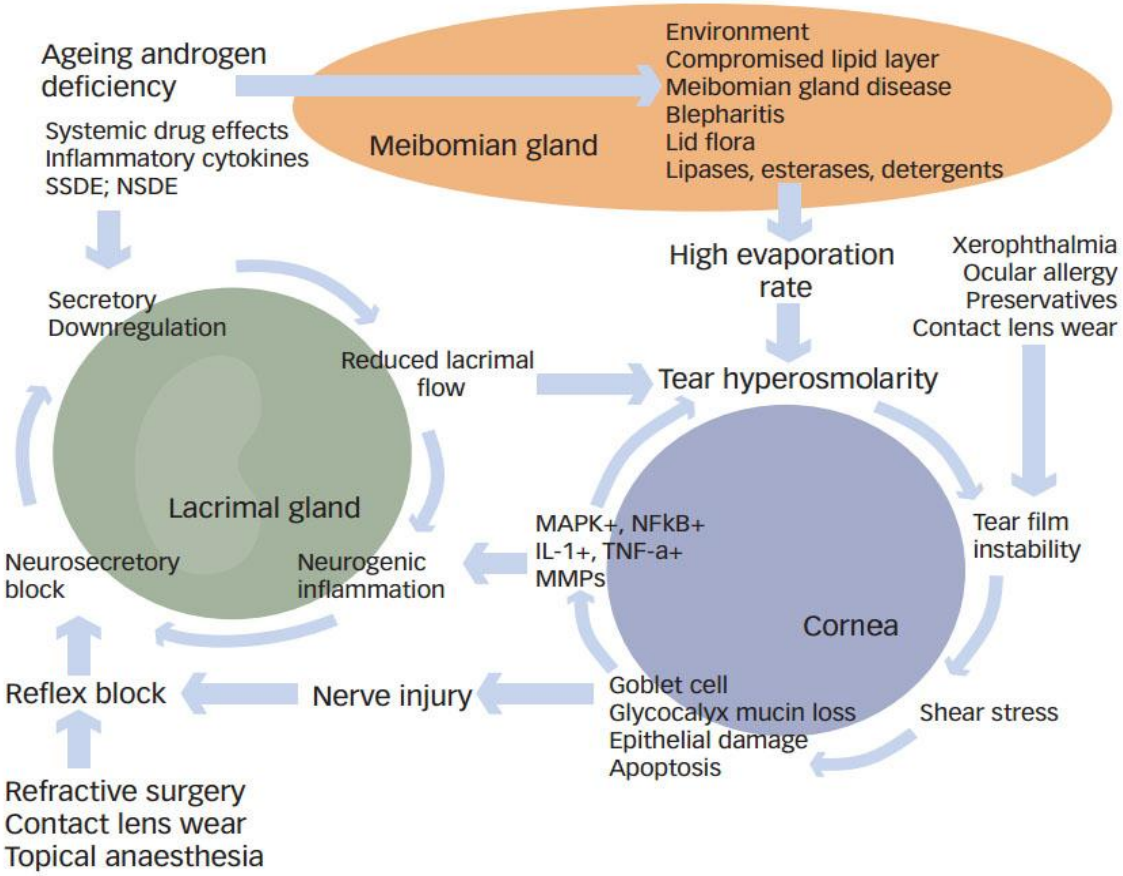

Figure 1.1: Risk factors for the development of the DES disease.

DES can result in dysfunction of one of the three main components of the ocular surface unit – the lacrimal gland, meibomian gland and cornea. Impairment of any one of these components perpetuates the dry eye condition *via* inflammatory, hyperosmolar and stress conditions that damage the other components of the ocular surface, driving disease progression **[23].**

1.3 DES diagnosis

The diagnostic approach of DES subgroups remains a challenging task clinically owing to the overlap of signs and symptoms. Moreover, there is currently no gold standard for the diagnosis and prognosis of the pathology. Hitherto, DES diagnosis is typically limited to symptom questionnaires and numeral/quantification clinical tests based on schirmer's test, tear film break-up time (TBUT) (evaluation of tear film quality), staining (Rose Bengal and fluorescein) of the corneal and conjunctival epithelium (identification of ocular surface damage) and osmometry (measurement of tear osmolarity) **[32].** However, considering a poor correlation between clinical tests and subjective symptoms, it is widely recognized that more objective diagnostic approaches that can monitor response to treatment are needed **[33, 34].** Several initial efforts utilized tear proteins for specific assays development as an objective test for the diagnosis of DES **[35-39].** For example, Boersma *et al* showed a good correlation between lysozyme C (LYZ) and lactotransferrin (LTF) concentrations in tears **[39]**. Decreased concentrations of LYZ or LTF in the tear fluid of DES patients were observed, with approximately 83 % diminished LTF levels in patients with severe dry eye. Goren and Goren demonstrated that LTF assay alone had about 70 % sensitivity (73 of 103 patients), while LTF assay plus Schirmer's test increased the sensitivity to about 85 % (87 of 103 patients) **[37]**. Unfortunately, there is paucity of proteomics studies in the literature for the development of effective diagnosis of DES. Further investigation of the protein content of human tear fluid has enormous potential for deepening our understanding of DES and development of novel noninvasive tear-based diagnostic technologies. The dynamics of tear proteins are indicative of the disease mechanisms and proteomic patterns in tear fluids may reflect functional changes of the main glands, especially the lacrimal and meibomian glands.

1.4 Tear film

The tear film is an extra-cellular fluid bathing the cells of the ocular surface and thus, closely related to its pathophysiological state. It is apparent from the definition that the tear film and ocular surface are altered in DES. Generally, the tear film is made up of three layers, composed of the mucin, aqueous and the lipid layer as shown in **Figure 1.2 [40-42]**. The lipids are derived principally from meibomian glands and comprise a complex mixture of different class of non-polar and polar lipids, as reported extensively in the review of Butovich **[43]**. The aqueous layer, secreted by lacrimal glands, contains electrolytes, proteins, peptides and small metabolites such as glucose and amino acids. The mucin layer primarily consisted

of O-linked carbohydrates with a protein core. To date, this complex molecular repertoire is not fully explored and deciphered. The maintenance of the tear film structure on the ocular surface is of great importance due to its diverse functions, especially in lubricatory, antimicrobial, host-defense and nutritional aspects in response to various environmental stimuli **[42, 44-46]**. Tear film comprises of water, electrolytes and large variety of proteins derived predominantly from the lacrimal and accessory gland secretions, which are under tight neural control. The disruption and/or compromise of any one layer of the tear film can result in the change of tear chemistry and as a result, DES develops.

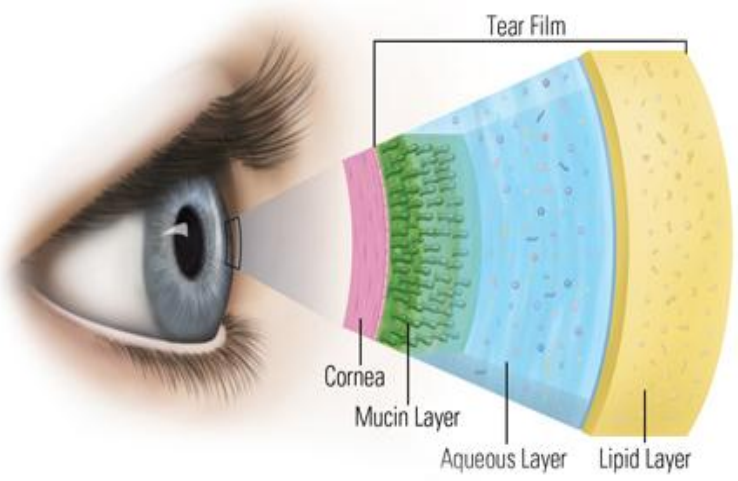

Figure 1.2: Three layers of tear film, which is composed of the mucus, aqueous and the lipid layer.
(Source: http://www.drbrendancronin.com.au/dry_eyes/)

1.5 Tear proteome analysis

In recent years, various proteomics approaches have been utilized to characterize the protein composition in the tear film and subsequently in the identification of protein markers for ocular diseases **[6, 47-56]**. In the meantime, the normal human tear proteome has significantly extended to ~1500 proteins, with more than 90 % of the total amount of tear proteins comprising of LYZ, LTF, lipocalin-1 (LCN1), secretory immunoglobulin A, lacritin and proline-rich proteins **[49, 50, 52, 57-61].** Many of them play important roles in the health of the tear film and ocular surface, namely, lacrimal gland secreted proteins, mucins, antimicrobial proteins/peptides, the S100 protein family, cystatins, 14-3-3 protein family and the matrix metalloproteinase family. In recent years, various proteomics techniques have been used to compare the tear protein profiles between DES and normal subjects, as tabulated

in **Table 1.1**. Identification of large number of tear proteins and molecular markers to diagnose ocular surface diseases have been intensively investigated employing multiple proteomic approaches. Differences in the identification of total proteins and protein biomarkers are extrapolated to the techniques used for analyzing the samples and to the tear sample collection methods employed. Additionally, other factors including the age of the person, severity of dryness of the ocular surface and contact lens use have been implicated in the pathogenesis of DES **[62-64].**

1.6 Mass spectrometry (MS) system

The MS system has emerged as an indispensable tool for protein analysis owing to its sensitivity, specificity, speed, versatility and accuracy of analysis. This tool can determine the amino acid sequences of peptides and characterize a wide variety of post-translational modifications (PTMs) **[65, 66]**. The MS system can also be employed to identify and quantify thousands of proteins from complex biological samples, which makes it an extremely powerful tool for systems biology studies **[66-70]**. On the other hand, there is also a dramatic increase observed in the use of MS system in the past decades for clinical diagnostics and research purposes **[69, 71]**. The MS system consists of three essential modules: an ion source, which transforms the molecules in a sample into ionized fragments; a mass analyzer that sorts the ions by their masses by applying magnetic and electric fields; and a detector, which measures the value of some indicator quantity and provides data for calculation of the abundances of each ion fragment present **[71]**. The ion source of the mass spectrometer ionizes the material under analysis (the analyte). The three primary methods for ionization of proteins/peptides include the electrospray ionization (ESI) (invented by J. Fenn), matrix-assisted laser desorption/ionization (MALDI) (developed by K. Tanaka and separately by M. Karas and F. Hillenkamp) and the surface-enhanced laser desorption ionization time of flight mass spectrometry (SELDI-TOF-MS) (developed by T. William Hutchens) **[72-77]**.

Table 1.1: Summary of the proteomics analysis of human tear proteome reporting the total number of tear proteins identified.

Tear collection method	Protein separation method	MS system	Protein search parameters	Total proteins	Quantification software	Disease/ Normal	Ref.
Schirmer strip	In-solution digestion & online reversed phase (RP)	LTQ-Orbitrap-XL	Significance threshold $P < 0.05$	435	Label-free quantitative (LFQ) with Peptide Prophet	DES_SS	**[78]**
Schirmer strip	Offline SCX & online RP	TripleTOF 5600	FDR ‹ 1 %	1543	None	Normal	**[57]**
Capillary tube	one-dimensional electrophoresis (1DE) & online RP	LTQ-Orbitrap Velos	FDR ‹ 1 %	185	iTRAQ with IsoQuant	Multiple sclerosis	**[79]**
Capillary tube	In-solution digestion & offline RP	MALDI-TOF/TOF 4800	unknown	78	iTRAQ with Protein Pilot	Vernal keratoconjunctivitis	**[80]**
Schirmer strip	1DE, RP-RP	MALDI-TOF/TOF	Mudpit Scoring $P < 0.05$	267	LFQ with in-house developed P2M (Proteomics Pipeline Mainz)	Contact lens & dry eye	**[50]**
Schirmer strip	In-solution digestion & online RP	LTQ-Orbitrap XL	Significance threshold $P < 0.05$	386	iTRAQ with inhouse program,	Dry eye	**[81]**
Schirmer strip	Online strong-cation-exchange (SCX)-RP	Q-TOF (Q-Star XL)	Significance threshold $P < 0.01$	93	iTRAQ with ProQUANT 1.0	Dry eye	**[52]**
Schirmer strip & capillary tube	1DE, two-dimensional electrophoresis (2DE) & Online SCX-RP	LTQ	Mowse scores › 80	97 40	None	Normal	**[58]**
Capillary tube	1DE & online RP	LTQ-Orbitrap, LTQ-FT	Mascot score › 27	491	None	Closed-eye	**[59]**
Schirmer strip	1DE & online RP	LTQ-Orbitrap XL	FDR ‹ 1 %	200	LFQ with MaxQuant	Dry eye	This study
Capillary tube	1DE & online RP	LTQ-Orbitrap XL	FDR ‹ 1 %	54	LFQ with MaxQuant	Basal and reflex	This study

The generated ions are then transported by magnetic or electric fields to the mass analyzer and are separated according to their mass-to-charge (*m/z*) ratio. There are many types of mass analyzers, namely, time-of-flight (TOF), linear quadrupole ion trap (LTQ) and Orbitrap **[71, 82-86]**. Each analyzer type has its strengths and limitations and many MS systems use two or more mass analyzers for tandem mass spectrometry (MS/MS) **[71]**. The Orbitrap analyzer, where ions are electrostatically trapped in an orbit around a central electrode and oscillate back and forth along the central electrode's long axis, possesses a high mass accuracy, high sensitivity and a good dynamic range compared to the other analyzers **[86]**. Thermo Fisher's LTQ-Orbitrap-XL™ is an example of the state-of-the-art MS system that provides economical access to the power of hybrid ion trap-Orbitrap analysis with outstanding mass accuracy, resolving power, high sensitivity and tandem MS capability for proteomics analysis (**Figure 1.3)**. In keeping with the mass range and performance of available MS systems, two approaches are used for characterizing proteins **[87, 88]**. In the first approach referred to as "top-down" strategy of protein analysis, intact proteins are ionized by either of the two techniques described above, and then introduced to a mass analyzer **[88]**. In the second approach known as the "bottom-up" protein analysis approach, proteins are enzymatically digested into smaller peptides using proteases such as trypsin or pepsin, either in-solution or in-gel after electrophoretic separation **[87]**. The collection of peptide products are then introduced to the mass analyzer. An important enhancement to the mass resolving and mass determining capabilities of MS system is using it in tandem with chromatographic separation techniques **[89-91]**. Liquid chromatography system separates compounds chromatographically prior to their introduction to the ion source and MS system. Generally, online coupling of a liquid chromatography (LC)-system with fast MS spectra acquisition and high mass accuracy ESI instruments in conjunction with fractionation on both protein and peptide level allows the analysis of very complex samples in a relatively short period of time **[92, 93]**.

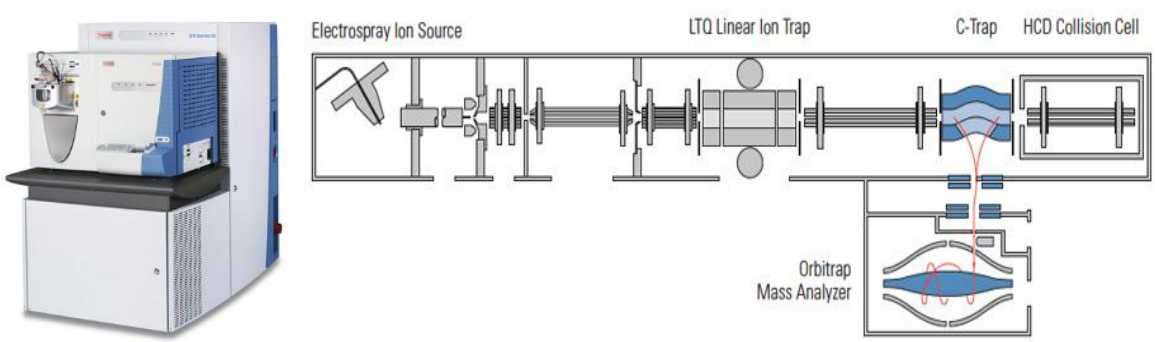

Figure 1.3: Schematic representation of the Thermo Fisher's LTQ-Orbitrap-XL™ system.
Combining patented Orbitrap™ technology with the most successful linear ion trap, the LTQ-Orbitrap-XL™ mass spectrometer provides fast, sensitive and reliable detection for identifications of compounds in complex mixtures.
(Source http://planetorbitrap.com/ltq-orbitrap-xl#tab:schematic

1.7 Protein quantification

Quantification of protein expression is a key aspect of proteomic experimentations. Several techniques, such as label-free, differential in-gel electrophoresis (DIGE), stable isotope labeling with amino acids in cell culture (SILAC), isotope-codes affinity tag (iCAT), isobaric tags for relative and absolute quantitation (iTRAQ) and absolute protein quantitation (AQUA) have emerged over the years for protein quantitation **[67, 94-98]**. Hitherto, protein quantification with isotopic labels has been largely utilized for tear proteins studies due to their quantitative accuracy, coverage and robustness. However, despite their success, they inherently require extra preparation steps of mixing differently labeled samples that consequently increase the complexity and often prohibit their use for biological questions that require the detection of vital proteome changes, mostly the low abundant tear proteins. On the contrary, the label-free quantification is the simplest, most economical and in addition, there is no limit on the number of samples that can be compared in contrast to the label-based methods **[68]**. In recent years, the development and improvement of the algorithms and tools in software namely, MaxQuant, Progenesis and OpenMS software suites provides an effective solution for label-free quantification, one that achieves state-of-the-art quantification accuracy and coverage **[69, 99-101].** Particularly, the MaxLFQ (a generic

method for label-free quantification) as part of the MaxQuant software suite has been demonstrated to accurately and robustly quantify small and high fold changes on a proteome scale and at present been successfully employed in diverse biological studies and has delivered excellent performance in benchmark comparisons with other software solutions **[70, 99, 102, 103]**.

1.8 Tear collection methods

There are no standard methods for tear collections and the two most commonly employed techniques are the Schirmer's strip and the glass capillary tube in respect to other absorbent-based methods **[49, 58, 104, 105]**. Schirmer's strip is advantageous in terms of patient compliance and is used routinely in ophthalmology, especially in the diagnosis of DES. A recent study demonstrated that higher protein concentration can be obtained with Schirmer's strip in comparison to capillary tear collection method **[58]**. However, this study had also demonstrated that the tear film collection method impacts the proteins present in the tear film and that care should be exercised in choosing a suitable tear collection method to best correlate to the experiment being conducted or the hypothesis that is being tested **[58]**. Hitherto, Schirmer's tear collection method has been proved to be a reliable method of tear collection in DES patients, with the ability to identify the differential protein expressions **[8, 50, 52, 57, 58, 78, 81]**.

1.9 DES Biomarkers

To date, many studies have showed the differentially expressed tear protein concentrations in DES. A complete list of protein biomarkers identified in DES subgroups compared to healthy subjects from the current study and the literature is tabulated in **Table 4.3**. Grus *et al* has employed SELDI-TOF to profile tear proteins from patients with DES and they found a significant increase in S100-A8 protein (S100A8) and decrement of LYZ, proline-rich protein 3, proline-rich protein 4 (PRR4) and α-1-antitrypsin **[47]**. The similar SELDI-TOF-MS system was employed by Boehm *et al* to differentially distinguish the tear proteome of patients with DRYaq, DRYlip and a combination of the two (DRYaqlip) compared to healthy controls (CTRL) **[106]**. They demonstrated that PRR4 expression level was diminished significantly in DRYaq and DRYaqlip groups compared to the CTRL. Mammaglobin-B (SCGB2A1) and lipophilin A as well as protein S100A8 were found to be increased in these patients. Remarkably, DRYlip patients revealed only slight alterations; the tear proteome of

these patients strongly deviated from the DRYaq or DRYaqlip groups. Meanwhile, Soria *et al* investigated the tear proteome of DRYaq and DRYlip patients compared to CTRL utilizing 2DE gels and the differentially expressed protein spots were identified employing MALDI-TOF/TOF **[107]**. Their results showed that the markers S100A6, protein S100-A9 (S100A9), S100A8, S100A4, glutathione S-transferase P (GSTP1) and annexin A1 (ANXA1) were found to be increased in abundance in both DRYaq and DRYlip groups, and together they discriminated best this group from the control group. In contrast, another group of proteins presented significant decrement in abundance in both DRYaq and DRYlip groups that include LCN-1, prolactin-inducible protein (PIP), LTF, zinc-alpha-2-glycoprotein (AZGP1), galectin-7 (LEG7), cystatin-S (CST4), Cystatin-SN (CST1), actin cytoplasmic 1 (ACTB) and SCGB2A1. Comparison of protein expression changes in DRYaq and DRYlip revealed decreased abundance of the same proteins. However, the extent of decrement associated with each pathology is clearly distinct. For example, LCN1, PIP, LTF and SCGB2A1 were found to be most strongly diminished in the DRYaq subgroup whereas AZGP1, LEG7, CST4, CST1 and ACTB were most evidently decreased in the DRYlip subgroup. Zhou *et al* used iTRAQ quantitative proteomics combined with nanoLC-MS/MS to identify potential tear biomarkers for dry eye and they found an increase of ENO1, alpha-2-HS-glycoprotein (AHSG), S100A8, S100A9, S100A4 and S100A11 and a decrease of PIP, LCN-1, LTF and LYZ **[52]**. Similarly, utilizing the iTRAQ tools, Srinivasan *et al* investigated the differentially expressed tear proteins in patients with mildly symptomatic aqueous deficiency (MDE), symptomatic aqueous deficiency (MSDE) and a combination group (MXDE) compared to healthy subjects (CTRL) **[81]**. In addition to the decreased abundance of commonly reported proteins, such as LCN1, LYZ and PIP across all DES sub-groups, their finding demonstrated a number of proteins that were significantly differentially expressed in subgroups of DES as follows: MDE *vs.* CTRL showed increment of 3 proteins and decrement of 15 proteins, MSDE *vs.* CTRL showed increment of 5 proteins and decrement of 18 proteins, MXDE *vs.* CTRL showed increment of 1 protein and decrement of 10 proteins.

Other DES studies have investigated Sjogren syndrome (SS) dry eye, which is a systemic autoimmune disease characterized by compromised lacrimal and salivary gland functions that causes severe dry eye and dry mouth. Aluru *et al* investigated the tear proteome of dry eye patients with primary SS (DES_pSS) compared to CTRL utilizing the 2DE and differential gel electrophoresis (DIGE) approaches, and the differentially expressed protein spots were

identified employing ESI-QTOF MS **[7]**. They found PPR4, extracellular glycoprotein lacritin (LACRT) and immunoglobulin J chain (IgJ) to be decreased in abundance in more than 95 % of the DES_pSS cases. In another study by Li *et al* label-free quantitative proteomics combined with LC-MS/MS methods were used to identify potential tear biomarkers for dry eye with Sjogren syndrome (DES_SS) and they found an increase in S100A8, S100A9, CDNA FLJ78387, annexin A2 isoform 1 (ANXA2), serotransferrin (TF), keratin 4, mucin-5AC precursor (fragment), ANXA1, keratin-type I cytoskeletal 10 (KRT10), complement C3 precursor (fragment) (C3) and ACTB, and decreased of growth-inhibiting protein 12, LCN-1, PIP, Ig alpha-1 chain C region (IGHA1), polymeric immunoglobulin receptor (PIGR), LACRT, LYZ, PRR4, CST4 and keratin-type II cytoskeletal 5 **[78]**.

One of the major risk factors for DES development has been associated with contact lens use **[48, 50].** A study by Funke *et al* revealed distinct similarities between contact lens users and DES patients using the proteomics approaches **[50]**. Moreover, Nichols *et al* highlighted the differential protein expressions in contact lens wearers with DES with respect to normal contact lens wearers **[48]**. Generally, these studies revealed that the up-regulation of inflammatory-related proteins (e.g. S100A8, S100A9) could play crucial protective functions in DES patients due to the reduced levels of major lacrimal proteins (e.g. LYZ, LTF and LCN-1) in tears. Furthermore, a recent study on the different subtypes of DES reported that specific alterations of the tear proteome reflect the different clinical phenotypes of DES **[106]**. This study found that aqueous-deficient dry eye seems to strongly influence the expression patterns of several proteins when compared to healthy subjects. However, only limited biomarker panels were identified in the aforementioned study due to the limitations in the methodology employed. Therefore, further in-depth investigation is necessary to unravel the pivotal intricate regulation profiles of tear proteins in the different DES subgroups. Potential usage of multiple tear proteins considering multiple disease characteristics (i.e. secretion deficiency, ocular surface inflammation and tear hyperosmolarity) will result in significant improvement over existing diagnostic accuracy for DES.

1.10 Reflex tears

Tear secretion can be categorized as basal and reflex. The reflex tears is produced in response to irritant chemical compounds, tactile or light stimulation and induces an upsurge in the tear volume. According to the DEWS (2007), reflex stimulation of the lacrimal gland is a compensatory mechanism designed to lower tear osmolarity and can be operative transiently and asymmetrically between eyes. Therefore, besides investigating the DES tear samples, further characterization of reflex tears is vital to unravel the key proteins, which are conjectured to possess essential functions in the protection of the ocular surface. However, only few studies demonstrated the differences in the composition of proteome in reflex tearing **[108-112]**. Therefore, we believe that there is still a missing link concerning important intricate proteome regulation profile of tears.

1.11 Proline-rich protein 4 (PRR4)

Proline-rich protein 4 (PRR4), synthesized in the acinar cells of human lacrimal gland, was discovered in 1995 by Dickson and Thiesse **[113]**. Transcriptome studies have demonstrated that this protein is highly expressed at the mRNA level and is important as a potential biomarker to determine the functional efficiency of the gland **[113, 114]**. However, the complete characteristic profiles of PRR4 at the protein level are still lacking, which hinders the complete understanding of the protein regulation in different ophthalmopathologies. Furthermore, the precise biological functions of PRR4 in tears are yet to be defined, which may have vital roles in the stability of the tear film and the protection of the ocular surface. Based on the salivary proline-rich proteins studies, it is believed that PRR4 may play crucial roles as an antimicrobial protein and lubricant in the protection of the ocular surface **[115-119]**. In retrospect, studies have demonstrated the correlation between DES and the decrement of truncated PRR4 in tear fluid of patients **[47, 56]**. Concordantly, studies by Saijyothi *et al* and Aluru *et al* demonstrated that significant decrement of PRR4 is found in all types of DES cases in their investigations, rendering this protein a potential biomarker for the pathology **[7, 8]**. These findings collectively attribute the decrement of PRR4 to the functional involvement of the lacrimal gland. Down regulation of PRR4 in tear fluid was also observed in contact lens users associated with DES **[48]**. Similarly, PRR4 level in tear fluid was also found to be significantly decreased in patients with thyroid-associated orbitopathy and diabetic proliferative retinopathy **[120, 121]**. However, PRR4 level in tear fluid of patients with keratoconus was found to remain unchanged compared to the healthy controls

[122]. Apart from being an abundant product of the lacrimal and salivary glands, the gene encoding for PRR4 was also identified to be highly expressed in the human submucosal glands **[113, 123, 124]**. Correspondingly, down-regulation of PRR4 in the sputum of smokers, as well as low expression of PRR4 gene from esophageal tumor tissue had been reported **[125, 126]**. In view of this, the potential of PRR4 as a biomarker for various clinical pathology is enormous. To date, utilization of both conventional and state-of-the-art proteomics platforms to study PRR4 and its probable functions, as well as its correlation to ocular surface pathology was not satisfactory due to limited information on the fundamental characteristics of this protein. The PTMs are especially important for investigation since they represent crucial trigger points in protein function and pathology. Hitherto, only two PRR4 isoforms with very limited information on their PTMs were reported in tear fluid **[49, 60, 61, 127]**. This is largely due to the incomplete visualization of PRR4 isoforms using gel electrophoresis and limited number of signature peptides identified in MS-based analysis.

2 OBJECTIVES

The discovery of tear biomarkers for ocular surface pathologies has provided an excellent paradigm for the scientific and clinical community to develop novel standardized methods for efficacious and early classification and diagnosis of the diseases, as well as for the identification of new molecular targets for therapy and treatments **[1, 35-39]**. It is noteworthy that tear fluid has been a subject of much interest for the discovery of new biomarkers. From a clinical perspective, the lack of compliance between clinical parameters and symptoms reported by DES patients has made it difficult to clearly discriminate between the subgroups of DES. This phenomenon has led to a need for alternative methods to improve existing clinical diagnosis to ensure a precise pathological classification of patients, mainly for categorization of confounding cases presenting insufficient signs and symptoms **[33]**. It is of utmost importance to distinguish the two major DES categories, which comprises the DRYaq subgroup (decrease in lacrimal gland secretion that produces aqueous tear fluid) and the DRYlip subgroup (evaporative dry eye commonly caused by meibomian gland dysfunction). It is equally imperative to differentiate the DES subgroups from other forms of symptomatic ocular surface diseases. Currently, there is no standardized diagnostic system based on clinically applicable biomarkers for an efficacious classification. Hence, in this study the proteomic profiles of the tear fluids of the two main DES subgroups patients, as well as the combination DES subgroup (DRYaqlip), were investigated. Furthermore, there are lack of in-depth investigations on the tear proteome profiles of reflex tears and PRR4 characteristics. Therefore, the main objectives of this study are as follows:

1: To identify and verify potential tear protein biomarker panels to distinguish the different DES subgroups.

2: To further evaluate the effect of reflex factor on the tear proteome of healthy subjects.

3: To identify and characterize the isoforms and PTMs of PRR4 in the basal tear fluid of healthy subjects.

In the present study, the intricate proteome regulation profiles of DES subgroups and reflex tears, as well as characterization of PRR4 were analyzed employing the bottom-up label-free MS-based proteomics approach utilizing the state-of-the art LC-MS/MS and bioinformatics tool. The ultimate outcome of this study would elucidate the intricate regulation profiles of potential biomarker panels responsible for the maintenance of tear film stability which, will

be translated into prospective diagnostic and prognostic use to ensure an appropriate control of DES in the clinical setting.

3 MATERIALS AND METHODS

3.1 Identification and verification of potential tear protein biomarker panels to distinguish DES subgroups

3.1.1 Tear sampling

3.1.1.1 Study samples

In this study, tear proteins of 80 patients were included and assigned into four groups: DES patients with a deficiency of tear fluid (DRYaq); DES patients with a lipid film dysfunction (DRYlip), patients showing characteristics of both groups DRYaq and DRYlip (DRYaqlip) and a group of control patients (CTRL). Each group comprises 20 subjects equally divided to male (M) and female (F), age between 21 to 79 years old. The classification of patients was carried out according to the guidelines of the Tear Film and Ocular Surface Society (TFOS, Ocular Surface, 2007) at the Department of Ophthalmology at the University Medical Center of the Johannes Gutenberg University, Mainz, following specific inclusion and exclusion criteria of basic secretory test (BST), TBUT, clinical parameters after Bron and Foulks Score and Lid-parallel Conjunctival Folds (LIPCOF) and extensively asking for the anamnesis and symptoms using Ocular Surface Disease Index (OSDI) questionnaire. Commentations of criteria selected for patient sub classification were as follows:

Group DRYaq: Patients with a BST ≤ 10 mm/ 5 min and no pathologic TBUT of > 10 s were classified as aqueous deficient patients, due to the fact that a reduced production/secretion of tear fluid will predominantly result in a lower BST value **[22, 128]**. With the purpose to get a representative insight into the tear proteome of patients suffering from different stages of aqueous deficient dry-eye, we chose a BST threshold of ≤ 10 mm/ 5 min, in accordance with previous studies of our group and others **[129-131].**

Group DRYlip: Patients with a TBUT ≤ 10 s and a BST value of > 10 mm/ 5 min were classified as lipid deficient dry eye. A dysfunctional, thinned lipid layer goes along with a pathological/ decreased TBUT **[132]**, which is due to the lower tear film stability **[133].** However, the TBUT is not necessarily correlated with a decreased BST value **[134]**. Thus, in the present study patients with a BST value > 10 mm/ 5 min and a TBUT ≤ 10 s were specifically classified as lipid deficient dry-eye (DRYlip) subjects, as they reveal a normal aqueous state but a pathological tear film stability. Further, the occurrence of a lipid layer deficiency was assured by inspecting meibomian glands **[135]**. Patients with a score ≥ 18

were classified as pathologic, respectively lipid deficient. Foulks and Bron suggested a threshold of > 10 **[135]**. Due to the higher specificity, we set a threshold of ≥ 18.

Group DRYaqlip: Patients with a BST value ≤10 mm/ 5 min and a TBUT ≤10 were classified as patients who suffer from a combined pathogenesis, means they are aqueous deficient as well as lipid deficient. It is generally accepted that symptoms of advanced stages of aqueous deficiency and lipid deficiency are overlapping and influencing each other. As suggested by Versura *et al*, a thin lipid layer results in an unstable tear film and an aqueous tear-deficient state **[131]**. Thus, we classified patients with a pathologic BST, TBUT and optionally a score ≥18 as aqueous and lipid deficient.

Excluded patients from this study were as follows: Patients suffering from Sjögren's syndrome, diabetes mellitus, allergy to local anesthetics and contact lens wearers. Patients who had undergone ophthalmic surgery during the last 6 months. Further, the use of any systemic drug suspected to have an influence on the tear production or systemic inflammatory processes led to exclusion of subjects (e.g., beta-blockers, selective serotonin reuptake inhibitors, oral contraceptives, postmenopausal estrogen therapy, local sympathomimetic drugs, nonsteroidal antirheumatic drugs [NSAR analgesics, such as ibuprofen, diclofenac, Voltaren, aspirin, Novalgin, Arcoxia], steroidal antirheumatic drugs, antihistamines).

Principally these four groups were classified by the following characteristics:

1. CTRL: BST > 10mm/ 5min, TBUT > 10s, Bron and Foulks Score < 18
2. DRYaq: BST < 10mm/ 5min, TBUT > 10s, Bron and Foulks Score < 18
3. DRYlip: BST > 10mm/ 5min, TBUT < 10s, Bron and Foulks Score > 18
4. DRYaqlip: BST < 10mm/ 5min, TBUT < 10s, Bron and Foulks Score > 18

From each individual, tear samples have been taken by a BST, a clinical standard test, using Schirmer’s strip. Schirmer’s strips have been placed into the lower eye lid for a few minutes, after having prepared the eye with mild anesthetic eye drops (Novesine). The samples were immediately stored at -80 ºC for subsequent analysis. The study was performed in strict adherence to the guidelines of the 1964 Declaration of Helsinki. Ethical clearance was obtained from the institutional ethics committee, “Landesärztekammer Rheinland-Pfalz“. All participants were informed of the possible risks, the goal of the study and privacy policy, and

an informed consent was signed according to the recommendations of the Declaration of Helsinki for investigation with human subjects.

3.1.1.2 Sample preparation

Tear proteins were extracted from the Schirmer's strips by soaking each strip in 500 µl phosphate-buffered saline (PBS) for 3 hours at 4 °C to elute the tear proteins. Subsequently, the total protein concentrations in the collected tear samples were determined using BCA Protein Assay Kit (Pierce, Rockford, IL) prior to further analysis.

3.1.2 Discovery study: LFQ analysis *via* 1DE & LC-ESI-MS/MS strategy

Label-free quantification of peptides *via* 1DE & LC-ESI-MS/MS strategy was employed to identify the change in protein abundance in the discovery data and to generate a list of candidate biomarker proteins of specific dry eye subgroups for subsequent verification. The complete proteomics experiments in this study, including both experimental protocols and data processing methods was conducted and presented according to the Minimum information about a proteomics experiment (MIAPE) guidelines **[136, 137]**. The MIAPE is a minimum information standard created by the Human Proteome Organization- Proteomics Standards Initiative (HUPO-PSI) for reporting proteomics experiments, allowing a critical evaluation of the whole process and the potential recreation of the work.

3.1.2.1 1DE

The tear samples for each assigned group (N=20) were pooled equally (2.5 µg per individual) to a total of 50 µg with three replicates. The reason for equal amount of protein collection and pooling from each patient within a group was to normalize the difference between subjects and to reduce individual variation. The tear samples were subjected to 1DE (50 µg/ well and sliced into 10 bands) using 4-12 % Bis-Tris Gels (Invitrogen, Karlsruhe, Germany) with MES running buffer under reducing conditions for approximately 60 minutes with a constant voltage of 150 V. SeeBlue™ Plus 2 (Invitrogen) was used as a protein molecular mass marker. The gels were stained with Colloidal Blue Staining Kit (Invitrogen) according to the manufacturer's instructions. The sliced gel pieces were subjected to trypsin digestion utilizing a method previously described **[138, 139]**. Briefly, the gel pieces were dehydrated with neat acetonitrile prior to disulfide bonds reduction with 10 mM DTT in 100 mM ammonium bicarbonate (NH_4HCO_3) and alkylation with 55 mM iodoacetamide in 100 mM NH_4HCO_3.

The reduced and alkylated protein mixtures were digested with sequence grade-modified trypsin (Promega, Madison, USA) for 16 hours at 37 °C with 10 mM NH_4HCO_3 in 10 % acetonitrile. Proteolysis was quenched by acidification of the reaction mixtures in each tube with 100 µl of extraction buffer [1:2 (v/v) of 5 % formic acid:acetonitrile] and incubated for 15 min at 37 °C in a shaker. The supernatant containing the peptides was collected and the remaining peptides in the gel pieces were extracted with two 20 minutes washes in extraction buffer. The supernatants were pooled and dried in a SpeedVac concentrator (Eppendorf, Darmstadt, Germany) prior to storage at -20 °C. The extracted peptides were purified on ZipTip® C18 columns (Millipore, Billerica, MA, USA) according to the manufacturer's instructions. This procedure was repeated four times for each sample and the combined eluate was concentrated to dryness in the SpeedVac concentrator and dissolved with 10 µl of 0.1 % TFA solution prior to LC-ESI-MS/MS analysis.

3.1.2.2 LC-ESI-MS/MS

The LC-ESI-MS/MS system utilized for this study has been extensively optimized **[50, 139]**. Basically, the peptide fractionation was conducted on the LC system that consisted of a Rheos Allegro pump (Thermo Scientific, Rockford, USA) and an HTS PAL autosampler (CTC Analytics AG, Zwingen, Switzerland) equipped with a BioBasic C18, 30 x 0.5 mm precolumn (Thermo Scientific, Rockford, USA) connected to a BioBasic Phenyl, 100 x 0.5 mm analytical column combined with a Jupiter 4 µ Proteo analytical, 150 x 0.5 mm column (Phenomenex, Torrence, USA). Solvent A was LC-MS grade water with 0.1 % (v/v) formic acid and solvent B was LC-MS grade acetonitrile with 0.1 % (v/v) formic acid. The gradient was run for 60 min per sample as follows; 0-5 min: 10 % B, 5-45 min: 10-45 % B, 45-50 min: 45-90 % B, 50-55 min: 90 % B, 55-60 min: 10 % B.

Continuum mass spectra data were acquired on an ESI-LTQ-Orbitrap-XL-MS system (Thermo Scientific, Bremen, Germany) and the general mass spectrometric conditions were: positive-ion electrospray ionization mode, spray voltage was set to 2.15 kV, the heated capillary temperature was set at 220 °C. The LTQ-Orbitrap was operated in the data-dependent mode of acquisition to automatically switch between Orbitrap-MS and LTQ-MS/MS acquisition. Survey full scan MS spectra (from *m/z* 300 to 1600) were acquired in the Orbitrap with a resolution of 30000 at *m/z* 400 and a target automatic gain control (AGC) setting of 5×10^5 ions. The lock mass option was enabled in MS mode and the polydimethylcyclosiloxane (PCM) *m/z* 445.120025 ions were used for internal recalibration

in real time **[140]**. The five most intense precursor ions were sequentially isolated for fragmentation in the LTQ with a CID fragmentation, the normalized collision energy (NCE) was set to 35% with activation time of 30 ms and dynamic exclusion of 60 s. The resulting fragment ions were recorded in the LTQ.

3.1.2.3 LFQ analysis

The acquired MS spectra were analyzed by MaxQuant computational proteomics platform version 1.4.1.2 and its built-in Andromeda search engine for peptide and protein identification, with LFQ and intensity-based absolute quantification (iBAQ) algorithm enabled **[70, 102, 103, 141]**. Tandem MS spectra were searched against Uniprot Human database (date, 15/05/2014) using default settings with peptide mass tolerance of ± 30 ppm, fragment mass tolerance of ± 0.5 Da, carbamidomethylation of cysteine was set as a fixed modification, while protein oxidation of methionine and acetyl (Protein N-term) were defined as variable modifications, enzyme: trypsin and maximum number of missed cleavages: 2. The false discovery rate (FDR) for peptide and protein identification was set to 0.01 with ≥ 6 amino acid residues and only "unique plus razor peptides" that belong to a protein were chosen to be included for quantification **[70]**. The output of the generated "proteingroups.txt" table was filtered for contaminants, reverse hits and minimum number of values "in at least one group" is 3 prior to Pearson correlation, statistical and clustering analysis using Perseus software. Unsupervised hierarchical clustering of the LFQ values was performed based on Euclidean distances on the Z-scored between mean values. For statistical analysis, two-samples t-test-based statistics with $P < 0.01$ was applied on Log2 transformed LFQ values to assert proteins regulation as significant for the specific groups **[102]**. The iBAQ values, which were calculated by dividing the summed peptide intensities for a given protein with the number of theoretically observable tryptic peptides, act as a degree of protein abundance were converted to percentage and employed to compare between proteins in each group **[142-144].** Proteins were classified as major protein if iBAQ values are larger than 0.5 % and minor if the iBAQ values are lower than 0.5 %.

3.1.3 Verification study: Targeted MS *via* AIMS strategy

The identified candidate biomarkers from the discovery stage were verified employing a targeted form of MS strategy called accurate inclusion mass screening (AIMS) **[145, 146]**. The main aim of employing the AIMS strategy for verification in the present study is to determine which are best able biomarker candidates to discriminate the specific DES

subgroups **[147]**. The identification of specific combinations of biomarker panels, which can be quantified robustly with sufficient assay sensitivity, specificity and precision are imperative before committing resources to quantitative assay configuration in the future. The experimentally observable peptides that each uniquely represents the protein biomarker candidates identified in DES groups were targeted compared to control tears in the discovery study. Selection of these peptides for the inclusion list was carried out manually based on the "msms.txt" file resulting from MaxQuant analysis governed by these criterions, fully tryptic, contains no missed cleavages, no modifications, peptide can only assume charge +2 and multiple charges were rejected. The peptides inclusion mass lists containing *m/z* and charge were generated and assigned to the instrument acquisition software before data acquisition.

The tear samples for each assigned group (N=20) were pooled equally (0.5 µg per individual) to a total of 10 µg with quadruplicate and subjected to in-solution digestion. The pooled tear samples were digested with sequence grade-modified trypsin [protease: protein ratio of 1:20 (w/w)] for 16 hours at 37 °C with 50 µl of 50 mM NH_4HCO_3 in 10 % acetonitrile. The digested samples were purified on ZipTip® C18 columns and the eluates were concentrated to dryness in the SpeedVac concentrator and dissolved with 10 µl of 0.1 % TFA solution prior to targeted MS analysis **[139]**.

For targeted MS analysis, the LC-ESI-MS/MS system was operated as described in **section 3.1.2.2** with several parameters adjusted to target only a specific set of peptides. The in-solution digested tear samples consisted of very complex mixtures especially the high abundant proteins. Hence, to yield optimum results, two LC gradients of 60 min (as described in **section 3.1.2.2**) and 120 min were utilized. The gradient for 120 min per sample is as follows: 0-5 min: 10 % B, 5-95 min: 10-50 % B, 95-105 min: 50-90 % B, 105-110 min: 90 % B, 110-115 min: 90-10 % B, 115-120 min: 10 % B. The adjusted parameters for inclusion list-dependent acquisition were as follows: the use of global parent list was enabled, the dynamic exclusion segment was disabled and the *m/z* tolerance around targeted precursors was ± 10 ppm. The acquired MS spectra were analyzed by MaxQuant for peptide and protein identification. Extracted spectra were searched against Uniprot Human database (date, 15/05/2014) using settings with peptide mass tolerance of ± 10 ppm, fragment mass tolerance of ± 0.5, peptide charge state of +2 and FDR for peptide and protein identification was set to 0.01. The output of the generated 'peptides.txt' from MaxQuant were exported in an excel workbook format (Microsoft Office Excel 2010) and the sum absolute intensity of the

signature peptides for each proteins were calculated and were transferred to Statistica (v8, StatSoft, Tulsa, OK) for t-test analysis (independent, by groups, $P< 0.05$).

3.2 Characterization of human reflex tear proteome in healthy volunteers

3.2.1 Tear sampling

Basal and reflex tears were repeatedly collected from 10 healthy volunteers (5 males and 5 females, age between 20 to 33 years old) who had no ocular diseases and were not contact lens wearer. Non-invasive capillary technique was utilized for basal tear fluid collection (~5 µl/ individual) as described elsewhere **[112, 139]**. Reflex tears were collected after briefly exposing the eye to freshly minced onion vapors to stimulate reflex tear production. To avoid contamination with basal tear fluid, the first 10 µl of fluid were discarded and 10 - 15 µl tears were collected within 2 minutes **[148, 149]**. The collected tear fluids were expelled into 0.2 ml PCR tubes and stored at -80 °C until further analysis. Protein concentration of the tears was determined using a Pierce BCA protein Assay Kit (Thermo Scientific, Rockford, USA) using BSA (Sigma-Aldrich, St Louis, USA) as standard. Informed consent was obtained from all participants prior to the study.

3.2.2 Discovery study: LFQ analysis *via* 1DE & LC-MS/MS strategy

3.2.2.1 1DE

Ten individual tear samples were repeatedly collected three times and pooled equally (10 µg per individual) to a total of 100µg each for basal and reflex tears with three biological replicates. The tear samples were subjected to 1DE (25 µg/ well and sliced into 10 bands) using 4-12 % Bis-Tris Gels (Invitrogen, Karlsruhe, Germany) with MES running buffer under reducing conditions for 60 minutes with a constant voltage of 150 V. SeeBlue™ Plus 2 (Invitrogen) was used as a protein molecular mass marker. The gels were stained with Colloidal Blue Staining Kit (Invitrogen) according to the manufacturer's instructions. The sliced gel pieces were subjected to trypsin digestion utilizing a method previously described in **section 3.1.2.1 [138, 139]**. The extracted peptides were purified on ZipTip® C18 columns (Millipore, Billerica, MA, USA) according to the manufacturer's instructions. This procedure was repeated three times for each sample and the combined eluate was concentrated to dryness in the SpeedVac concentrator and dissolved with 10 µl of 0.1 % TFA solution prior to LC-MS/MS analysis.

3.2.2.2 LC-ESI-MS/MS

The LC-ESI-MS/MS system utilized for this study has been described in detail in **section 3.1.2.2 [139]**.

3.2.2.3 LFQ analysis

The acquired MS spectra were analyzed utilizing MaxQuant computational proteomics platform version 1.4.1.2 for peptide and protein identification as well as for LFQ analysis **[70, 102, 103, 141]**. Tandem MS spectra were searched against Uniprot Human database (date, 15/5/2014) using standard settings with peptide mass tolerance of ± 30 ppm, fragment mass tolerance of ± 0.5 Da with LFQ algorithm selected. The FDR for peptide and protein identification was set to 0.01 with ≥ 6 amino acid residues and only "unique plus razor peptides" that belong to a protein were chosen to be included for quantification **[70]**. Carbamidomethylation of cysteine was set as a fixed modification, while protein N-terminal acetylation and oxidation of methionine were defined as variable modifications, enzyme: trypsin and maximum number of missed cleavages: 2. The output of the generated "proteingroups.txt" table was filtered for contaminants, reverse hits and minimum number of values "in at least one group" is 3 prior to statistical analysis using Perseus software. First, the normalized LFQ intensities of protein abundance were Log2 transformed for further analyses. Subsequently, two-samples t-test-based statistics with P values < 0.05 was applied to assert proteins expression as significant for the reflex group **[102]**.

3.2.3 Verification study 1: 2DE & LC-ESI-MS/MS strategy

High abundant reflex and basal tear proteins were differentially analyzed employing the 2DE and LC-ESI-MS/MS system. Ten individual tear samples were repeatedly collected three times and pooled equally (6 µg per individual) to a total of 60 µg each for basal and reflex tears with three biological replicates and subjected for 2DE analysis as described in detail elsewhere **[139]**. Briefly, the 2DE was performed as follows: tear protein samples (60 µg/ gel) were diluted in 125 µl rehydration buffer (7 M urea, 2 M thiourea, 4 % CHAPS, 40 mM DTT, 0.002 % bromophenol blue, 2 % pH 3-10 non-linear IPG buffer) and applied on 7 cm IPG strips (GE Healthcare, Piscataway, NJ). Isoelectric focusing (IEF) strips were focused on an IPGphor-II (GE Healthcare, Piscataway, NJ) with passive rehydration for 2 hours and active rehydration with a 9 steps IEF **[139]**. The IEF strips were then reduced and alkylated, and the proteins were separated for 60 min with a constant voltage of 150 V. SeeBlue™ Plus 2 was used as a protein molecular mass marker and the gels were stained with Colloidal Blue Staining Kit. The 2DE gels images were analyzed using REDFIN Solo software (Ludesi, Malmo, Sweden) and ImageJ software (http://imagej.nih.gov/ij/) **[150]**. The REDFIN software was employed for warping and visualizing the differentially expressed protein spots

in the 2DE gels. Protein spots that localized to the same position were matched and the intensities of each of the similar spots across the gels were calculated by utilizing ImageJ software. Data obtained from the ImageJ software were exported in an excel workbook format (Microsoft Office Excel 2010) and the intensities of the protein spots were transferred to Statistica (v8, StatSoft, Tulsa, OK) for t-test analysis (independent, by groups, $P< 0.05$). All the differentially expressed protein spots from basal and reflex tears in 2DE gels were manually excised and subjected to in-gel digestion prior to LC-ESI-MS/MS analysis.

3.2.4 Verification study 2: Targeted MS *via* AIMS strategy

Targeted MS *via* the AIMS strategy by means of an "inclusion list" in the MS instrument method was utilized for verification analysis **[145, 146]**. Basal and reflex tears were collected from 5 healthy volunteers (3 males and 2 females, age between 28 to 33 years old) and subjected to in-solution digestion and analyzed individually by the AIMS strategy **[139]**. Each tear sample was adjusted to 10 µg and was digested with sequence grade-modified trypsin [protease:protein ratio of 1:20 (w/w)] for 16 hours at 37 °C with 50 µl of 50 mM NH_4HCO_3 in 10 % acetonitrile. The digested samples were dried in SpeedVac concentrator and subsequently purified on ZipTip® C18 columns according to the manufacturer's instructions. Next, the eluates were concentrated to dryness in the SpeedVac concentrator and dissolved with 10 µl of 0.1 % TFA solution prior to targeted MS analysis. For targeted MS analysis, the LC-ESI-MS/MS system was operated as described in **section 3.1.2.2**. However, the use of global parent list was enabled and the dynamic exclusion segment was disabled and the parent mass width was set to 10 ppm for both high and low *m/z* **[139]**. Raw files were processed using Thermo Proteome Discoverer software v.1.1.0.263 (Thermo Scientific, Bremen, Germany) and the following specified parameters were applied for database-search: database, SwissProt_140101 (542258 sequences; 192776118 residues) and NCBInr_110225 (13135398 sequences; 4494708239 residues); taxonomy, *Homo sapiens*; proteolytic enzyme, trypsin; peptide mass tolerance, ± 30 ppm; fragment mass tolerance, ± 0.5 Da and peptide charge state, 2+ using MASCOT v2.2.07 (Matrix Science, London, UK). Proteins search were run under stringent MudPIT scoring with significance threshold set to $p \leq 0.01$ and FDR of 1 %. Data obtained from the Thermo Proteome Discoverer software were exported in an excel workbook format (Microsoft Office Excel 2010) and the sum absolute intensity of the signature peptides for each proteins were calculated and were transferred to Statistica (v8, StatSoft, Tulsa, OK) for t-test analysis (independent, by groups, $P< 0.05$).

3.3 Characterization of Lacrimal Proline-Rich Protein 4 (PRR4) in Human Tear Proteome

3.3.1 Tear sampling

Tears were collected from 61 healthy volunteers (29 males and 33 females, age between 20 to 33 years old) who had no ocular diseases and were either contact lens wearers (N=12) or non-contact lens wearers (N=49). Standard non-invasive capillary technique was employed for basal tear fluid collection (~5 µl/ individual) as described elsewhere **[112]**. Briefly, the tears were collected by cautiously applying the tip of a 5 µl glass microcapillary tube (Hirschmann® Laborgerate, Eberstadt, Germany) to the corner of the eye. The collected tear fluids were expelled into 0.2 ml PCR tubes and stored at -80 °C until further analysis.

Study 1 (PRR4 characterization from pooled samples)

Ten tear samples from the sixty one volunteers (5 males and 5 females) were randomly selected and pooled for the identification of the PRR4 rich-region in 1DE gels (25 µg/ well; two lanes of the gel were combined and sliced into 14 bands) after tryptic digestion and analyzed utilizing LC-MALDI-MS/MS and LC-ESI-MS/MS systems. Subsequently, the pooled tear samples were also used for the identification of PPR4 spots and their PTMs in 2DE gels after tryptic and endoproteinase Asp-N digestion, and analyzed utilizing MALDI-MS/MS and LC-ESI-MS/MS systems.

Study II (PRR4 characterization from individual samples)

Sixty one tear samples (29 males and 33 females) were analyzed individually to identify and determine the distribution of PRR4 isoforms. This experiment was conducted based on the targeted data acquisition of signature PRR4 peptides representing specific PRR4 isoforms by analyzing the PRR4-rich region in the 1DE gels utilizing MALDI-MS/MS and, by analyzing the in-solution tryptic digestion tear samples utilizing LC-ESI-MS/MS systems.

3.3.2 1DE and 2DE

Tear samples (25 µg/ well) were subjected to 1DE using 4-12 % Bis-Tris Gels (Invitrogen, Karlsruhe, Germany) with MES running buffer under reducing conditions for 60 minutes with a constant voltage of 150 V. Briefly, the 2DE was performed as follows: tear protein samples (60 µg/ gel) were diluted in 125 µl rehydration buffer containing 7 M urea, 2 M thiourea, 4 % CHAPS, 40 mM DTT, 0.002 % bromophenol blue, 2 % pH 3-10 non-linear

(NL) IPG buffer and applied on 7 cm IPG strips (GE Healthcare, Piscataway, NJ). Isoelectric focusing (IEF) strips were focused on an IPGphor-II (GE Healthcare, Piscataway, NJ) with passive rehydration for 2 hours and active rehydration with a 9 steps IEF using the following voltage setting: 20 V for 12 hours (step and hold), 500 V for 1 hour (gradient), 500 V for 1 hour (step and hold), 1000 V for 30 min (gradient), 1000 V for 1 hour (step and hold), 4000 V for 30 min (gradient), 4000 V for 2 hours (step and hold), 8000 V for 2 hours (gradient) and 8000 V for 2 hours (step and hold). The IEF strips were then reduced in equilibration solution of 6 M urea, 75 mM tris Tris-HCl pH 8.8, 29.3 % glycerol, 2 % sodium dodecyl sulfate (SDS), 0.002 % bromophenol blue containing 1 % w/v DTT for 15 min and alkylated in equilibration solution containing 2.5 % w/v iodoacetamide for 15 min with gentle shaking. The IEF strips were placed on top of a 4-12 % Bis-Tris NuPAGE ZOOM gel (Invitrogen, Karlsruhe, Germany) and sealed with agarose solution (0.5 % agarose, 0.002 % bromophenol blue in MES SDS electrophoresis buffer) and the proteins were separated for 60 min with a constant voltage of 150 V. SeeBlue™ Plus 2 (Invitrogen, Karlsruhe, Germany) was used as a protein molecular mass marker. The gels were stained with Colloidal Blue Staining Kit (Invitrogen, Karlsruhe, Germany) according to the manufacturer's instructions. The 2DE gels were analyzed employing Melanie Viewer v7.0 software (GeneBio, Geneva, Switzerland). All the abundant protein spots in 2DE especially in the PRR4-rich region identified from 1DE, were manually excised and subjected for in-gel digestion.

3.3.3 In-gel digestion

The extracted gel pieces were subjected to trypsin or endoproteinase Asp-N digestion utilizing a method previously described in **section 3.1.2.1 [138, 139]**. The reduced and alkylated protein mixtures were digested with sequence grade-modified trypsin or endoproteinase Asp-N (Promega, Madison, USA) for 16 hours at 37 °C with 10 mM NH_4HCO_3 in 10 % acetonitrile. Proteolysis was quenched by acidification of the reaction mixtures in each tube with 100 µl of extraction buffer [1:2 (vol/vol) of 5 % formic acid: acetonitrile] and incubated for 15 min at 37 °C in a shaker. The supernatant containing the peptides was collected and the remaining peptides in the gel pieces were extracted with two 20 minutes washes in extraction buffer. The supernatants were pooled and dried in SpeedVac concentrator prior to storage at -20 °C. The dried peptides were purified on ZipTip® C18 columns (Millipore, Billerica, MA, USA) according to the manufacturer's instructions. This procedure was repeated twice for each sample and the combined eluate was concentrated to

dryness in the SpeedVac concentrator and dissolved with 15 µl of 0.1 % TFA solution prior to MS analysis.

3.3.4 MALDI-MS/MS analysis

MALDI-MS/MS analysis was conducted by depositing 2 µl of purified peptides which were dissolved in 0.1 % TFA on a 386 MTP PolishedSteel™ MALDI target plate (Bruker Daltonics, Bremen) without fractionation (each individual sample per spot with three technical replicates). The samples were dried at room temperature and 2 µl of 2 mg/mL α-cyano-4- hydroxy cinnamic acid (CHCA) matrix in 0.1 % TFA, 50 % acetonitrile were applied to each dried spot. In addition, 2 µL Peptide Calibration Standard 2 (Bruker Daltonics, Bremen, Germany) were prepared. Mass spectra were acquired using an ULTRAFLEX II MALDI-TOF/TOF (Bruker Daltonics, Bremen, Germany) and the system was operated by the FlexControl and FlexAnalysis version 2.4 (Bruker Daltonics, Bremen, Germany) software. Mass spectra were acquired based on following parameters: reflector polarity, positive; mass range, 900-3700 Da; laser frequency, 100Hz; accumulation, 500 shots (10x50 short steps)/ spot. Sequencing of the acquired mass spectra was done using the laser-induced dissociation (LID)-LIFT TOF mode with following parameters: accumulation, 500 shots (5x100 short steps)/ spot; S/N threshold ≥ 10; intensity threshold ≥ 800. Raw mass spectra were processed using Biotools software v3.0 (Bruker Daltonics, Bremen, Germany) for protein data interpretation and the following specified parameters were applied for database search: databases, SwissProt_111101.fasta, 533049 sequences, 189064225 residues and NCBInr_110225.fasta, 13135398 sequences, 4494708239 residues; taxonomy, *Homo sapiens*; proteolytic enzyme, trypsin; peptide mass tolerance, ± 80 ppm; fragment mass tolerance, ± 0.8 Da; global modification, Carbamidomethylation of cysteine; variable modification, Oxidation of methionine; peptide charge state, 1+ and one missed cleavage using MASCOT v2.2.07 (Matrix Science, London, UK). Proteins search were run under stringent MudPIT scoring with significance threshold set to $p \leq 0.01$ and FDR of 1 %.

3.3.5 LC-MALDI-MS/MS analysis

The LC-MALDI-MS/MS system is well established in our laboratory and has been described in detail elsewhere **[50]**. Briefly, the peptide elution was followed by off-line fractionation on a 386 MTP PolishedSteel™ MALDI target plate. Each slice extract was fractionated over 24 spots with a frequency of 40 seconds per spot (14 gel slices x 24 spots = 336 spots). The fractionated eluates were dried at room temperature and 2 µL of 2 mg/mL CHCA matrix in

0.1 % TFA, 50 % acetonitrile were applied to each dried fraction spot. In addition, 15 spots with 2 µL Peptide Calibration Standard 2 were prepared. The continuum mass spectra were acquired using an ULTRAFLEX II MALDI-TOF/TOF and the system was operated in an automated mode by incorporating WARPLC™ software (Bruker Daltonics, Bremen, Germany), FlexControl and FlexAnalysis version 2.4 software. Mass spectra acquiring parameters and the data interpretation parameters were performed described in **section 3.3.4**.

3.3.6 LC-ESI-MS/MS analysis

The LC-ESI-LTQ-Orbitrap MS system is well established in our laboratory and has been described in detail in **section 3.1.2.2 [50, 139]**. Raw files were processed using Thermo Proteome Discoverer software v. 1.1.0.263 (Thermo Scientific, Bremen, Germany) and the following specified parameters were applied for database-search: database, NCBInr_110225.fasta, 13135398 sequences, 4494708239 residues; taxonomy, *Homo sapiens*; proteolytic enzyme, trypsin or endoproteinase Asp-N; peptide mass tolerance, ± 10 ppm; fragment mass tolerance, ± 0.8 Da; global modification, carbamidomethylation of cysteine; variable modification, oxidation (M); peptide charge state, 1+, 2+, 3+ and 4+; and one max missed cleavage. Proteins search were run under stringent MudPIT scoring with significance threshold set to $p \leq 0.01$ and FDR of 1 %.

3.3.7 PRR4 PTMs identifications

For identification of PTMs of PRR4 in the 2DE gel, a trial version of PEAKS Studio 7 (32bit) software was utilized **[151, 152]**. The search parameters were set as follows: parent mass error tolerance: ± 20 ppm, fragment mass error tolerance: 0.6 Da, precursor mass search type: monoisotopic with charge states of +1 to +4, max missed cleavages per peptide: 0, non-specific cleavage: 0, fixed modifications: carbamidomethylation (+57.02), variable modifications: 52 common modifications listed in built-in modifications section in PEAKS 7 software and maximum allowed variable PTM per peptide: 1. The result filtration parameters were set as follows: De novo score (ALC %) threshold: ≥50; Peptide −10 lgP≥17.5; Protein −10 lgP≥20; FDR (Peptide-Spectrum Matches): 1 %. Each PTM was further manually validated through PTM-specific neutral loss and *a*, *b* and/or *y* fragmentation ions series.

3.3.8 Targeted MS *via* AIMS strategy

Sixty one tear samples were subjected for in-solution digestion and analyzed individually by targeted data acquisition approach *via* AIMS strategy utilizing LC-ESI-MS/MS systems. Each tear samples (10 µg) were digested with sequence grade-modified trypsin [protease: protein ratio of 1:20 (w/w)] for 16 hours at 37 °C with 50 µl of 10 mM NH_4HCO_3 in 10 % acetonitrile. The digested samples were dried in SpeedVac concentrator and subsequently purified on C18 StageTips^{TM} (Thermo Scientific, Bremen, Germany) according to the manufacturer's instructions. Next, the eluates were concentrated to dryness in the SpeedVac concentrator and dissolved with 10 µl of 0.1 % TFA solution prior to MS analysis. The primarily identified PRR4 isoforms signature peptides were selected and assigned into the global parent mass list according to the MS Mass (*m/z*) and MS Charge State. The LTQ-Orbitrap was operated in the data-dependent mode of acquisition to automatically switch between Orbitrap-MS and LTQ-MS/MS acquisition as describe in **section 3.1.2.2**. However, the use of global parent list was enabled and the dynamic exclusion segment was disabled. The parent mass width was set to 10 ppm for both high and low *m/z*. Raw files were processed using Thermo Proteome Discoverer software and the following specified parameters were applied for database-search: database, NCBInr_110225.fasta, 13135398 sequences, 4494708239 residues; taxonomy, *Homo sapiens*; proteolytic enzyme, trypsin; peptide mass tolerance, ± 10 ppm; fragment mass tolerance, ± 0.8 Da and peptide charge state, 1+, 2+, 3+ and 4+.

4 RESULTS

4.1 Identification and verification of potential tear protein biomarker panels to distinguish DES subgroups

The representative tear protein profiles of DES subgroups and CTRL resolved in 1DE gel are depicted in **Figure 4.1**. Notable differences were observed at band three, seven and ten, that represent serum albumin (ALB), PRR4 and SCGB2A1, respectively. A total of 200 proteins were detected by the discovery approach as presented in **Appendix 1.** Of these proteins, 117 overlapped with CTRL and all DES subgroups, as shown in the Venn diagram in **Figure 4.2**. The exclusively identified proteins for each group were only 8, 4, 28 and 20 proteins in the CTRL, DRYlip, DRYaq and DRYaqlip, respectively. The degree of variances in the proteome between the groups was investigated through Pearson correlation using their protein intensities extracted from the MaxQuant analysis. Generally, there is excellent technical reproducibility of the entire experimental workflow, which reveals Pearson correlation of 0.96 ± 0.01 for DRYaq and 0.97 ± 0.01 for CTRL, DRYlip and DRYaqlip as shown in **Figure 4.3**. On average, correlation between DRYlip-CTRL was 0.96 ± 0.01, and slightly lower correlations were observed between the DRYaq-CTRL (0.89 ± 0.01) and DRYaqlip-CTRL (0.87 ± 0.01). Hence, this demonstrated high similarities between the proteome of CTRL and DRYlip, as well as DRYaq and DRYaqlip. In addition, this analysis indicates that reproducible data were generated from the pooled tear samples, which enabled further statistical analysis.

In order to reveal differentially expressed proteins in the DES subgroups compared to CTRL, LFQ values of the identified proteins extracted from MaxQuant analysis were employed for statistical analysis utilizing the Perseus software. To more easily visualize the data, a heat map with unsupervised hierarchical clustering of the data was generated, as shown in **Figure 4.4**. The heat map revealed two major clusters (cluster 1: CTRL & DRYlip, cluster 2: DRYaq & DRYaqlip) and the triplicate measurements perfectly segregated according to their groups. This shows that MS-based proteomics can correctly group DES proteomes according to the subgroups. Correspondingly, the proteins lists were also clustered into two main clusters, which also demonstrated almost similar expression profiles between CTRL-DRYlip and DRYaq-DRYaqlip. In order to identify a subset of proteins that significantly differentiate the dry eye subgroups compared to CTRL, a two samples t-test ($P < 0.01$) was performed. **Figure 4.5** shows the pairwise differences in the proteome of dry eye subgroups compared to CTRL

and the total number of proteins that were significantly differentially expressed are as follows: DRYlip/CTRL - 22 proteins; DRYaq/CTRL - 58 proteins; DRYaqlip/CTRL - 67 proteins. The summary of the significantly differentially expressed proteins in the different DES subgroups compared to CTRL is as shown in **Table 4.1** (complete name of the proteins in **Appendix 1**).

Next, with the aim to elucidate the abundance of the regulated proteins identified between DES subgroups and CTRL, normalized iBAQ intensities to the sum of all intensities were utilized because the value of iBAQ is proportional to the relative expression level of protein. iBAQ values larger than 0.5 % was counted as major protein and minor if the iBAQ values are lower than 0.5 %. **Figure 4.6** shows that only top 20 major proteins from the total of 200 proteins make up almost 95.52 ± 0.32 %, 96.36 ± 0.65 %, 91.0 ± 0.13 % and 92.55 ± 0.56 % of the total identified proteome in CTRL, DRYlip, DRYaq and DRYaqlip, respectively. Moreover, LYZ, LCN1, LTF and PIP make up as much as 60 % of the total proteome of the CTRL tears.

Table 4.2 demonstrated the overview of the relative expression level of the significantly differentially expressed proteins in DES subgroups compared to CTRL and the total major proteins were as follows: DRYlip/CTRL - 6 proteins; DRYaq/CTRL - 9 proteins; DRYaqlip/CTRL - 13 proteins. Among the major proteins differentially expressed in DRYlip/CTRL, ALB was decreased and IGHA1, ENO1 and SCGB2A were increased. On the contrary, almost similar cluster of major proteins were differentially expressed in DRYaq/CTRL and DRYaqlip/CTRL, namely decrement of AZGP1, IGHA1, PRR4, LACRT and ENO1, and increment of ALB, IGHG1, S100A8, S100A9, ENO1, PIGR and GSTP1. However, the expression level of major proteins LTF and LYZ were observed to be decreased in abundance in the DRYaqlip/CTRL. Generally, the aforementioned iBAQ analysis revealed that most of the significantly differentially expressed proteins were classified as minor proteins in this study.

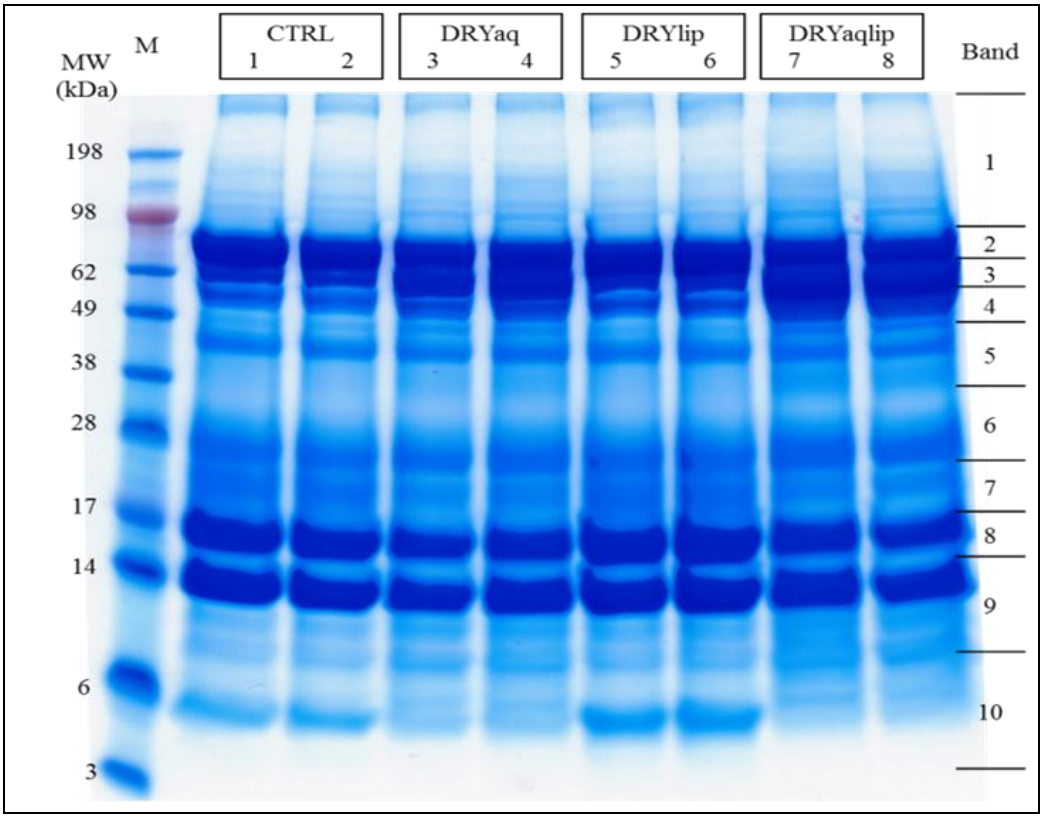

Figure 4.1: Representative CTRL, DRYaq, DRYlip and DRYaqlip tear protein profiles resolved in 1DE gel after colloidal blue staining.
Notable differences between DES subgroups and CTRL are observed at band three, seven and ten, which abundantly represent ALB, PRR4 and SCGB2A1, respectively.

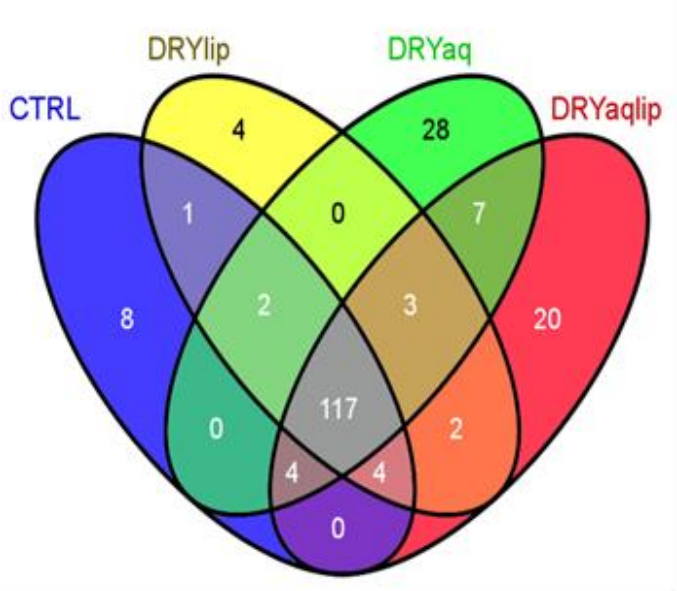

Figure 4.2: The Venn diagram depicts the overlap of the non-redundant proteins identified in the control and DES subgroups of discovery proteomics analysis.

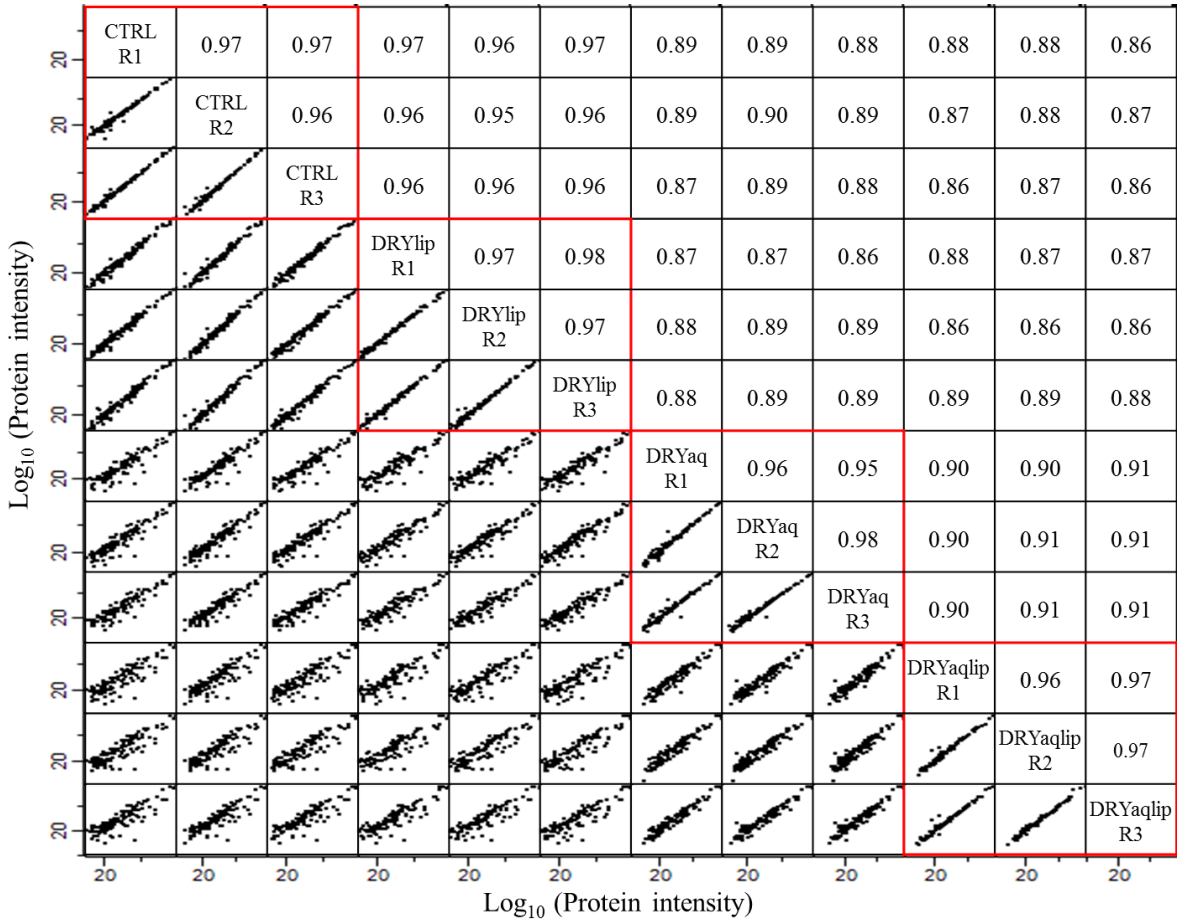

Figure 4.3: The degree of variances in the proteome between the DES subgroups and control group investigated through Pearson correlation using their protein intensities extracted from the MaxQuant analysis are shown.

Technical replicates of the same group are highly correlated, which reveals average Pearson coefficients of 0.96 ± 0.01. Generally, correlation between DRYlip-CTRL was 0.96 ± 0.01, and slightly lower correlations were observed between DRYaq-CTRL (0.89 ± 0.01) and DRYaqlip-CTRL (0.87 ± 0.01).

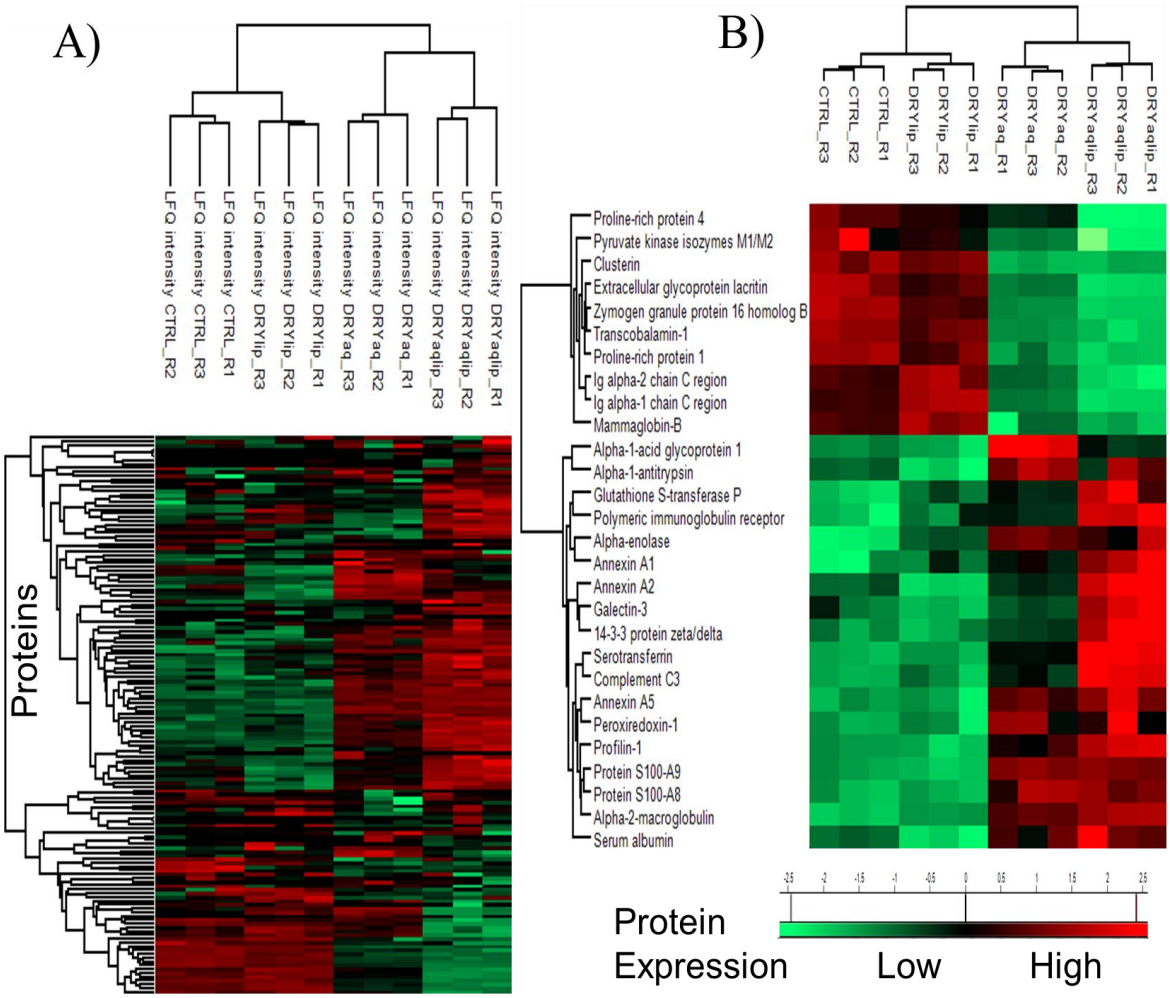

Figure 4.4: LFQ intensities of the 200 proteins were used to identify significantly differentially expressed proteins between DES subgroups and control. LFQ intensity ranges from highest intensity (red) to lowest (green). (A) The heat map shows hierarchical clustering analysis that separates the samples into two main clusters (cluster 1: CTRL & DRYlip, cluster 2: DRYaq & DRYaqlip). (B) The heat map shows a subset of 28 proteins considered highly differentially expressed between the DES subgroups.

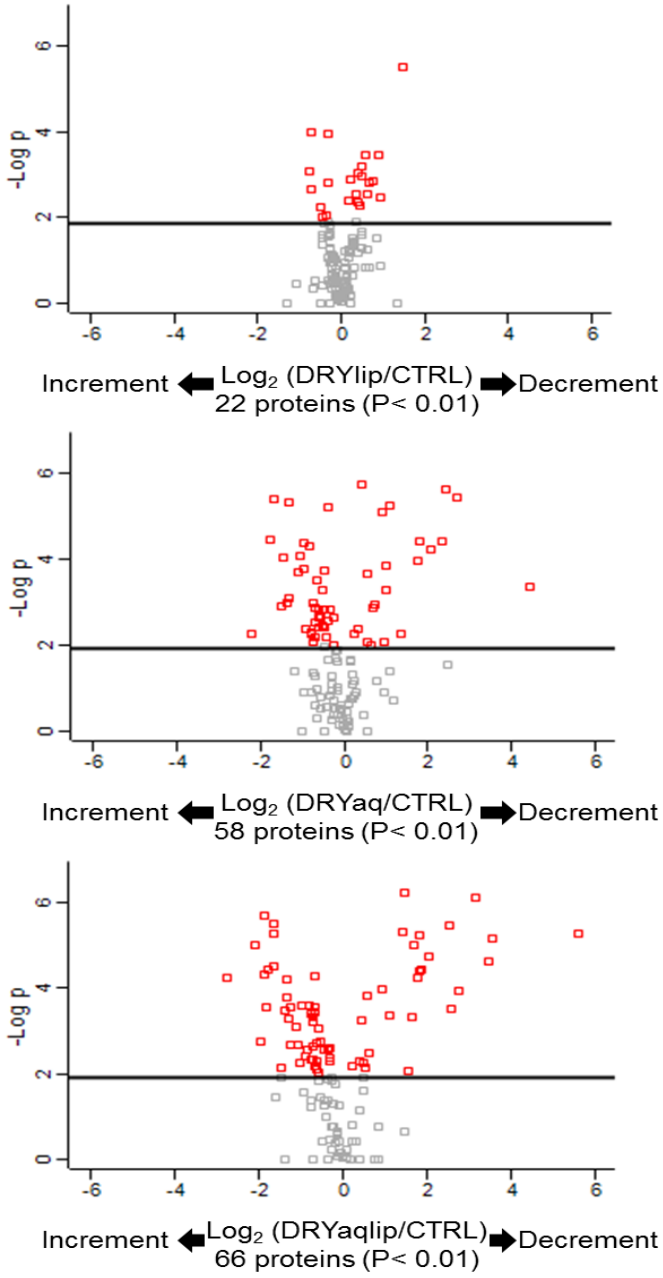

Figure 4.5: These plots show the pairwise differences in the proteome of each dry eye subgroup compared to control.

X-axis represents the log fold differences of the identified proteins based on their intensity. Spots on the left represent the increased and the right the decreased proteins. *Y*-axis represents the (minus) log P values from the statistical analysis. Significantly altered proteins (P< 0.01) are annotated as red squares.

Table 4.1: Summary of the differentially expressed proteins (LFQ values) in DES subgroups compared to control employing 1DE and LC-ESI-MS/MS strategy.

	LFQ values subjected for Two samples t-test; Threshold p-value < 0.01					
	DRYlip/CTRL		DRYaq/CTRL		DRYaqlip/CTRL	
Gene names	Significant	p value	Significant	p value	Significant	p value
LYZ	n.s	8.9E-02	n.s	2.5E-01	decrement	1.1E-04
LTF	n.s	4.7E-01	n.s	2.3E-02	decrement	5.5E-04
IGHA1	increment	1.1E-04	decrement	7.7E-06	decrement	5.6E-07
AZGP1	n.s	6.5E-01	decrement	5.4E-06	decrement	5.6E-06
CST4	n.s	9.8E-02	n.s	5.0E-01	decrement	7.5E-03
PRR4	n.s	3.1E-02	decrement	1.4E-03	decrement	3.4E-06
LACRT	n.s	2.7E-02	decrement	3.8E-05	decrement	7.0E-06
IGHA2	n.s	2.4E-02	decrement	1.4E-04	decrement	3.7E-05
ACTB	n.s	1.2E-01	decrement	5.4E-03	decrement	6.5E-03
SCGB2A1	increment	9.7E-03	n.s	2.8E-02	decrement	1.2E-04
SCGB1D1	increment	2.2E-03	decrement	8.4E-03	decrement	1.9E-05
IGJ	n.s	1.5E-02	n.s	5.8E-01	decrement	5.6E-03
HSPB1	decrement	6.2E-04	decrement	4.2E-03	decrement	4.6E-04
PGK1	n.s	1.3E-02	increment	1.4E-03	decrement	1.6E-04
DMBT1	n.s	5.6E-02	decrement	2.2E-04	decrement	5.0E-06
CLU	n.s	3.0E-01	decrement	3.9E-05	decrement	5.5E-05
PROL1	n.s	5.7E-02	decrement	4.5E-04	decrement	5.4E-06
MDH1	n.s	2.7E-02	increment	1.5E-03	decrement	3.2E-03
KRT1	decrement	3.3E-03	decrement	5.3E-04	decrement	4.3E-04
ZG16B	decrement	1.1E-03	decrement	2.3E-06	decrement	7.8E-07
TCN1	n.s	4.3E-02	decrement	3.5E-06	decrement	2.4E-05
KRT10	decrement	3.4E-04	n.s	1.2E-01	decrement	4.9E-03
CTSB	n.s	4.8E-02	decrement	1.1E-04	decrement	3.1E-04
KRT9	decrement	3.1E-06	decrement	6.1E-05	decrement	9.9E-06
PKM	n.s	2.3E-01	decrement	8.5E-03	decrement	8.3E-03

Table 4.1: (continued)

	LFQ values subjected for Two samples t-test; Threshold p-value < 0.01					
	DRYlip/CTRL		DRYaq/CTRL		DRYaqlip/CTRL	
Gene names	**Significant**	**p value**	**Significant**	**p value**	**Significant**	**p value**
IGHG1	decrement	4.1E-03	increment	6.1E-06	increment	4.3E-03
S100A9	n.s	3.8E-02	increment	3.3E-05	increment	3.6E-05
GSTP1	n.s	1.3E-02	increment	5.0E-04	increment	2.8E-03
S100A8	n.s	9.2E-01	increment	1.1E-03	increment	3.3E-04
ENO1	increment	1.0E-04	increment	4.8E-06	increment	5.2E-04
ANXA1	n.s	9.7E-02	increment	9.8E-03	increment	2.7E-03
PIGR	n.s	7.1E-02	increment	2.6E-03	increment	3.5E-04
IGHG2	n.s	6.8E-02	increment	4.0E-03	increment	2.6E-04
SERPINB1	decrement	4.6E-03	n.s	3.5E-01	increment	8.5E-04
ANXA2	decrement	9.0E-04	n.s	2.4E-02	increment	2.8E-04
ORM1	n.s	8.8E-02	increment	4.9E-05	increment	5.1E-03
TF	n.s	3.5E-01	increment	4.0E-05	increment	5.1E-06
PRDX1	n.s	9.2E-01	increment	2.1E-03	increment	9.4E-03
PEBP1	n.s	1.7E-01	increment	1.0E-03	increment	7.9E-04
YWHAZ	n.s	4.3E-01	n.s	2.0E-02	increment	2.3E-03
TPI1	n.s	1.9E-01	n.s	9.5E-02	increment	4.6E-04
S100A11	n.s	3.2E-02	decrement	5.4E-03	increment	2.7E-04
CSTB	decrement	1.6E-03	increment	1.2E-03	increment	3.0E-06
AKR1C1	n.s	2.8E-01	increment	6.4E-03	increment	2.8E-04
UBB	n.s	4.8E-01	n.s	1.6E-01	increment	5.7E-03
PFN1	n.s	6.5E-02	increment	9.3E-05	increment	1.0E-05
ALDOA	n.s	4.6E-01	n.s	2.3E-02	increment	2.6E-04
AKR1A1	decrement	1.4E-03	n.s	2.3E-01	increment	6.1E-04
FBP1	n.s	7.4E-01	increment	8.7E-03	increment	2.1E-03
PPIA	n.s	1.0E+00	increment	8.2E-04	increment	1.8E-03

Table 4.1: (continued)

	LFQ values subjected for Two samples t-test; Threshold p-value < 0.01					
	DRYlip/CTRL		DRYaq/CTRL		DRYaqlip/CTRL	
Gene names	**Significant**	**p value**	**Significant**	**p value**	**Significant**	**p value**
FABP5	n.s	1.2E-01	increment	5.6E-03	increment	5.5E-05
ALDH3A1	n.s	9.4E-01	increment	4.9E-03	increment	3.8E-03
C3	n.s	4.9E-01	increment	1.4E-03	increment	5.1E-05
TGM2	n.s	4.5E-01	n.s	1.2E-01	increment	4.7E-03
GSN	n.s	2.5E-02	increment	8.5E-05	increment	3.0E-05
A2M	increment	1.5E-03	increment	3.9E-06	increment	2.1E-06
PARK7	n.s	1.1E-01	increment	6.3E-03	increment	2.1E-03
GLOD4	n.s	3.1E-01	increment	5.6E-03	increment	2.0E-03
RBP4	n.s	4.4E-01	n.s	1.0E+00	increment	5.3E-03
CFH	n.s	5.0E-02	increment	1.9E-04	increment	6.0E-05
ITIH4	n.s	4.6E-01	n.s	3.9E-02	increment	7.6E-03
SFN	n.s	2.4E-01	increment	1.3E-03	increment	1.6E-04
UBA1	n.s	7.5E-01	n.s	1.1E-02	increment	6.5E-03
IGLL5	increment	5.8E-03	n.s	4.6E-02	n.s	9.4E-01
SERPINA1	decrement	2.8E-03	increment	1.8E-04	n.s	4.1E-02
LCN2	increment	8.5E-04	n.s	7.0E-02	n.s	2.4E-01
ALDH1A1	n.s	2.3E-01	decrement	1.8E-06	n.s	2.2E-01
HP	decrement	2.9E-03	increment	2.2E-03	n.s	4.0E-01
ORM2	decrement	5.4E-03	increment	3.7E-03	n.s	6.1E-01
TTR	n.s	1.9E-01	increment	2.9E-03	n.s	1.6E-01
HSPA1A	n.s	4.1E-02	decrement	1.0E-02	n.s	7.4E-02
GC	n.s	7.1E-01	increment	1.7E-04	n.s	1.8E-01
ANXA3	n.s	4.7E-01	increment	4.2E-03	n.s	1.1E-01
GDI2	decrement	3.4E-04	n.s	3.1E-01	n.s	8.9E-01

Note: non-significant (n.s).

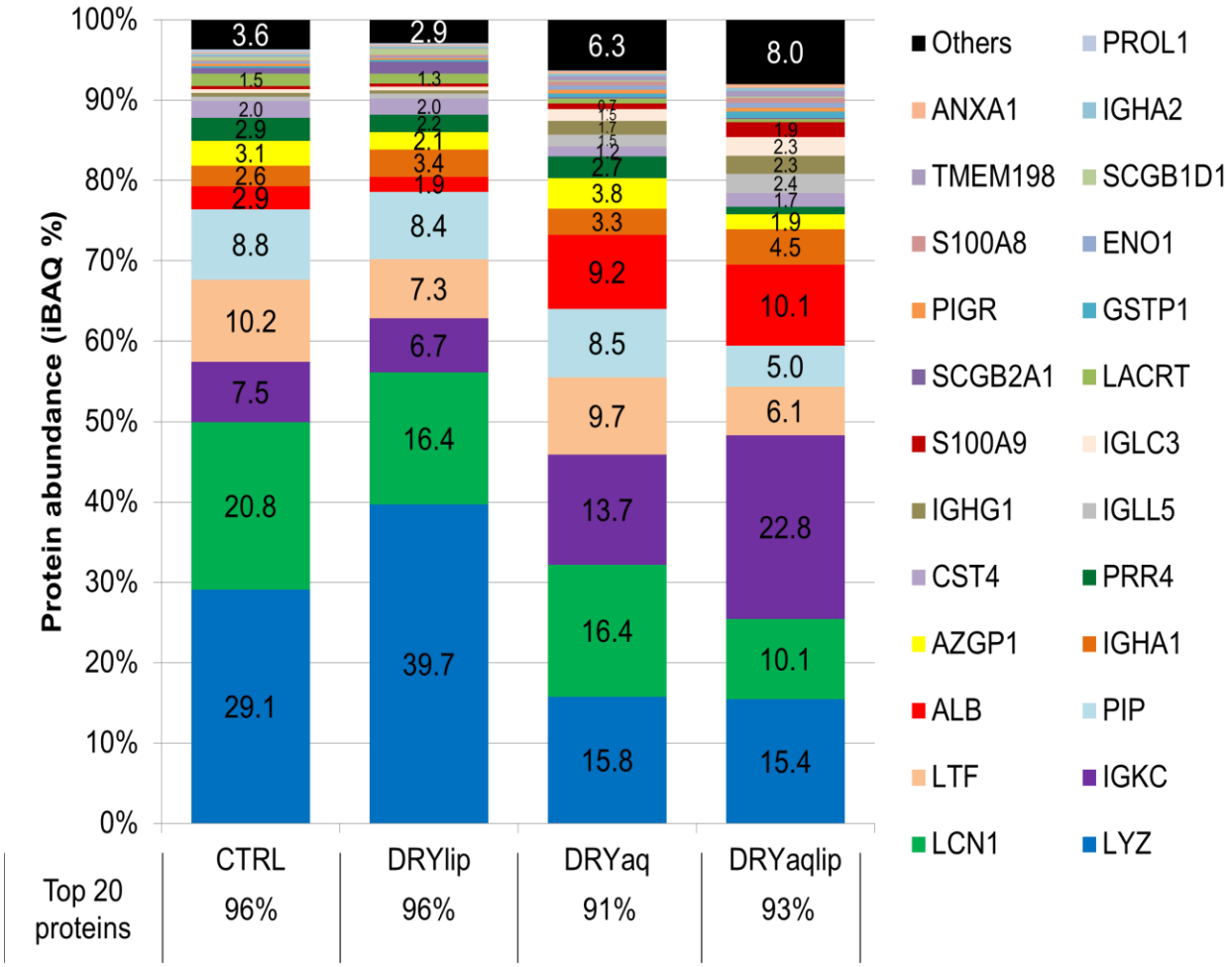

Figure 4.6: The iBAQ intensities of the 200 proteins extracted from MaxQuant analysis were used to compare the degree of protein abundance between proteins in each group for DES subgroups and control.

Top 20 major proteins from the total of 200 proteins make up almost 90 % of the total identified proteome in CTRL and DES subgroups tears.

Table 4.2: Summary of the relative expression level (iBAQ values) of the differentially expressed proteins in DES subgroups compared to control employing 1DE and LC-ESI-MS/MS strategy.

	iBAQ values (%)							
	CTRL		DRYlip		DRYaq		DRYaqlip	
Gene names	Mean %	SD %	Mean %	SD %	Mean %	SD %	Mean %	SD %
LYZ	29.161	3.311	39.231	9.346	15.595	3.439	15.429	2.511
LTF	10.244	0.438	7.435	1.956	9.733	1.419	6.110	0.551
AZGP1	3.071	0.203	2.100	0.565	3.822	0.405	1.890	0.108
PRR4	2.884	0.508	2.199	0.350	2.694	0.290	0.868	0.038
ALB	2.863	0.018	1.895	0.517	9.242	0.458	10.059	1.170
IGHA1	2.578	0.205	3.435	1.381	3.287	0.576	4.456	0.286
CST4	2.013	0.162	2.025	0.732	1.226	0.459	1.742	0.298
LACRT	1.491	0.306	1.294	0.436	0.573	0.067	0.338	0.029
SCGB2A1	0.749	0.054	1.547	0.634	0.209	0.071	0.171	0.001
IGLL5	0.560	0.044	0.643	0.136	1.446	0.269	2.355	0.405
IGHG1	0.501	0.138	0.377	0.137	1.683	0.194	2.262	0.289
S100A9	0.445	0.074	0.386	0.061	0.691	0.027	1.891	0.465
SCGB1D1	0.429	0.074	0.797	0.121	0.201	0.042	0.151	0.015
IGLC3	0.422	0.012	0.494	0.093	1.530	0.352	2.315	0.055
PROL1	0.412	0.047	0.276	0.071	0.092	0.007	0.034	0.015
PIGR	0.315	0.008	0.298	0.100	0.503	0.022	0.486	0.009
IGHA2	0.286	0.025	0.284	0.058	0.349	0.078	0.334	0.009
GSTP1	0.226	0.020	0.175	0.030	0.395	0.027	0.760	0.021
S100A8	0.199	0.046	0.186	0.035	0.403	0.093	0.662	0.021
ANXA1	0.196	0.038	0.107	0.025	0.286	0.003	0.486	0.063
ENO1	0.182	0.026	0.150	0.013	0.581	0.023	0.628	0.057
ZG16B	0.131	0.013	0.093	0.018	0.044	0.004	0.023	0.007
IGJ	0.124	0.005	0.098	0.040	0.141	0.015	0.135	0.005
LCN2	0.096	0.007	0.109	0.014	0.144	0.012	0.274	0.018
SERPINB1	0.093	0.002	0.040	0.007	0.184	0.020	0.367	0.020
HSPB1	0.091	0.021	0.053	0.008	0.153	0.014	0.110	0.017
ACTB	0.086	0.016	0.077	0.018	0.246	0.017	0.250	0.032
ALDH1A1	0.079	0.006	0.054	0.021	0.118	0.010	0.175	0.010
IGHG2	0.078	0.008	0.055	0.019	0.254	0.045	0.385	0.048
ORM1	0.077	0.015	0.040	0.005	0.296	0.027	0.276	0.025
SERPINA1	0.072	0.005	0.047	0.012	0.239	0.084	0.283	0.062
DMBT1	0.072	0.006	0.077	0.014	0.118	0.011	0.050	0.002
TCN1	0.071	0.009	0.044	0.008	0.056	0.018	0.023	0.004
ANXA2	0.061	0.003	0.041	0.010	0.173	0.016	0.297	0.025
TF	0.052	0.005	0.031	0.009	0.351	0.029	0.239	0.012
CLU	0.050	0.001	0.036	0.010	0.032	0.008	0.035	0.001
PRDX1	0.044	0.006	0.040	0.025	0.120	0.026	0.183	0.022
HP	0.041	0.001	0.021	0.005	0.165	0.012	0.127	0.022

Table 4.2: (continued)

	iBAQ values (%)							
	CTRL		DRYlip		DRYaq		DRYaqlip	
Gene names	Mean %	SD %	Mean %	SD %	Mean %	SD %	Mean %	SD %
YWHAZ	0.038	0.003	0.033	0.007	0.116	0.016	0.151	0.011
PEBP1	0.035	0.006	0.035	0.004	0.089	0.004	0.169	0.016
KRT1	0.031	0.002	0.015	0.004	0.081	0.015	0.025	0.004
S100A11	0.027	0.012	0.017	0.019	0.004	0.001	0.108	0.013
TPI1	0.025	0.004	0.022	0.006	0.080	0.027	0.143	0.019
UBB	0.021	0.002	0.021	0.003	0.009	0.001	0.072	0.024
CSTB	0.021	0.002	0.016	0.007	0.024	0.009	0.093	0.015
ORM2	0.019	0.003	0.007	0.002	0.057	0.013	0.052	0.008
PFN1	0.018	0.006	0.015	0.005	0.024	0.003	0.066	0.011
PGK1	0.015	0.003	0.021	0.012	0.068	0.009	0.068	0.010
TTR	0.015	0.010	0.015	0.008	0.038	0.010	0.041	0.014
C3	0.014	0.001	0.012	0.003	0.036	0.004	0.037	0.002
CTSB	0.014	0.001	0.009	0.002	0.011	0.001	0.005	0.002
AKR1C1	0.013	0.002	0.010	0.004	0.029	0.004	0.081	0.005
AKR1A1	0.012	0.001	0.007	0.001	0.037	0.006	0.056	0.002
PPIA	0.011	0.000	0.005	0.004	0.041	0.004	0.050	0.003
HSPA1A	0.010	0.001	0.007	0.001	0.021	0.001	0.027	0.001
TGM2	0.010	0.002	0.008	0.002	0.025	0.003	0.034	0.002
KRT10	0.010	0.001	0.005	0.001	0.115	0.012	0.012	0.004
GSN	0.009	0.000	0.008	0.003	0.025	0.009	0.021	0.004
FBP1	0.009	0.004	0.008	0.002	0.044	0.024	0.054	0.007
ALDOA	0.008	0.002	0.010	0.002	0.033	0.007	0.064	0.014
ALDH3A1	0.008	0.003	0.009	0.004	0.055	0.009	0.042	0.006
ANXA5	0.008	0.002	0.007	0.004	0.032	0.001	0.054	0.004
PKM	0.007	0.002	0.005	0.001	0.006	0.002	0.001	0.002
MDH1	0.007	0.002	0.007	0.002	0.020	0.003	0.027	0.000
GDI2	0.007	0.001	0.002	0.001	0.014	0.001	0.008	0.002
FABP5	0.006	0.003	0.008	0.001	0.025	0.007	0.048	0.005
PARK7	0.004	0.000	0.002	0.001	0.006	0.001	0.016	0.001
HSPG2	0.003	0.001	0.003	0.000	0.004	0.001	0.001	0.000
KRT9	0.003	0.001	0.001	0.000	0.002	0.000	0.002	0.000
GC	0.003	0.001	0.002	0.001	0.021	0.004	0.011	0.003
ANXA3	0.002	0.001	0.002	0.001	0.007	0.002	0.009	0.001
A2M	0.002	0.000	0.003	0.001	0.020	0.002	0.021	0.003
ASS1	0.001	0.000	0.001	0.000	0.004	0.000	0.003	0.001
RBP4	0.001	0.000	0.001	0.000	0.002	0.002	0.007	0.000
SFN	0.001	0.000	0.001	0.001	0.003	0.000	0.004	0.000
CFH	0.001	0.000	0.001	0.000	0.004	0.001	0.007	0.005
GLOD4	0.001	0.000	0.001	0.000	0.005	0.000	0.010	0.000
UBA1	0.001	0.001	0.001	0.000	0.004	0.000	0.003	0.000
IH4	0.001	0.000	0.001	0.000	0.005	0.001	0.005	0.000

The comprehensive gene ontology cellular compartments (GOCC), molecular functions (GOMF) and biological process (GOBP) analysis of the 77 differentially expressed proteins were manually curated from the Uniprot database, and listed in **Table 4.3**. The summary of the GOCC analysis of these proteins in DRYlip/CTRL, DRYaq/CTRL and DRYaqlip/CTRL are shown in **Figure 4.7**. In general, GOCC analysis of DRYlip/CTRL showed several of extracellular and cytoplasm proteins. Preponderance of extracellular region proteins were identified in DRYaq/CTRL (decrement of 12 proteins and increment of 18 proteins) and DRYaqlip/CTRL (decrement of 17 proteins and increment of 19 proteins). Remarkably, the differentially expressed proteins in the DRYaq/CTRL and DRYaqlip/CTRL groups showed a drastic increase in cytoplasmic proteins with ~23 proteins, compared to the decrease of 7 proteins. Notable increased of cell membrane, mitochondria and nucleus proteins compared to decreased proteins were also observed in the DRYaq/CTRL and DRYaqlip/CTRL groups.

The summary of the GOBP analysis of the significantly differentially expressed tear proteins in DRYlip/CTRL, DRYaq/CTRL and DRYaqlip/CTRL are shown in **Figure 4.8**. In general, GOBP analysis of these proteins in DRYlip/CTRL showed only several proteins associated with antibacterial, immune response, protease inhibitor and metabolic enzymes. High numbers of antibacterial proteins were identified in DRYaq/CTRL (decrement of 3 proteins and increment of 6 proteins) and DRYaqlip/CTRL (decrement of 7 proteins and increment of 7 proteins). Differentially expressed proteins in the DRYaq/CTRL and DRYaqlip/CTRL showed a drastic increase of metabolic enzymes with 14 proteins compared to decrease of ~6 proteins. Noteworthy increase of immune response and inflammatory response proteins compared to decreased proteins were also observed in DRYaq/CTRL and DRYaqlip/CTRL.

Table 4.3: Summary of the protein profiles in the current study and from the literatures search.
The GOCC, GOMF and GOBP analysis of the identified biomarkers were manually curated from the Uniprot database (http://www.uniprot.org/).

Gene names	Expression profiles in this study			iBAQ values	GOCC	GOMF & GOBP	Expression profiles from literatures	
	DRYlip/CTRL	DRYaq/CTRL	DRYaqlip/CTRL				Profiles	DES [Citations]
ALB	DOWN	UP	UP	Major	Extracellular region	Carrier/binding protein	UP	DRY_CL [48]
AZGP1	n.s	DOWN	DOWN	Major	Extracellular region	Zinc-binding/Lipid degradation/Cell adhesion	DOWN	DRYaq & DRYlip [107], DRY_MDE & DRY_MSDE [81]
CST4	n.s	n.s	DOWN	Major	Extracellular region	Cysteine protease inhibitor/Antimicrobial	DOWN	DRYlip [107], DRY_SS [78], DRY_MDE & DRY_MSDE [81]
ENO1	UP	UP	UP	Major	Cell membrane/ Cytoplasm/Membrane/Nucleus	Lyase/Repressor/Glycolysis/Plasminogen activation/Transcription regulation	UP	DRYaqlip [52]
GSTP1	n.s	UP	UP	Major	Cytoplasm/Mitochondrion/Nucleus	Transferase	UP	DRYaq & DRYlip [107]
IGHA1	UP	DOWN	DOWN	Major	Extracellular region	Antibacterial/Immune response	DOWN	DRY_SS [78], DRY_MSDE [81]
LACRT	n.s	DOWN	DOWN	Major	Extracellular region	Positive regulation of secretion/Prosecretory mitogen/collagen binding,	DOWN	DRY_CL [48], DRYaq, DRY_pSS, DRY_SJS & DRY_RA [7], DRY_SS [78], DRY_MDE & DRY_MSDE [81]
LTF	n.s	n.s	DOWN	Major	Extracellular region	Antimicrobial/Hydrolase/Serine protease	DOWN	DRYaq & SS [153]; DRYaqlip [52]; DRYaq, DRY_pSS, DRY_SJS & DRY_RA [7]; DRYaq [107], DRY_SS [78], DRY_MDE & DRY_MSDE [81]
LYZ	n.s	n.s	DOWN	Major	Extracellular region	Antimicrobial/Hydrolase	DOWN	DRYaqlip [6], DRY_SS [78], DRY_MDE & DRY_MSDE [81]
PIGR	n.s	UP	UP	Major	Cell membrane/ Membrane/Extracellular region	Immunoglobulin transcytosis in epithelial cells mediated by polymeric immunoglobulin receptor	DOWN	DRY_SS [78], DRY_MDE & DRY_MSDE [81]
PRR4	n.s	DOWN	DOWN	Major	Extracellular region	Unknown	DOWN	DRYaq [47]; DRY_CL [48]; DRY_pSS & DRY_SJS [8]; DRYaq, DRY_pSS, DRY_SJS & DRY_RA [7], DRYaq & DRYaqlip [106], DRY_SS [78], DRY_MDE & DRY_MSDE [81]
S100A8	n.s	UP	UP	Major	Cell membrane/Cytoplasm/Cytoskeleton/Membrane/Extracellular region	Antimicrobial/Apoptosis/Autophagy/Chemotaxis/Immunity/Inflammatory response/Innate immunity	UP	DRYaq [47], DRYaqlip [52], DRYaq & DRYaqlip [106], DRYaq & DRYlip [107], DRY_SS [78]

Table 4.3: (continued)

Gene names	Expression profiles in this study			iBAQ values	GOCC	GOMF & GOBP	Expression profiles from literatures	
	DRYlip/CTRL	DRYaq/CTRL	DRYaqlip/CTRL				Profiles	DES [Citations]
S100A9	n.s	UP	UP	Major	Cell membrane/ Cytoplasm/Cytoskeleton/Membrane/Extracellular region	Antimicrobial/Apoptosis/Autophagy/Chemotaxis/Immunity/Inflammatory response/Innate immunity	UP	DRYaqlip [52], DRYaq & DRYlip [107], DRY_SS [78]
SCGB1D1	UP	DOWN	DOWN	Major	Extracellular region	Protein heterodimerization activity/Androgen receptor signaling pathway	DOWN UP	DRY_CL [48], DRYaq & DRYaqlip [106], DRY_MDE & DRY_MSDE [81]
SCGB2A1	UP	n.s	DOWN	Major	Extracellular region	Protein heterodimerization activity/Androgen receptor signaling pathway	DOWN DOWN UP	DRYaq [107] DRY_MDE & DRY_MSDE [81] DRYaq & DRYaqlip [106],
ACTB	n.s	DOWN	DOWN	Minor	Cytoplasm/cytoskeleton	Motility/ATP-binding/Nucleotide-binding/Cell adhesion/Structure	DOWN UP	DRYaq & DRYlip [107] DRY_SS [78]
ALDH3A1	n.s	UP	UP	Minor	Cytoplasm	Oxidoreductase	UP	DRY_SS [78], DRY_MDE [81]
ANXA1	n.s	UP	UP	Minor	Cell membrane/Cell projection/Cytoplasm	Phospholipase A2 inhibitor	UP	DRYaq & DRYlip [107], DRY_SS [78]
ANXA2	DOWN	n.s	UP	Minor	Basement membrane/Extracellular matrix/Extracellular region	Calcium-dependent phospholipid binding	UP	DRY_SS [78]
ANXA5	n.s	UP	UP	Minor	Cytoplasm/External side of plasma membrane/Focal adhesion	Calcium-dependent phospholipid binding	DOWN	DRY_SS [78]
C3	n.s	UP	UP	Minor	Extracellular region	Immune/Inflammatory response	UP	DRY_SS [78], DRY_MDE [81]
CLU	n.s	DOWN	DOWN	Minor	Cytoplasm/Cytoplasmic vesicle/Endoplasmic reticulum/Membrane,/Microsome/Mitochondrion/Nucleus/Extracellular region	Cytoprotective/Misfolded protein binding/Chaperone/Anti-apoptotic/Immunity	UP	DRY_SS [78]
CSTB	DOWN	UP	UP	Minor	Cytoplasm/Nucleus	Cysteine-type endopeptidase inhibitor activity	DOWN	DRY_SS [78]
GC	n.s	UP	n.s	Minor	Extracellular region	Vitamin D-binding	UP	DRY_MSDE [81]
HP	DOWN	UP	n.s	Minor	Extracellular region	Antimicrobial/Hemoglobin binding	UP	DRY_MDE [81]
HSPA1A	n.s	DOWN	n.s	Minor	Cytoplasm	Chaperone/Host cell receptor for virus entry/Receptor/Stress response	UP	DRY_SS [78]
IGHA2	n.s	DOWN	DOWN	Minor	Extracellular region	Antibacterial/Immune response	DOWN	DRY_MSDE [81]

Table 4.3: (continued)

Gene names	Expression profiles in this study			iBAQ values	GOCC	GOMF & GOBP	Expression profiles from literatures	
	DRYlip/CTRL	DRYaq/CTRL	DRYaqlip/CTRL				Profiles	DES [Citations]
IGJ	n.s	n.s	DOWN	Minor	Extracellular region	Antibacterial/Immune response/IgA binding	DOWN	DRYaq, DRY_pSS, DRY_SJS & DRY_RA [7], DRY_MDE & DRY_MSDE [81]
KRT1	DOWN	DOWN	DOWN	Minor	Cytoskeletal intermediate filaments	Carbohydrate binding/Structural molecule activity	UP	DRY_SS [78]
KRT10	DOWN	n.s	DOWN	Minor	Cytoskeletal intermediate filaments	Structural constituent of epidermis/Keratinocyte differentiation	UP	DRY_SS [78]
ORM1	n.s	UP	UP	Minor	Extracellular region	Apparent modulator of acute-phase immune activity	UP	DRYaqlip [52], DRY_SS [78]
PRDX1	n.s	UP	UP	Minor	Cytoplasm	Antioxidant/Oxidoreductase/Peroxidase	UP	DRY_MSDE [81]
PROL1	n.s	DOWN	DOWN	Minor	Extracellular region	Protease inhibitor	DOWN	DRY_MSDE [81]
SERPINA1	DOWN	UP	n.s	Minor	Endoplasmic reticulum/Extracellular region	Serine protease inhibitor/Acute phase/Blood coagulation/ Hemostasis	UP	DRYaq [47], DRYaq & DRYaqlip [106]
TCN1	n.s	DOWN	DOWN	Minor		Cobalamin binding	DOWN	DRY_MDE [81]
TF	n.s	UP	UP	Minor	Extracellular region	Ferric iron binding and transport to proliferating cells	UP	DRY_SS [78]
ZG16B	DOWN	DOWN	DOWN	Minor	Extracellular region/Extracellular vesicular exosome	Unknown	DOWN	DRY_MSDE [81]
IGHG1	DOWN	UP	UP	Major	Extracellular region	Antibacterial/Immune response	New findings	
IGLC3	n.s	n.s	UP	Major	Extracellular region	Antibacterial/Immune response	New findings	
IGLL5	UP	n.s	n.s	Major	Extracellular region		New findings	
A2M	UP	UP	UP	Minor	Extracellular region	Protease inhibitor/Antimicrobial	New findings	
AKR1A1	DOWN	n.s	UP	Minor	Apical plasma membrane/Extracellular region	Oxidoreductase	New findings	
AKR1C1	n.s	UP	UP	Minor	Cytoplasm	Oxidoreductase	New findings	
ALDH1A1	n.s	DOWN	n.s	Minor	Cytoplasm	Oxidoreductase/Aldehyde dehydrogenase (NAD) activity	New findings	

Table 4.3: (continued)

Gene names	Expression profiles in this study			iBAQ values	GOCC	GOMF & GOBP	Expression profiles from literatures	
	DRYlip/CTRL	DRYaq/CTRL	DRYaqlip/CTRL				Profiles	DES [Citations]
ALDOA	n.s	n.s	UP	Minor	Cytoplasm	Lyase/Glycolysis	New findings	
ANXA3	n.s	UP	n.s	Minor	Cytoplasm/Extracellular vesicular exosome	Phospholipase A2 inhibitor	New findings	
ASS1	n.s	UP	n.s	Minor	Cytoplasm/Membrane/cytosol	Ligase/Amino-acid biosynthesis/ Arginine biosynthesis/Urea cycle	New findings	
CFH	n.s	UP	UP	Minor	Extracellular region	Heparan sulfate proteoglycan binding/Complement alternate pathway/Immunity	New findings	
CTSB	n.s	DOWN	DOWN	Minor	Lysosome/Extracellular region	Protease inhibitor/Antimicrobial	New findings	
DMBT1	n.s	DOWN	DOWN	Minor	Extracellular region/Cytoplasm	Protein transport/Scavenger receptor, binds surfactant protein D	New findings	
FABP5	n.s	UP	UP	Minor	Cytoplasm	Fatty acid binding/Epidermis development/ Response to wounding	New findings	
FBP1	n.s	UP	UP	Minor	Cytoplasm/cytosol/Extracellular vesicular exosome	Fructose 1,6-bisphosphate 1-phosphatase activity	New findings	
GDI2	DOWN	n.s	n.s	Minor	Cytoplasm/Membrane	GTPase activation	New findings	
GLOD4	n.s	UP	UP	Minor	Mitochondrion	Unknown	New findings	
GSN	n.s	UP	UP	Minor	Amyloid/Cytoplasm/Cytoskeleton/Extracellular region	Calcium ion binding/Actin filament polymerization	New findings	
HSPB1	DOWN	DOWN	DOWN	Minor	Cytoplasm/Cytoskeleton/Spindle	Chaperone/Stress response	New findings	
HSPG2	n.s	DOWN	DOWN	Minor	Basement membrane/Extracellular matrix/Extracellualr region	Carrier/growth factor binding/Metal-binding	New findings	
IGHG2	n.s	UP	UP	Minor	Extracellular region	Antibacterial/Immune response	New findings	
ITIH4	n.s	n.s	UP	Minor	Extracellular region	Endopeptidase inhibitor activity/Acute phase	New findings	
KRT9	DOWN	DOWN	DOWN	Minor		Structural constituent of epidermis/Keratinocyte differentiation	New findings	
LCN2	UP	n.s	n.s	Minor	Extracellular region	Iron ion binding/ Apoptosis/Immunity	New findings	

Table 4.3: (continued)

Gene names	Expression profiles in this study			iBAQ values	GOCC	GOMF & GOBP	Expression profiles from literatures	
	DRYlip/CTRL	DRYaq/CTRL	DRYaqlip/CTRL				Profiles	DES [Citations]
MDH1	n.s	UP	DOWN	Minor	Cytoplasm	Oxidoreductase/Tricarboxylic acid cycle	New findings	
ORM2	DOWN	UP	n.s	Minor	Extracellular region	Apparent modulator of acute-phase immune activity	New findings	
PARK7	n.s	UP	UP	Minor	Cell membrane/ Cytoplasm/ Membrane/Mitochondrion/Nucleus	Chaperone/Hydrolase/Protease/Autophagy/Fertilization/Inflammatory response/Stress response	New findings	
PEBP1	n.s	UP	UP	Minor	Cytoplasm	Serine protease inhibitor	New findings	
PFN1	n.s	UP	UP	Minor	Cytoplasm/Cytoskeleton	Proline-rich region binding/Actin binding	New findings	
PGK1	n.s	UP	DOWN	Minor	Cytoplasm	Kinase/Transferase/Glycolysis	New findings	
PKM	n.s	DOWN	DOWN	Minor	Cytoplasm/Nucleus	Kinase/Transferase/Glycolysis	New findings	
PPIA	n.s	UP	UP	Minor	Cytoplasm/Extracellular region	Accelerate the folding of protein/Catalyzes the cis-trans isomerization of proline imidic peptide bonds in oligopeptides/Rotamase/Host-virus interaction/Peptide binding	New findings	
RBP4	n.s	n.s	UP	Minor	Extracellular region	Retinol transporter activity	New findings	
S100A11	n.s	DOWN	UP	Minor	Cytoplasm/Nucleus	Calcium-dependent protein binding	New findings	
SERPINB1	DOWN	n.s	UP	Minor	Cytoplasm	Serine-type endopeptidase inhibitor activity/ Antimicrobial	New findings	
SFN	n.s	UP	UP	Minor	Cytoplasm/Nucleus/Extracellular region	Protein kinase C inhibitor activity/Apoptotic process	New findings	
TGM2	n.s	n.s	UP	Minor	Cytosol/Focal adhesion/Plasma membrane/Exctracellualr vesicular exosome/Mitochondria	Acyltransferase/Transferase/Protein-glutamine gamma-glutamyltransferase activity	New findings	
TPI1	n.s	n.s	UP	Minor	Cytosol/Extracellular vesicular exosome/Extracellular space	Triose-phosphate isomerase activity/ Gluconeogenesis/Glycolysis/Pentose shunt	New findings	
TTR	n.s	UP	n.s	Minor	Amyloid/Cytoplasm/Extracellular region	Thyroid hormone-binding	New findings	

Table 4.3: (continued)

Gene names	Expression profiles in this study			iBAQ values	GOCC	GOMF & GOBP	Expression profiles from literatures	
	DRYlip/CTRL	DRYaq/CTRL	DRYaqlip/CTRL				Profiles	DES [Citations]
UBA1	n.s	n.s	UP	Minor	Cytoplasm/Mitochondrion/Nucleus	Ubiquitin conjugation pathway/ ATP-binding/Nucleotide-binding	New findings	
UBB	n.s	n.s	UP	Minor	Cytoplasm/Nucleus	Activation of MAPK activity	New findings	
YWHAZ	n.s	n.s	UP	Minor	Cytoplasm	Binds to a large number of partners, usually by recognition of a phosphoserine or phosphothreonine motif	New findings	

Note: The abbreviations used in this table are as follows; Sjögren syndrome (SS), contact lens-related dry eye (DRY_CL), dry eye associated with Sjogren's syndrome (DRY_SS), dry eye associated with Stevens-Johnson syndrome (DRY_SJS), dry eye associated with rheumatoid arthritis (DRY_RA), mildly symptomatic with aqueous deficiency (DRY_MDE) and symptomatic aqueous deficiency (DRY_MSDE), non-significant (n.s).

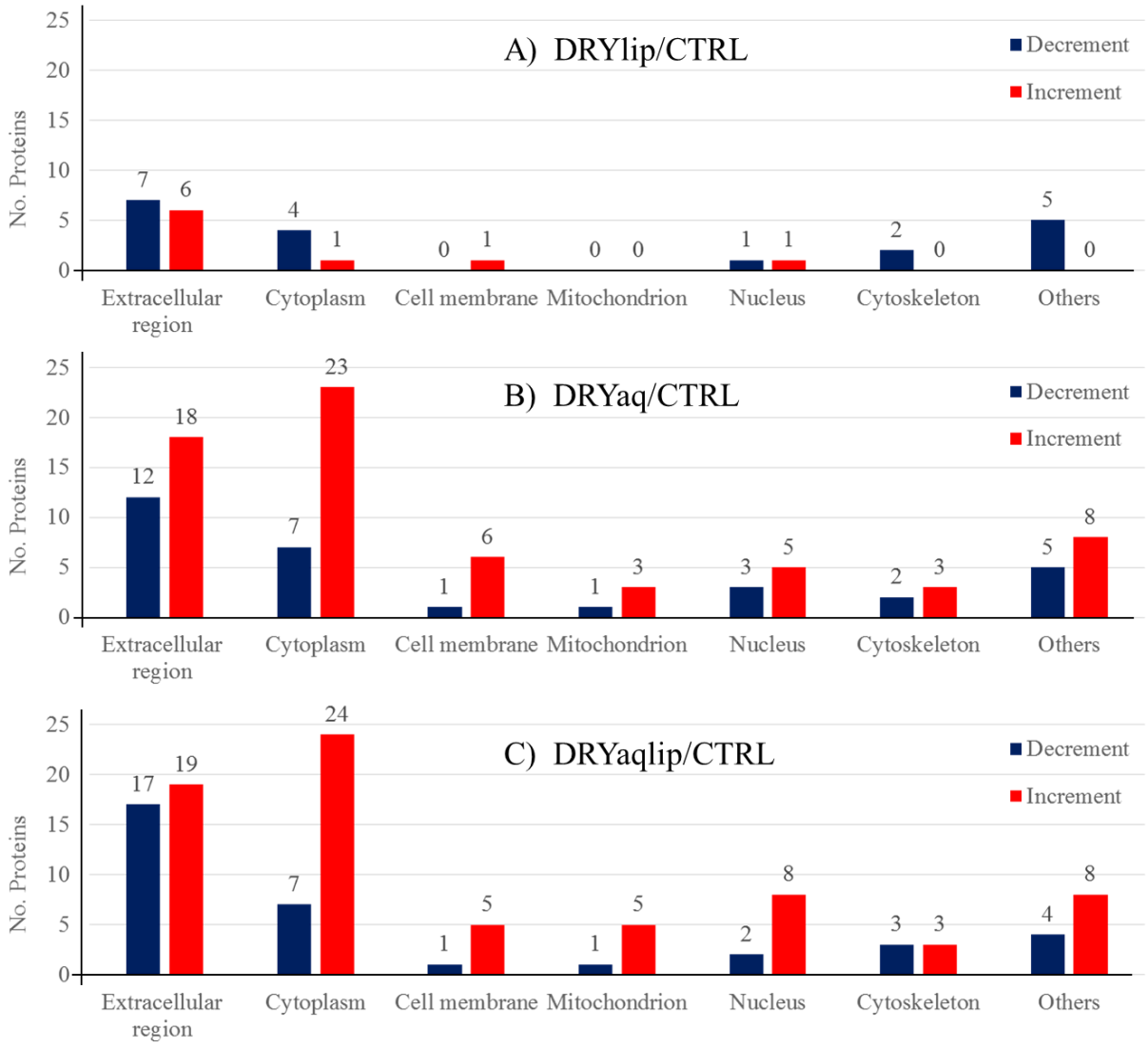

Figure 4.7: Gene ontology cellular components (GOCC) analysis of the significantly differentially expressed tear proteins in (A) DRYlip/CTRL, (B) DRYaq/CTRL and (C)DRYaqlip/CTRL.

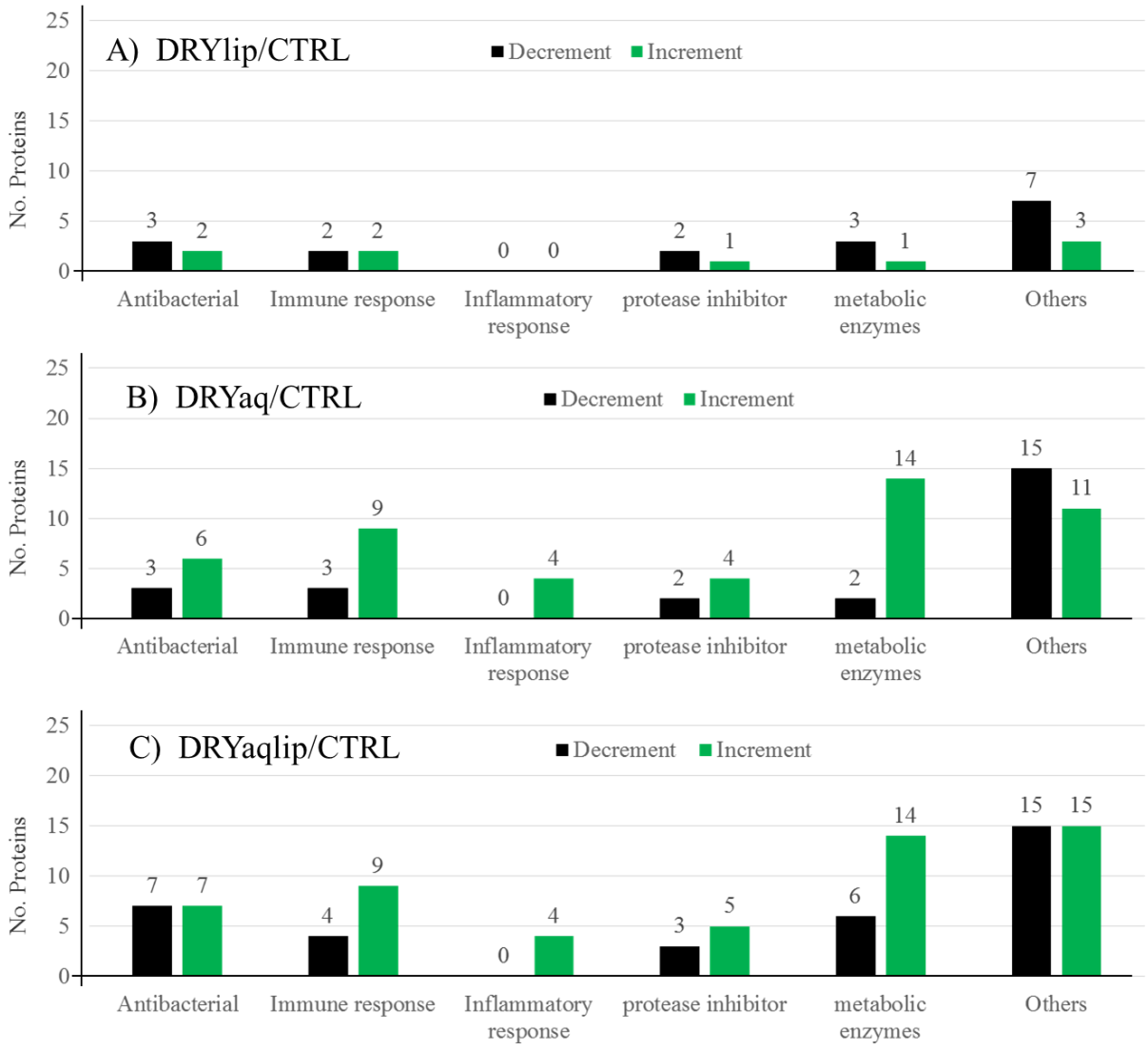

Figure 4.8: Gene ontology biological process (GOBP) analysis of the significantly differentially expressed tear proteins in (A) DRYlip/CTRL, (B) DRYaq/CTRL and (C) DRYaqlip/CTRL.

Finally, a rapid and robust approach *via* in-solution digestion of the pooled tear samples and AIMS analysis have been successfully utilized to further verify some of the major differentially expressed tear proteins in DES subgroups compared to the CTRL group. **Table 4.4** shows the detailed AIMS analysis of the signature peptides based on representative precursor ions for specific proteins. This analysis ascertained the differentially expressed profiles of 13 proteins in DES subgroups compared to CTRL that comprises PRR4, zymogen granule protein 16 homolog B (ZG16B), SCGB2A1, deleted in malignant brain tumors 1 protein (DMBT1), proline-rich protein 1 (PROL1), LACRT, aldehyde dehydrogenase, dimeric NADP-preferring (ALDH3A1), alpha-enolase (ENO1), TF, S100A8, S100A9, phosphatidylethanolamine-binding protein 1 (PEBP1) and alpha-1-acid glycoprotein 1 (ORM1). **Figure 4.9** shows the profiles of selected proteins differentially expressed in DRY subgroups compared to CTRL. Two signature peptides for PRR4 were utilized in the AIMS analysis because these two peptides are essential for exact identification and quantification of this protein.

Table 4.4: Summary of the differentially expressed proteins in DES subgroups compared to CTRL tears employing AIMS strategy.

Gene names	Peptides [AA-sequences]	m/z [Da]	Charge [+]	MZ + [Da]	Score	Two samples t-test; (*Significant P< 0.05)					
						DRYlip/CTRL		DRYaq/CTRL		DRYaqlip/CTRL	
						Significant	p value	Significant	p value	Significant	p value
PRR4	FPSVSLQEASSFFQR	865.43	2	1728.85	344	decrement	0.0004	decrement	0.0000	decrement	0.0000
	FPSVSLQEASSFFR	801.40	2	1600.79	340						
ZG16B	YFSTTEDYDHEITGLR	973.94	2	1945.87	127	decrement	0.0016	decrement	0.0000	decrement	0.0000
SCGB2A1	TINSDISIPEYK	690.35	2	1378.70	197	n.s	0.0588	decrement	0.0008	decrement	0.0000
DMBT1	FGQGSGPIVLDDVR	730.38	2	1458.75	187	n.s	0.1682	decrement	0.0228	decrement	0.0000
PROL1	FSQAVILSQLFPLESIR	974.55	2	1947.08	200	decrement	0.0081	decrement	0.0001	decrement	0.0000
LACRT	SILLTEQALAK	593.85	2	1185.70	255	n.s	0.3401	n.s	0.0521	decrement	0.0436
ALDH3A1	SLEEAIQFINQR	724.38	2	1446.75	135	n.s	0.1853	n.s	0.3497	increment	0.0083
ENO1	GNPTVEVDLFTSK	703.86	2	1405.71	155	n.s	0.2672	increment	0.0256	increment	0.0037
TF	HSTIFENLANK	637.33	2	1272.65	84	n.s	0.3587	increment	0.0000	increment	0.0000
S100A8	ALNSIIDVYHK	636.85	2	1271.69	142	increment	0.0229	increment	0.0004	increment	0.0000
PEBP1	GNDISSGTVLSDYVGS GPPK	975.48	2	1948.94	98	n.s	0.7171	increment	0.0007	increment	0.0000
ORM1	YVGGQEHFAHLLILR	876.98	2	1751.95	127	n.s	0.4548	increment	0.0004	increment	0.0000
S100A9	NIETIINTFHQYSVK	903.97	2	1805.93	342	increment	0.0001	increment	0.0000	increment	0.0000

Note: non-significant (n.s).

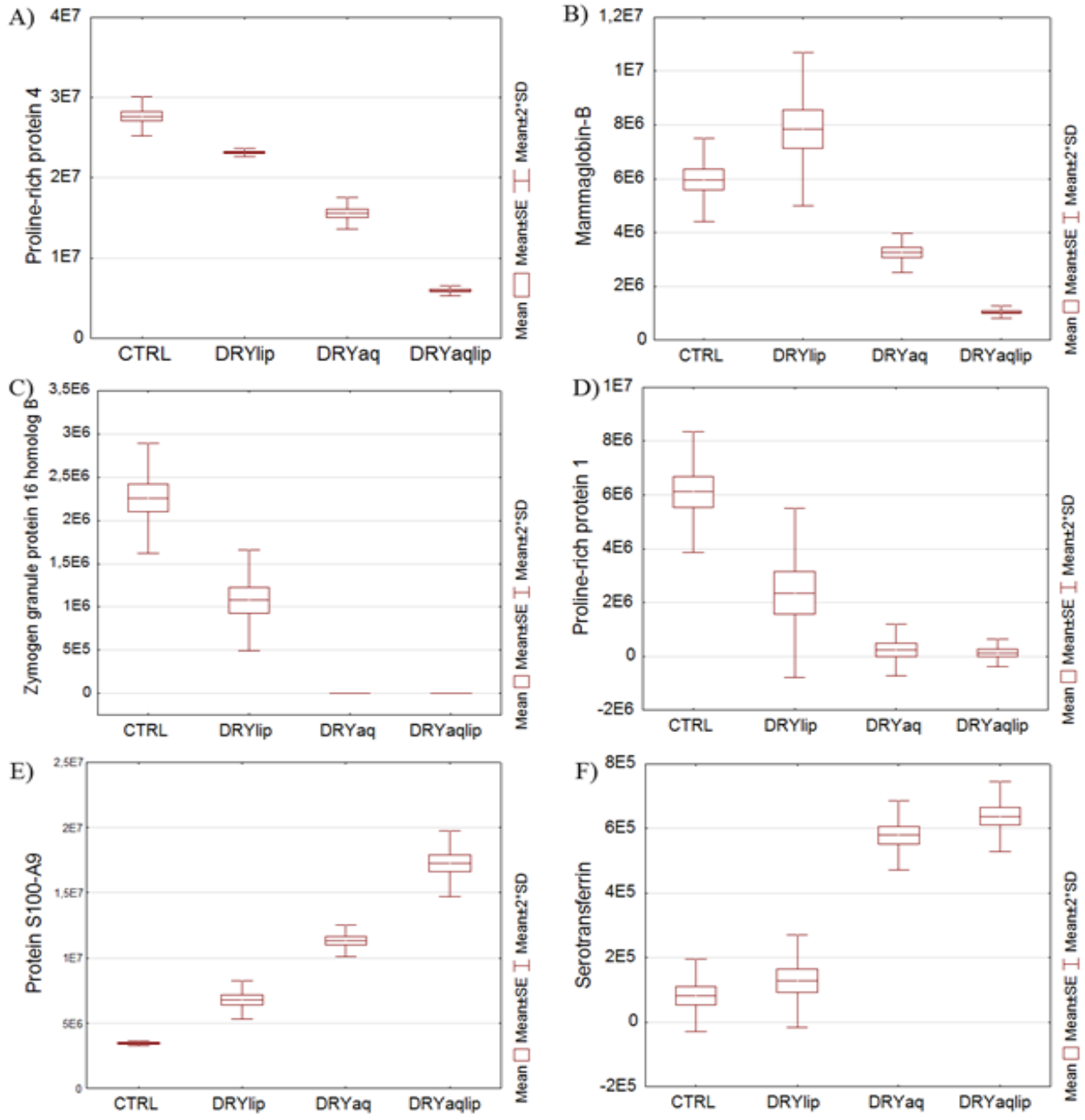

Figure 4.9: Box plots show some of the differentially expressed proteins profiles between DES subgroups and control after AIMS analysis.

(A) PRR4 (B) SCGB2A1 (C) ZG16B (D) PRP1 (E) S100A9 and (F) TF. The *y*-axis represents the mean absolute intensities of the signature peptides of 4 independent experiments of pooled tear samples (N=20) from each groups. Boxes represent the ME ± SE, rectangles the ME ± SD. *p<0.05, significance compared with CTRL.

4.2 Characterization of human reflex tear proteome in healthy subjects

The representative protein profiles of basal and reflex tears resolved in 1DE gel are depicted in **Figure 4.10**. This gel shows the distribution of the most abundant proteins in the basal and reflex tears. It is noteworthy that band four in the gel, which predominantly represent IGHA1, showed a high band intensity in the basal tears and was almost absent in the reflex tear samples. Bands six and seven represent to a large extent two distinct with slightly diffuse profiles of PRR4 which showed relatively more intense smearing profiles in basal tears than in the reflex tears. In addition, differences were also observed at band eight and band ten; these bands highly represent LCN1 and SCGB2A1, respectively. A total of 54 proteins were detected by the discovery strategy as presented in **Appendix 1.** In order to reveal the differentially expressed proteins in the reflex tears compared to basal tears, LFQ values of the identified proteins extracted from MaxQuant analysis were employed for statistical analysis utilizing the Perseus software. A subset of 15 proteins was found to be differentially expressed in reflex tears compared to basal tears as tabulated in **Table 4.5**. The reflex tear proteome showed increased abundance in PRR4, ZG16B, ALB, LACRT, LCN1 and mesothelin (MSLN). On the contrary, decreased abundance in PIGR, IGHA1, Ig alpha-2 chain C region (IGHA2), SCGB2A1, Ig kappa chain C region (IGKC), Ig lambda-1 chain C regions, Ig lambda-3 chain C regions, IgJ and clusterin (CLU) were showed. Other abundant proteins e.g. LTF, LYZ, AZGP1 and PIP remained constant**.**

Analysis of the basal and reflex tear proteomes employing 2DE and LC-ESI-MS/MS with Ludesi REDFIN 3 and ImageJ softwares demonstrated only few noteworthy differentially expressed proteins spots, as illustrated in **Figure 4.11**. The majority of tear proteins visualized in the 2DE gels appear as large protein spots reflecting their high level of expression of the abundant proteins. The 2DE gels analysis revealed distinctly different patterns of acidic PRR4 entities specific to basal and reflex tears. The most notable differences were found to be the PRR4 spots [*a* to *c* (M_r/ pI: 28 - 30 kDa/ 3.0 - 3.5) and *d* to *g* (M_r/ pI: 24 - 25 kDa/ 4.7 - 5.4), as shown in **Figure 4.11.** Increased abundance of highly acidic PRR4 spots (*a, b* and *c*) and decreased abundance of the less acidic PRR4 spots (*d* to *g*) were clearly depicted in the 3D visualization, as presented in **Figure 4.11D and E**. The relative intensities profile of the PRR4 spots for reflex tears compared to the basal tears are tabulated in the **Table 4.6**. This expression pattern of PRR4 spots in 2DE gels corroborates with the expression profiles in 1DE, where the highly acidic PRR4 spots (*a, b* and *c*)

represent largely band 6 and the less acidic PRR4 spots (*d* to *g*) represent band 7. Correspondingly, increased abundance of highly acidic PRR4 spots compared to less acidic PRR4 spots in reflex tears resulted in more intense smearing profile in the 1DE gel (**Figure 4.10**). The plausible reason for why highly acidic PRR4 spots failed to resolve into discrete bands/ spots in the 1DE/2DE gels is because of the limitation of the gel electrophoresis method to resolve proteins that are too acidic **[154]**. The other differentially expressed proteins observed in the 2DE gels were IGHA1 (S2), CST4 (S6), SCGB2A1 (S7) and ALB (S8) as tabulated in **Table 4.6.** Abundant protein spots of LTF (S1), AZGP1 (S3), LCN1 (S4) and LYZ (S5) were non-significantly regulated.

In addition, a rapid and robust approach employing in-solution digestion of the individual tear samples and AIMS strategy have been utilized to further confirm the significant differences in the proteins expression level in reflex tears. **Table 4.7** shows the detailed analysis of the selected peptides based on the representative precursor ions for basal and reflex tear. Overall, this analysis ascertained the increased abundance of three proteins; PRR4, ZG16B and ALB, decreased abundance of five proteins; IGHA1, PIGR, CLU, CST4/ CST1 and SCGB2A1, and the four not differentially expressed abundant proteins; LTF, PIP, LCN1 and LYZ. **Figure 4.12** represents the box plots for four of the proteins profiles in reflex and basal tear samples, which are the PRR4, ZG16B, IGHA1 and PIGR. For PRR4, signature peptide of FPSVSLQEASSFFR at *m/z* 1601.80 (maximum ion score of 124) was chosen instead of QLSLPR at *m/z* 703.43 (maximum ion score of 47) for quantification analysis because the precursor ion could be detected with very high intensity and identified with high ion scores **[139]**. The summary of the differentially expressed proteins in reflex tears compared to basal tears employing the label-free MS strategies were tabulated in **Table 4.8**. Although the discovery study identified 15 proteins to be differentially expressed in the reflex tears, only six proteins, PRR4, IGHA1, SCGB2A1, ALB, LTF and LYZ, demonstrated similar expression levels in the verifications studies. The limitation of the 2DE analysis of the tear proteins is that the 2DE gels are not suitable to determine the expression levels of the low abundant proteins. Hence, the AIMS approach was instrumental to verify the additional four proteins; PIGR, ZG16B, CLU and PIP.

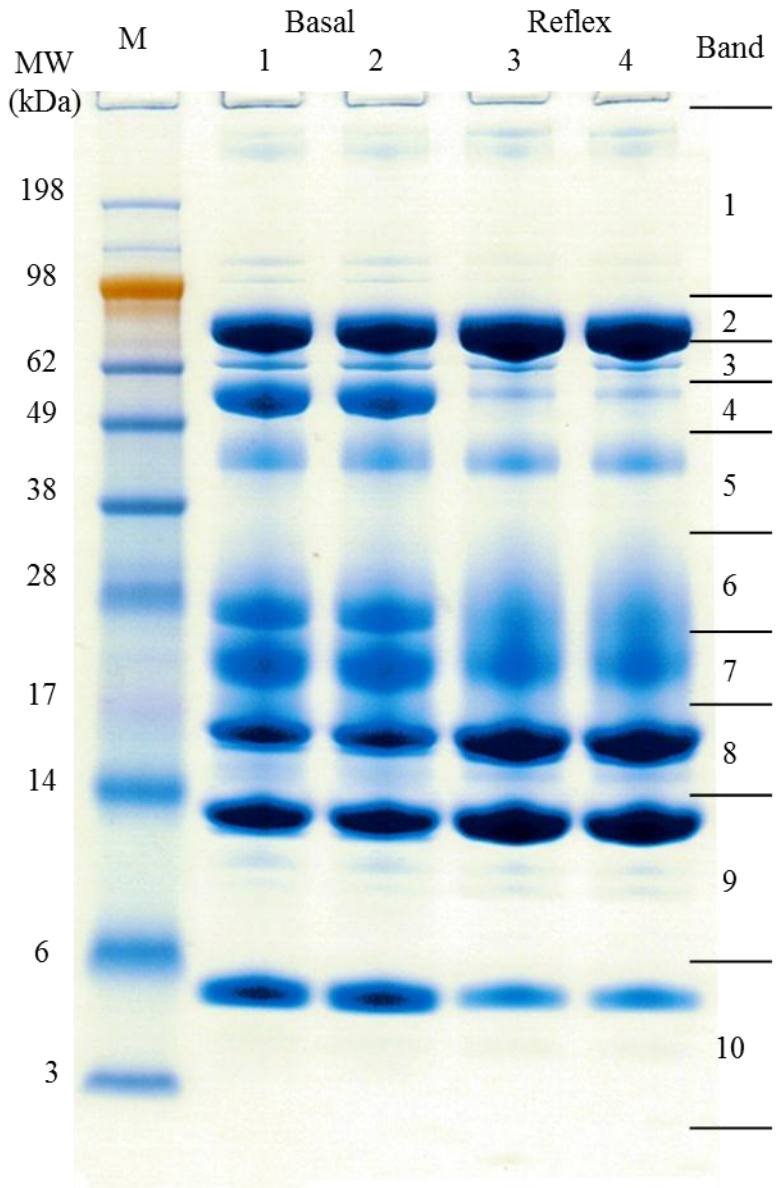

Figure 4.10: Representative basal and reflex tear protein profiles resolved in 1DE gel after colloidal blue staining.

Notable differences between basal and reflex tears were observed at band four, six, seven, eight and ten.

Table 4.5: Summary of the differentially expressed proteins in reflex tears compared to basal tears employing 1DE and LC-ESI-MS/MS strategy.

Gene names	Razor + unique peptides	Unique + razor sequence coverage [%]	Mol. weight [kDa]	Sequence length	t-test difference	t-test P values	P values <0.05
ZG16B	4	26.0	22.7	208	-1.570	0.00007	Increment
LCN1	12	67.0	19.3	176	-0.550	0.00066	Increment
ALB	28	48.4	69.4	609	-1.943	0.00332	Increment
PRR4	2	10.4	15.1	134	-0.808	0.00626	Increment
LACRT	6	35.5	14.2	138	-0.958	0.00952	Increment
MSLN	12	23.0	69.0	630	-0.400	0.01642	Increment
PIGR	24	34.0	83.3	764	3.953	0.00004	Decrement
IGLL5	6	35.0	23.1	214	1.260	0.00026	Decrement
IGKC	6	80.2	11.6	106	1.703	0.00089	Decrement
IGHA2	3	22.1	36.5	340	2.318	0.00106	Decrement
SCGB2A1	6	51.6	10.9	95	1.786	0.00118	Decrement
IGLC3	2	27.4	11.2	106	1.071	0.00169	Decrement
IGJ	3	23.3	18.1	159	1.382	0.00221	Decrement
IGHA1	14	53.5	37.7	353	0.670	0.01420	Decrement
CLU	6	16.3	52.5	449	0.941	0.04528	Decrement

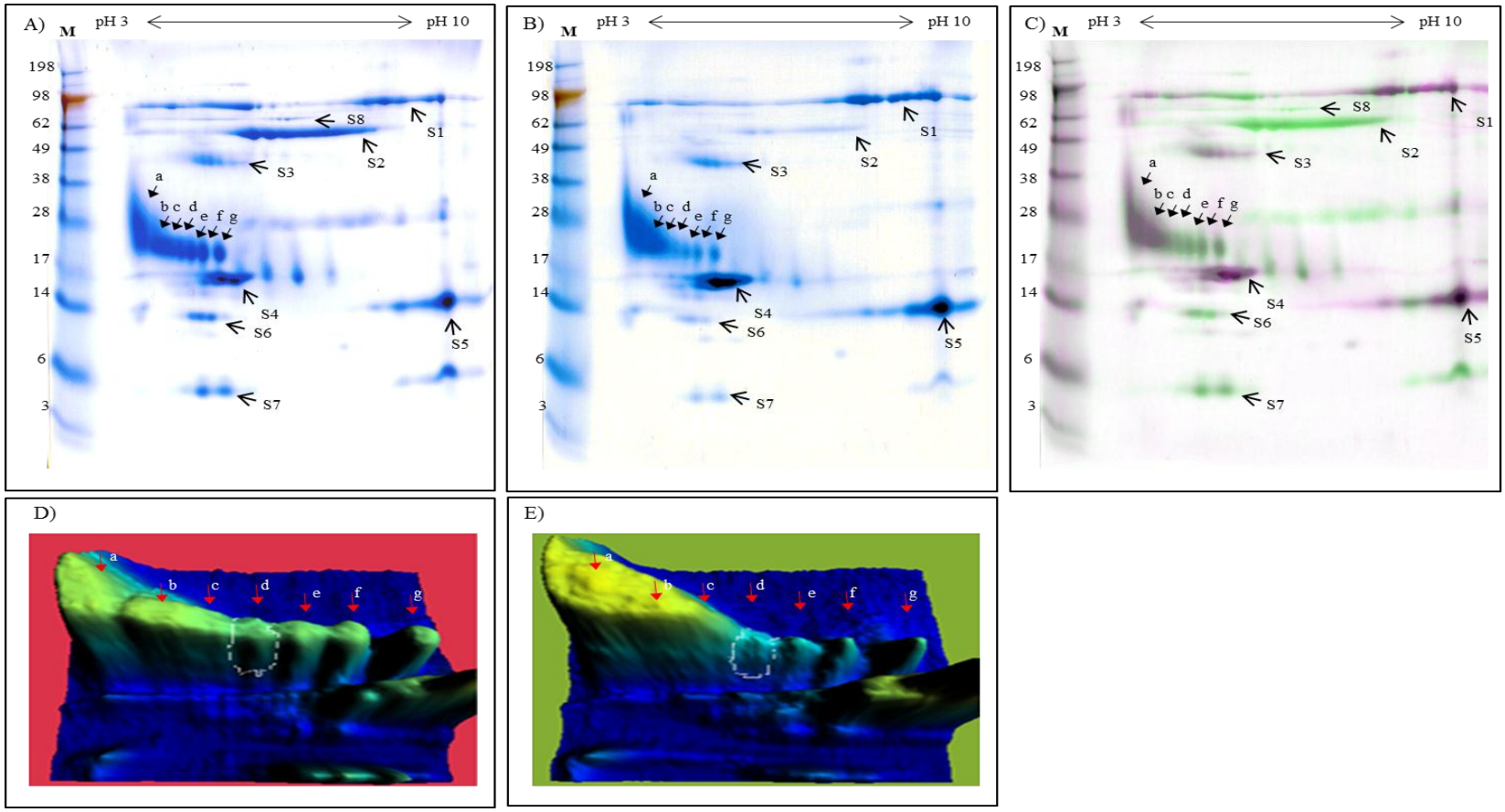

Figure 4.11: 2DE & LC-ESI-MS/MS analysis of the basal and reflex tear proteome

A) 2DE gel of the basal tears illustrates the seven abundant proteins (S1- S7) and seven PRR4 spots (*a* to *g*). B) 2DE gel of reflex tears shows notable increased abundance of PRR4 highly acidic spots (*a* to *c*) and decreased abundance of IGHA1 spot (S2) compared to basal tears. C) 2DE gels analyzed with Ludesi REDFIN software shows the decrement of less acidic PRR4 spots (*d* to *g*), IGHA1 (S2), CST4 (S6) and SCGB2A1 (S7) as green spots. D) 3D view of PRR4 spots (*a* to *g*) in basal tears. E) 3D view of PRR4 spots (*a* to *g*) in reflex tears which shows sharp increment of highly acidic spots (*a* to *c*) and decrement of less acidic spots (*d* to *i*) compared to basal tears.

Table 4.6: Summary of the differentially expressed proteins in reflex tears compared to basal tears employing 2DE and LC-ESI-MS/MS strategy.

Spot(s)	Gene names	Basal Intensity		Reflex Intensity		t-test difference	t-test P values	P values <0.05
		Mean	SD	Mean	SD			
S8	ALB	12861	4974	38807	1211	-8.7791	0.0009	Increment
a, b, c	PRR4	73690	17025	133814	21596	-3.7868	0.0193	Increment
S4	LCN1	62984	9473	78288	7479	-2.1964	0.0930	Non-significant
S1	LTF	77425	18205	91894	13775	-1.0977	0.3340	Non-significant
S5	LYZ	28885	2500	29128	1536	-0.1431	0.8931	Non-significant
d, e, f, g	PRR4	141576	22256	91120	6815	3.7546	0.0199	Decrement
S6	CST4	40215	4495	21317	6263	4.2458	0.0132	Decrement
S7	SCGB2A1	33765	3670	17124	5292	4.4755	0.0110	Decrement
S2	IGHA1	101326	9429	24003	6417	11.7422	0.0003	Decrement

Table 4.7: Summary of the differentially expressed proteins in reflex tears compared to basal tears employing AIMS strategy.

Gene names	Max. Mascot Score	*m/z* [Da]	MH+[Da]	Charge [+]	Max. IonScore	Peptides [AA-sequences]	[AA-position]	t-test difference	t-test P values	P values <0.05
PRR4	6916	801.40	1601.80	2	124	FPSVSLQEASSFFR	107-120	0.0120	-3.231	Increment
ZG16B	3327	973.94	1946.88	2	99	YFSTTEDYDHEITGLR	63-78	0.0018	-4.600	Increment
ALB	565	756.42	1511.84	2	79	VPQVSTPTLVEVSR	59-72	0.0000	-14.812	Increment
PIGR	3587	625.84	1250.67	2	104	DGSFSVVITGLR	115-126	0.0000	21.077	Decrement
IGHA1	1489	770.86	1540.73	2	99	DASGVTFTWTPSSGK	154-168	0.0000	9.079	Decrement
CLU	471	937.50	1873.99	2	72	LFDSDPITVTVPVEVSR	183-194	0.0058	3.734	Decrement
CST4	14670	982.46	1963.92	2	141	EQTFGGVNYFFDVEVGR	75-91	0.0176	2.979	Decrement
CST1	998	957.97	1914.94	2	117	QQTVGGVNYFFDVEVGR	75-91	0.0464	2.354	Decrement
SCGB2A1	2680	690.35	1379.70	2	93	TINSDISIPEYK	32-43	0.0047	3.876	Decrement
LTF	6008	768.92	1536.84	2	110	YLGPQYVAGITNLK	111-124	0.0526	-2.273	Non-significant
PIP	4050	907.98	1814.97	2	103	TYLISSIPLQGAFNYK	70-85	0.4333	-0.825	Non-significant
LCN1	3134	661.31	1321.63	2	73	NNLEALEDFEK	140-150	0.2842	1.148	Non-significant
LYZ	7133	700.84	1400.68	2	99	STDYGIFQINSR	69-80	0.6721	-0.439	Non-significant

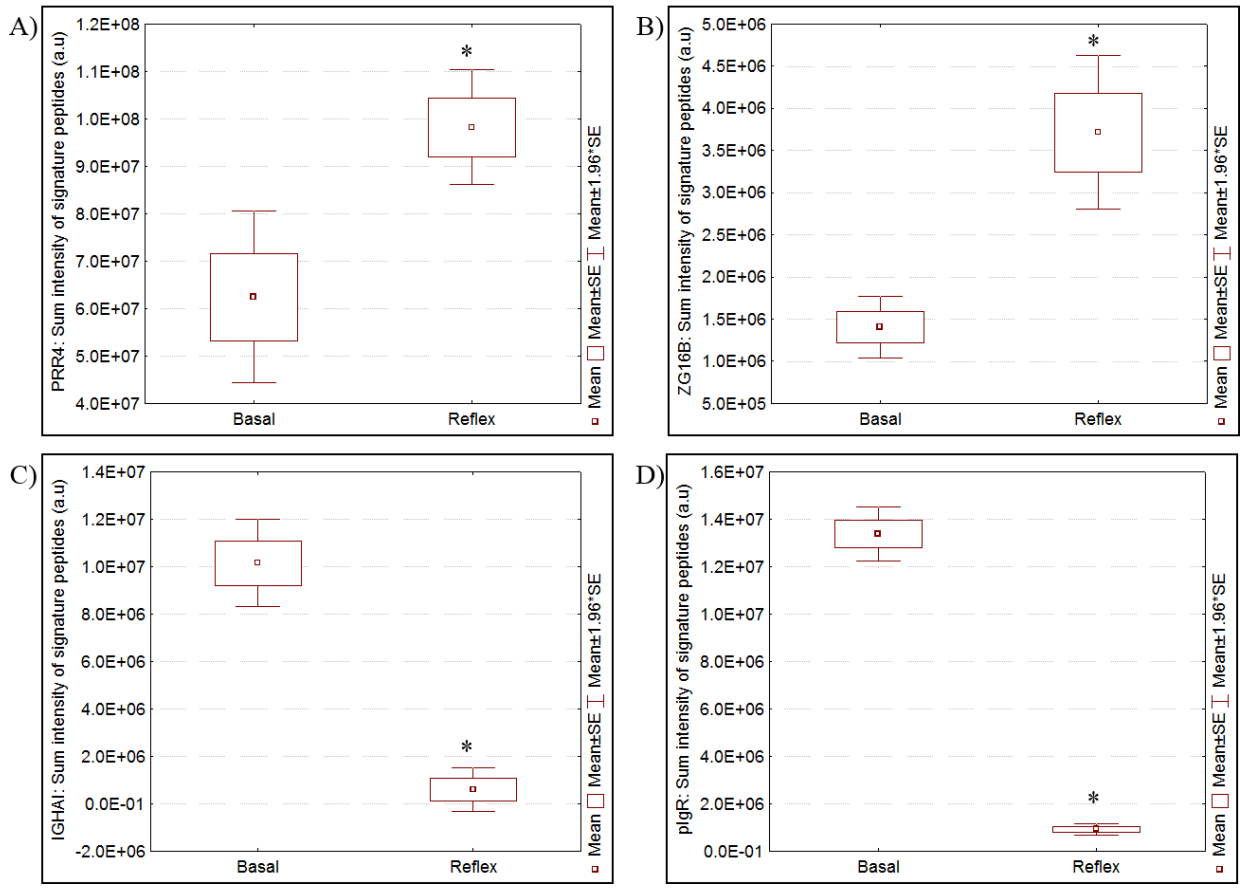

Figure 4.12: Box plots show some of the differentially expressed protein profiles in reflex tears compared to basal tears after AIMS analysis

A) PRR4, B) ZG16B, C) IGHAI and D) PIGR. The *y*-axis represents the mean absolute intensities of the signature peptides of 5 biological experiments. Boxes represent the ME ± SE, rectangles the ME ± SD. *$p<0.05$, significance compared with basal.

Table 4.8: Summary of the differentially expressed proteins in reflex tears compared to basal tears employing the label-free MS strategies

Gene names	Proteins	1DE & LC-ESI-MS/MS	2DE & LC-ESI-MS/MS	AIMS
IGHA1	Ig alpha-1 chain C region	Decrement	Decrement	Decrement
SCGB2A1	Mammaglobin-B	Decrement	Decrement	Decrement
CST4	Cystatin-S	Non-significant	Decrement	Decrement
PRR4	Proline-rich protein 4	Increment	Increment	Increment
ALB	Serum albumin	Increment	Increment	Increment
LCN1	Lipocalin-1	Increment	Non-significant	Non-significant
LTF	Lactotransferrin	Non-significant	Non-significant	Non-significant
LYZ	Lysozyme C	Non-significant	Non-significant	Non-significant
PIGR	Polymeric immunoglobulin receptor	Decrement	-	Decrement
CLU	Clusterin	Decrement	-	Decrement
CST1	Cystatin-SN	Non-significant	-	Decrement
ZG16B	Zymogen granule protein 16 homolog B	Increment	-	Increment
PIP	Prolactin-inducible protein	Non-significant	-	Non-significant

4.3 Characterization of Lacrimal Proline-Rich Protein 4 (PRR4) in Human Tear Proteome

The PRR4-rich region in tear fluid (bands seven and eight) was identified in 1DE gel based on the specific signal peaks after LC-MALDI-MS/MS and LC-ESI-MS/MS analysis, as shown in **Figure 4.13.** Two PRR4 isoforms were found from the approximately 200 proteins identified in the pooled tear samples from SwissProt and NCBI databases. Very high intensity signal peaks corresponding to PRR4 (SwissProt: Q16378, NCBI: gi/ 154448886) were detected at *m/z* 1729.84 (ion score 127) and *m/z* 1792.95 (ion score 63) after LC-MALDI-MS/MS analysis, as shown as overlaid MS spectrum of band 8 in **Figure 4.13B**. Additionally, pHL E1F1 (NCBI: gi/1050983), an annotated hypothetical conserved protein related to PRR4, was also identified based on the high intensity signal peaks at *m/z* 1601.84 (ion score 127) and *m/z* 1921.10 (ion score 60). Similarly, two PRR4 isoforms were also identified based on the signal peaks at *m/z* 1601.80 (ion score 124), *m/z* 1729.86 (ion score 119), *m/z* 1792.94 (ion score 36) and *m/z* 1920.99 (ion score 59) after LC-ESI-MS/MS analysis, as shown in **Figure 4.13C**. In general, high intensity signal peaks at *m/z* 1601.8 and *m/z* 1729.8 were easily identified employing the LC-MALDI-MS/MS and LC-ESI-MS/MS methods with high ion scores. However, high intensity peaks at *m/z* 1792.9 and *m/z* 1920.9 shown in **Figure 4.13B** yielded low ion scores for both methods and were poorly identified, as shown in **Figure 4.13C**.

Proline-rich protein 4 in pooled tear samples was further detected in 2DE employing the MALDI-MS/MS and LC-ESI-MS/MS. As a result, 10 PRR4 spots (S1 to S10) with vast polymorphisms were identified in 2DE gel, as illustrated in **Figure 4.14A,** which corresponded to the PRR4-rich region in the 1DE shown in **Figure 4.13A**. The PRR4 isoforms spots were identified in the 2DE gel as S1 to S5 with a train of five spots (M_r/ pI: 24 - 25 kDa/ 4.7 - 5.4), S6 to S7 with broad smearing pattern (M_r/ pI: 28 - 30 kDa/ 3.0 - 3.5), and S8 to S10 (M_r/ pI: 17.7 - 20.0 kDa/ 6.0 - 6.6). Manual inspection of these spots by MALDI-MS analysis showed that each spot predominantly consists of signal peaks at *m/z* 1601.8, 1729.9, 1792.9 and 1921.0 for PRR4 isoforms with total intensity between 70 - 87 % for these spectra per spot as shown in **Figure 4.14B**. The detailed characteristics of the identified PRR4 isoforms are tabulated in **Table 4.9**. After searching the continuum tandem MS data generated from PRR4 spots employing LC-ESI-MS/MS, four types of biological modifications were identified, which are methylation, oxidation, acetylation and

pyroglutamate formation. Besides, one artificial modification of sodium adduct formation on glutamic acid (E) at positions 114 and 130 were identified. The summary of all the identified PTMs in PRR4 isoforms spots in 2DE are presented in **Table 4.9**. The O-methylation of PRR4 isoforms occurred on glutamic acid (E) at positions 52, 114 and 130. The CID spectrum of unmodified and methylated peptides FPSVSLQE$^{\#}$ASSFFR shown in **Figure 4.15** identified the precise methylated amino acid residue by matched fragmented *b*-ions and *y*-ions from the peptides. The oxidation occurred on tryptophan (W) at position 134, pyroglutamate formation occurred on glutamine (Q) at position 101 and acetylation occurred on aspartic acid (D) at position 43 and 122 in the PRR4 isoforms. Generally, most of the aforementioned PTMs were detected in the acidic spots especially at S6 and S7. The unmodified counterparts of all the modified peptides were also identified from each spot, as tabulated in **Table 4.9**, indicating that the PRR4 isoforms are a heterogeneous mixture in each spot, which could have possibly resulted in smear regions around these spots.

The determination of PRR4 isoforms distribution among 61 volunteers was carried out by individual sample analysis based on the identified PRR4 rich-region (**Figure 4.13A)** after trypsin digestion and direct MALDI-MS analysis without fractionation. In parallel, a rapid and robust approach employing in-solution digestion has been successfully utilized to determine the PRR4 isoforms of tear samples and analyzed individually by targeted data acquisition approach utilizing LC-ESI-MS/MS system. Only the unmodified PRR4 isoforms signature peptides (**Table 4.9)** were selected and assigned into the global parent mass list for this targeted data acquisition approach. This is because the modified peptides were relatively very low in abundance compared to the unmodified peptides to be identified in the crude tears samples. **Table 4.10** shows the detailed characteristics of PRR4 isoforms identified based on the representative signal peaks, which had been clustered into six postulated groups. Protein identification by tandem MS analysis for group P1 (signal peaks at *m/z* 1601.94 and 1921.17) and P2 (signal peaks at *m/z* 1729.82 and 1792.89) yielded pHL E1F1 and PRR4, respectively. On the other hand, group P3 (signal peaks at *m/z* 1601.93 and 1793.10) was not identified as a protein since it has not been annotated in the existing *Homo sapiens* database. However, these signal peptides yielded another hypothetical conserved protein predicted similar to pHL E1F1 isoform 2 (NCBI: gi/55667085) from *Pan troglodytes* database, with a substitution of arginine (R) with glutamine (Q) at position 120 compared to PRR4. Therefore, this PRR4 isoform is designated as PRR4-N3 in this study. Group P4 shows three signal peaks at *m/z* 1601.75, 1729.80 and *m/z* 1792.90, and tandem MS analysis identified PRR4

and PRR4-N3 in this group. Similarly, group P5 (signal peaks at *m/z* 1792.76, 192.96 and 1601.76) yielded pHL E1F1 and PRR4-N3. Lastly, group P6 shows four signal peaks at *m/z* 1601.8, 1729.9, 1792.9 and 1921.0, and can thus be postulated that two or three PRR4 isoforms might exist in this group. In this study, majority of the singular PRR4 isoform identified was as pHL E1F1 from group P1 with 21 volunteers compared to PRR4 from group P2 (n=1) and PRR4-N3 from group P3 (n=2). On the other hand, higher number of volunteers (n=20) were shown to have both pHL E1F1 and PRR4-N3 isoforms in their tears as postulated in group P5, compared to other combinations as postulated in group P4 (n=6) and P6 (n=11). It is noteworthy that PRR4 is the only isoform annotated in the SwissProt database, whereas all three isoforms of PRR4 are annotated in the NCBI database.

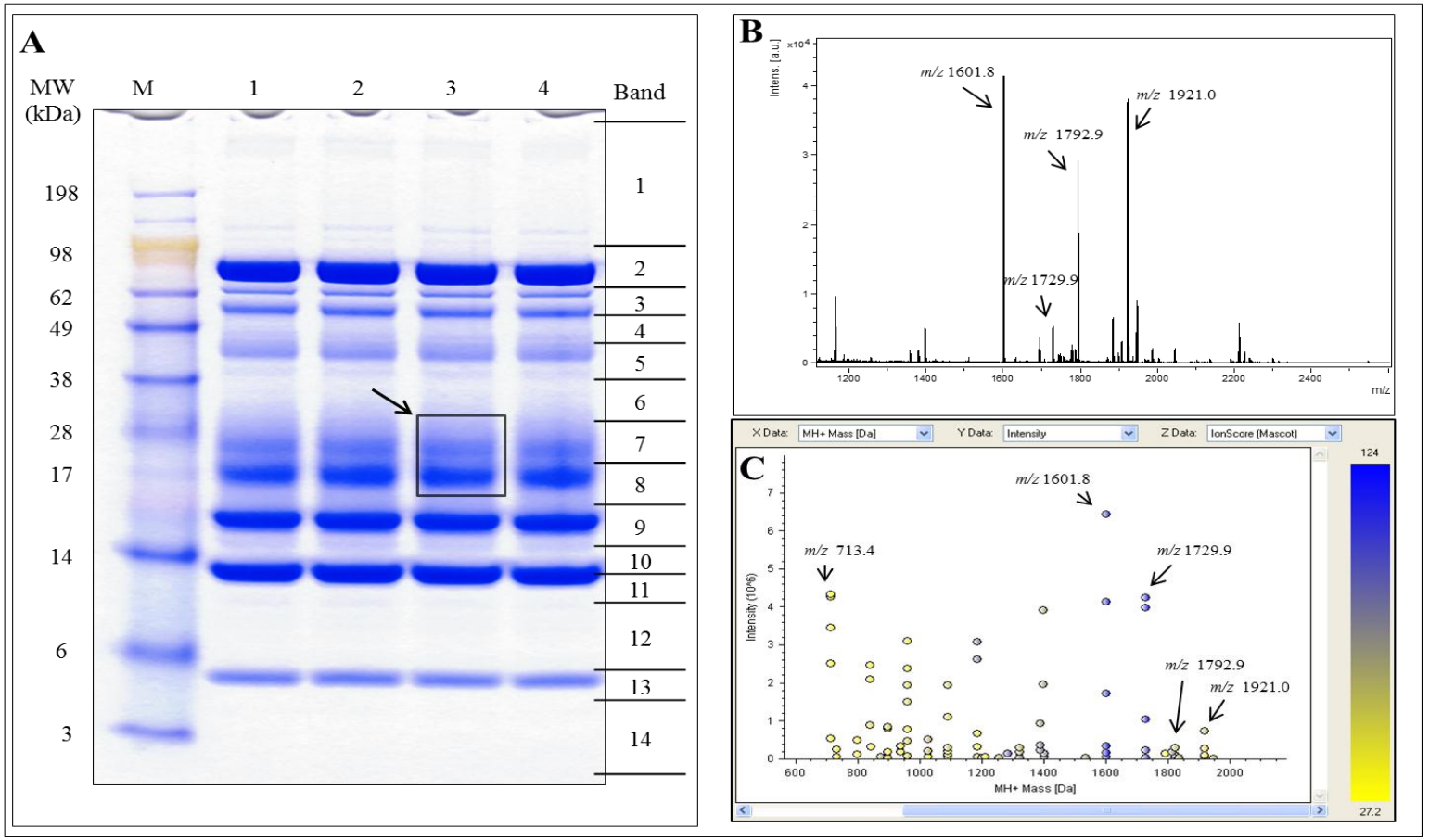

Figure 4.13: (A) 1DE gel of colloidal blue stained tear proteins. Arrow indicates PRR4 rich-region (bands 7 and 8). **(B)** Overlaid MS spectrum of band 8 after LC-MALDI-MS analysis. The values on the *y*-axis indicate mass peak intensities in arbitrary units of the identified mass spectra (*x*-axis). **(C)** Overlaid MS spectrum of band 8 after LC-ESI-MS/MS analysis. The values on the *y*-axis indicate mass peak intensities in arbitrary units of the identified mass spectra (*x*-axis) and the *z*-axis indicate the ion scores of the peaks **[139]**.

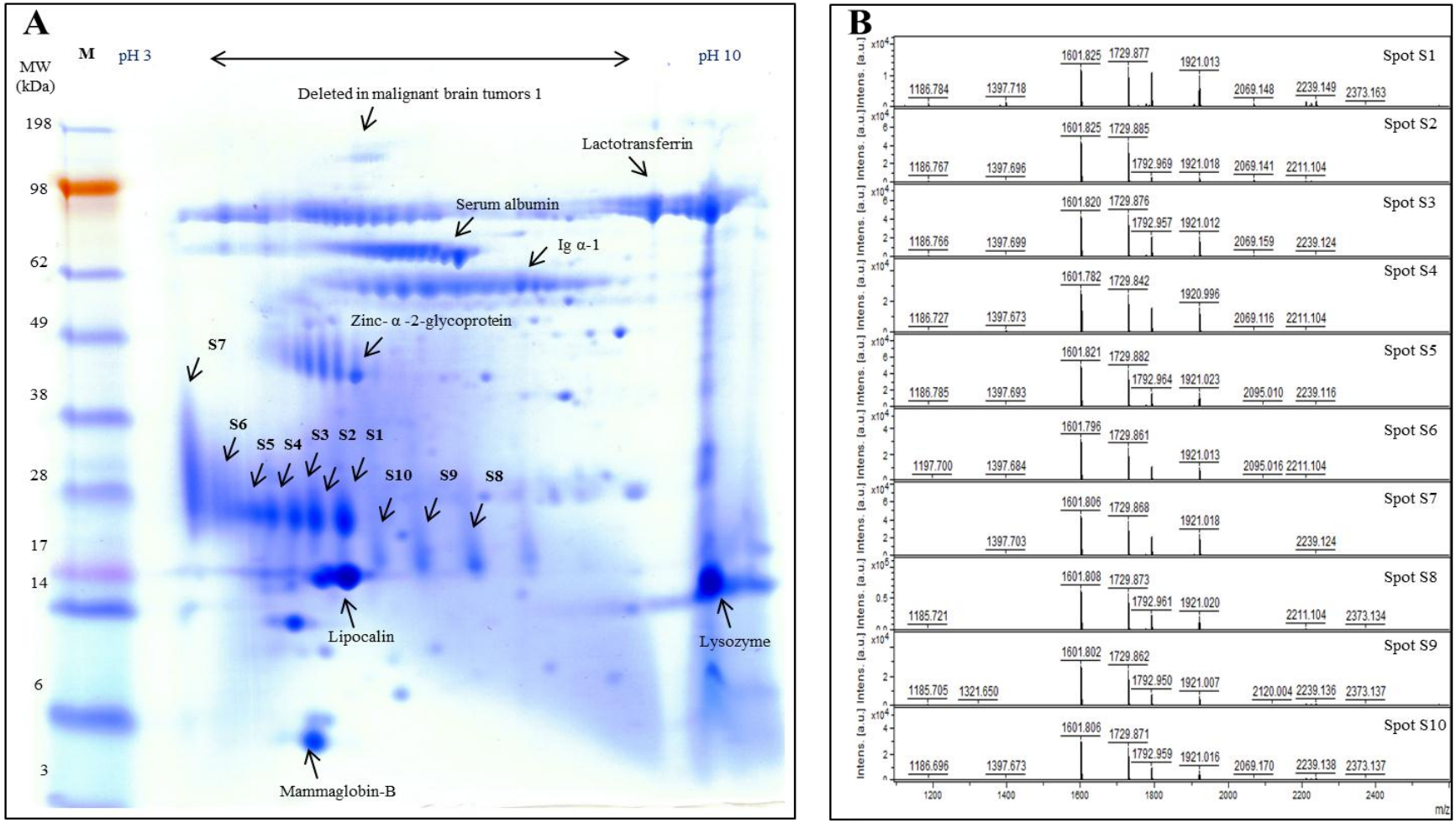

Figure 4.14: (A) 2DE gel of pooled capillary-collected tear proteins (n=10) stained with colloidal blue staining. The spots marked S1 to S10 show the differential expression of PRR4 isoforms. **(B)** Representative MS spectrum of each PRR4 spots (S1 to S10) after MALDI-MS analysis. The values on the *y*-axis indicate mass peak intensities in arbitrary units of the identified mass spectra (*x*-axis) **[139]**.

Table 4.9: Summary of the identified PRR4 isoforms and PTMs profiles from pooled healthy tear fluid sample (n=10) by 2DE and MS systems [139].

Digestion	Peptides [AA-sequences]	[AA-position]	m/z [Da]	Charge [+]	MH +[Da]	Ion score (-)10lgP	Modifications	PRR4 isoforms	
								PRR4	pHL E1F1
Asp,N	DQGPQRPPPEGLLPRPPG	43-60	636.675	3	1907.001	151	Unmodified	√	√
Asp,N	DQGPQRPPPE(+14.02)GLLPRPPG	43-60	961.517	2	1921.017	65	Methylation (+14.02)	√	√
Asp,N	D(+42.01)QGPQRPPPEGLLPRPPG	43-60	975.516	2	1949.012	123	Acetylation (N-term) (+42.01)	√	√
Trypsin	HPPPPPFQNQQRPPR	82-96	896.972	2	1791.928	52	Unmodified	√	x
Trypsin	HPPPPPFQNQQRPPQR	82-97	961.002	2	1919.987	59	AA substitution R to Q	x	√
Trypsin	QLSLPR	101-105	713.431	1	712.423	53	Unmodified	√	√
Trypsin	Q(-17.03)LSLPR	101-105	696.405	1	695.397	53	Pyro-glu from Q (-17.02)	√	√
Trypsin	FPSVSLQEASSFFQR	107-121	865.432	2	1728.847	200	Unmodified	√	x
Trypsin	FPSVSLQE(+14.02)ASSFFQR	107-121	872.439	2	1742.863	44	Methylation (+14.02)	√	x
Trypsin	FPSVSLQE(+21.98)ASSFFQR	107-121	876.421	2	1750.829	57	Sodium adduct (+21.98)	√	x
Trypsin	FPSVSLQEASSFFR	107-120	801.402	2	1600.789	200	AA substitution Q to R	x	√
Trypsin	FPSVSLQE(+14.02)ASSFFR	107-120	808.409	2	1614.804	118	Methylation (+14.02)	x	√
Trypsin	FPSVSLQE(+21.98)ASSFFR	107-120	812.393	2	1622.770	92	Sodium adduct (+21.98)	x	√
Asp,N	DRPARHPQEQPLW	122-134	815.416	2	1628.817	135	Unmodified	√	√
Asp,N	DRPARHPQEQPLW(+15.99)	122-134	823.414	2	1644.812	107	Oxidation (+15.99)	√	√
Asp,N	DRPARHPQE(+14.02)QPLW	122-134	822.425	2	1642.833	93	Methylation (+14.02)	√	√
Asp,N	D(+42.01)RPARHPQEQPLW	122-134	836.422	2	1670.828	68	Acetylation (N-term) (+42.01)	√	√
Trypsin	HPQEQPLW	127-134	517.756	2	1033.498	96	Unmodified	√	√
Trypsin	HPQEQPLW(+15.99)	127-134	525.755	2	1049.493	62	Oxidation (+15.99)	√	√
Trypsin	HPQE(+21.98)QPLW	127-134	528.747	2	1055.480	78	Sodium adduct (+21.98)	√	√
								Sequence coverage (%)	
								63.43	63.43

Table 4.9: (continued)

Digestion	Peptides [AA-sequences]	Identified peptides in each 2DE spot [a](Mr/ kDa; pI) by LC-ESI-Orbitrap XL MS									
		Spot 1 (23.7; 5.4)	Spot 2 (24.0; 5.2)	Spot 3 (24.3; 5.1)	Spot 4 (24.6; 4.9)	Spot 5 (24.9; 4.7)	Spot 6 (28.2; 4.0)	Spot 7 (29.7; 3.5)	Spot 8 (17.8; 6.6)	Spot 9 (18.4; 6.3)	Spot 10 (20.0: 6.0)
Asp,N	DQGPQRPPPEGLLPRPPG	131	46	55	28	169	179	106	48	32	69
Asp,N	DQGPQRPPPE(+14.02)GLLPRPPG	x	7	5	2	x	x	1	4	5	x
Asp,N	D(+42.01)QGPQRPPPEGLLPRPPG	8	10	12	10	46	61	49	13	12	7
Trypsin	HPPPPPFQNQQRPPR	35	43	39	57	30	94	119	37	5	5
Trypsin	HPPPPPFQNQQRPPQR	25	37	19	31	32	76	116	41	3	4
Trypsin	QLSLPR	7	12	13	12	11	24	43	1	3	2
Trypsin	Q(-17.03)LSLPR	x	x	x	2	2	5	12	1	x	2
Trypsin	FPSVSLQEASSFFQR	8	9	8	14	18	39	58	12	7	12
Trypsin	FPSVSLQE(+14.02)ASSFFQR	x	x	x	x	1	1	2	x	x	x
Trypsin	FPSVSLQE(+21.98)ASSFFQR	2	2	2	2	3	3	3	2	1	3
Trypsin	FPSVSLQEASSFFR	40	56	53	51	60	60	72	53	19	26
Trypsin	FPSVSLQE(+14.02)ASSFFR	x	1	1	2	3	3	9	2	1	2
Trypsin	FPSVSLQE(+21.98)ASSFFR	5	6	6	8	7	20	49	6	5	5
Asp,N	DRPARHPQEQPLW	141	24	24	20	146	122	77	25	19	45
Asp,N	DRPARHPQEQPLW(+15.99)	1	3	3	8	1	7	x	6	4	x
Asp,N	DRPARHPQE(+14.02)QPLW	11	4	4	x	5	30	16	x	4	x
Asp,N	D(+42.01)RPARHPQEQPLW	x	4	3	2	x	x	x	2	2	x
Trypsin	HPQEQPLW	14	23	10	15	15	35	62	11	5	6
Trypsin	HPQEQPLW(+15.99)	x	4	1	1	x	11	14	1	x	1
Trypsin	HPQE(+21.98)QPLW	5	4	5	6	5	7	7	3	3	4
		Total intensity of PRR4 spectra/ spot (%) by MALDI-MS									
		84.60 ± 2.26	86.42 ± 1.95	90.38 ± 3.59	90.94 ± 3.06	87.37 ± 2.08	94.18 ± 1.04	92.49 ± 2.81	85.71 ± 7.87	80.24 ± 7.33	78.65 ± 9.21

Note: Apparent molecular weight and pI of protein spots identified in this study ([a]), identified (√) and not identified (x).

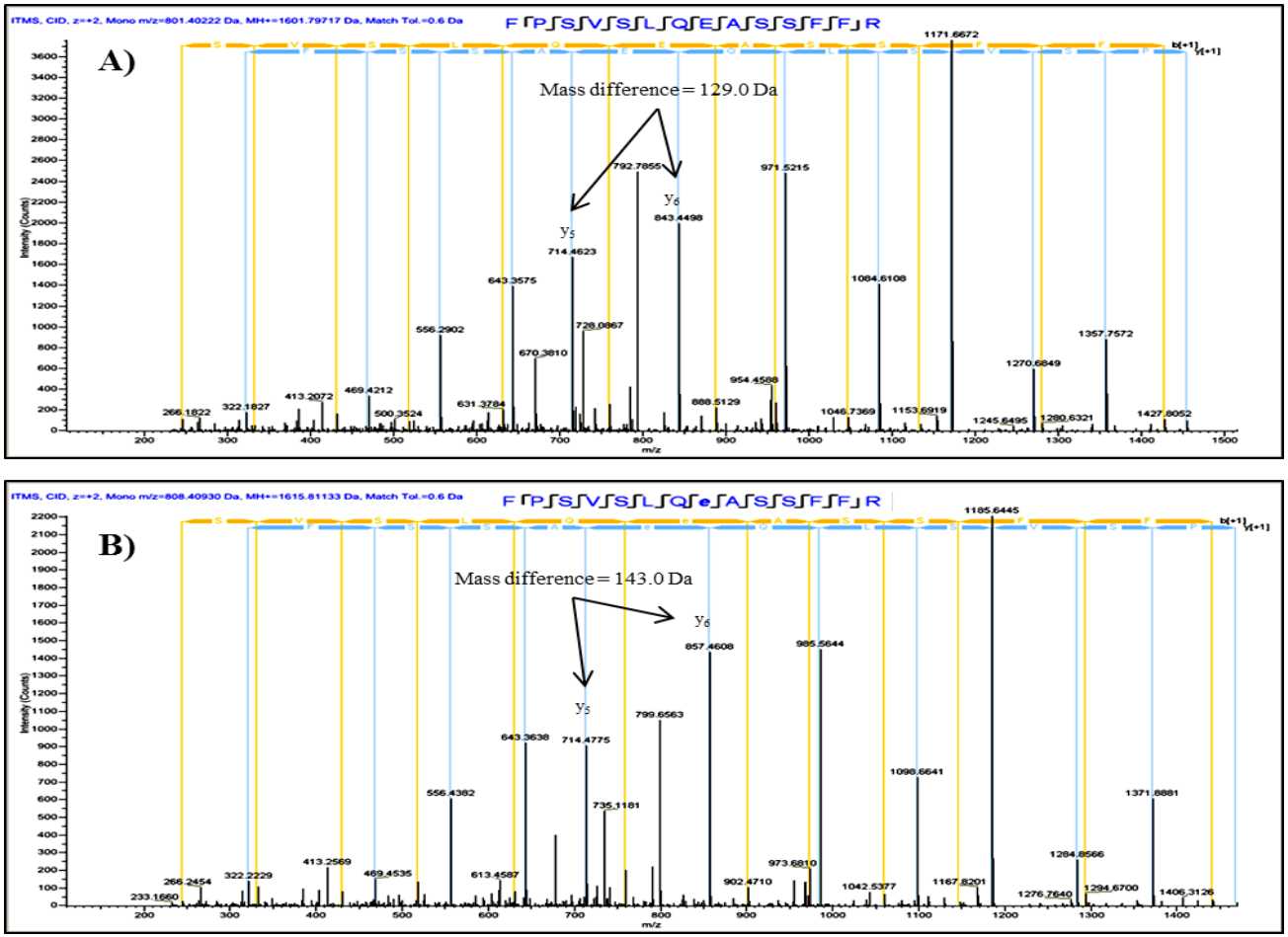

Figure 4.15: Tandem MS spectra of both unmodified and methylated peptide FPSVSLQE#ASSFF.

A) CID spectrum of the unmodified peptide (2+ ion, *m/z* 1601.80 with ion score of 124) displays mass difference between *y*5 and *y*6 ion as 129.0 Da. **B)** CID spectrum of the O-methylated peptide (2+ ion, *m/z* 1615.81 with ion score of 106) displays mass difference between *y*5 and *y*6 ion as 143.0 Da. Mass difference of 14.0 Da between both peptides pinpoint the methylation of glutamic acid ($E^{\#}$) **[139]**.

Table 4.10: Summary of the identified PRR4 isoforms profiles from healthy tear fluid samples (n=61) by MS systems [139]

Group	#Volunteers		Accession	Protein	Peptides [AA-sequences]	1DE-MALDI TOF/TOF MS				
	Male	Female				Mascot score	SC %	MH+ [Da]	Ion score	Total intensity of PRR4 spectra/spot (%)
P1	10	11	gi1050983	pHL E1F1 [*Homo sapiens*]	R.FPSVSLQEASSFFR.R	158	22	1601.86	132	83.67 ± 2.97
					R.HPPPPPFQNQQRPPQR.G			1921.08	64	
					R.HPQEQPLW.-			x	x	
					R.QLSLPR.F			x	x	
P2	0	1	gi154448886	proline-rich protein 4 isoform 2 [*Homo sapiens*]	R.FPSVSLQEASSFFQR.D	146	22	1729.83	127	69.53 ± 1.72
					R.HPPPPPFQNQQRPPR.R			1792.92	61	
					R.HPQEQPLW.-			x	x	
					R.QLSLPR.F			x	x	
P3	2	0	gi55667085	PREDICTED: similar to pHL E1F1 isoform 2 [*Pan troglodytes*]	R.FPSVSLQEASSFFR.R	122	21	1601.81	122	86.35 ± 1.15
					R.HPPPPPFQNQQRPPR.R			1792.96	70	
					R.HPQEQPLW.-			x	x	
					R.QLSLPR.F			x	x	
P4	4	2	gi154448886	proline-rich protein 4 isoform 2 [*Homo sapiens*]	R.FPSVSLQEASSFFQR.D	142	22	1729.86	122	86.08 ± 1.15
					R.HPPPPPFQNQQRPPR.R			1792.96	61	
					R.HPQEQPLW.-			x	x	
					R.QLSLPR.F			x	x	
			gi55667085	PREDICTED: similar to pHL E1F1 isoform 2 [*Pan troglodytes*]	R.FPSVSLQEASSFFR.R	174	21	1601.8	126	
					R.HPPPPPFQNQQRPPR.R			1792.96	86	
					R.HPQEQPLW.-			x	x	
					R.QLSLPR.F			x	x	

Table 4.10: (continued)

Group	#Volunteers		Accession	Protein	Peptides [AA-sequences]	1DE-MALDI TOF/TOF MS				
	Male	Female				Mascot score	SC %	MH+ [Da]	Ion score	Total intensity of PRR4 spectra/spot (%)
P5	7	13	gi1050983	pHL E1F1 [*Homo sapiens*]	R.FPSVSLQEASSFFR.R	151	22	1601.75	122	84.32 ± 2.24
					R.HPPPPPFQNQQRPPQR.G			1920.94	67	
					R.HPQEQPLW.-			x	x	
					R.QLSLPR.F			x	x	
			gi55667085	PREDICTED: similar to pHL E1F1 isoform 2 [*Pan troglodytes*]	R.FPSVSLQEASSFFR.R	148	21	1601.75	118	
					R.HPPPPPFQNQQRPPR.R			1792.88	70	
					R.HPQEQPLW.-			x	x	
					R.QLSLPR.F			x	x	
P6	6	5	gi1050983	pHL E1F1 [*Homo sapiens*]	R.FPSVSLQEASSFFR.R	136	22	1601.82	112	83.15 ± 3.13
					R.HPPPPPFQNQQRPPQR.G			1921.05	60	
					R.HPQEQPLW.-			x	x	
					R.QLSLPR.F			x	x	
			gi154448886	proline-rich protein 4 isoform 2 [*Homo sapiens*]	R.FPSVSLQEASSFFQR.D	143	22	1729.88	116	
					R.HPPPPPFQNQQRPPR.R			1792.98	63	
					R.HPQEQPLW.-			x	x	
					R.QLSLPR.F			x	x	
			gi55667085	PREDICTED: similar to pHL E1F1 isoform 2 [*Pan troglodytes*]	R.FPSVSLQEASSFFR.R	145	21	1601.82	118	
					R.HPPPPPFQNQQRPPR.R			1792.98	63	
					R.HPQEQPLW.-			x	x	
					R.QLSLPR.F			x	x	

Table 4.10: (continued)

Group	#Volunteers		Accession	Protein	Peptides [AA-sequences]	In-solution LC-ESI-LTQ-Orbitrap-XL MS					
	Male	Female				Mascot score	SC %	m/z [Da]	Charge (+)	MH+ [Da]	Ion score
P1	10	11	gi1050983	pHL E1F1 [*Homo sapiens*]	R.FPSVSLQEASSFFR.R	11304	32.84	801.40	2	1601.80	124
					R.HPPPPPFQNQQRPPQR.G			961.00; 641.00; 481.00	2; 3; 4	1920.99	60
					R.HPQEQPLW.-			1034.50; 517.75	1; 2	1034.50	42
					R.QLSLPR.F			713.43; 357.21	1; 2	713.43	39
P2	0	1	gi154448886	proline-rich protein 4 isoform 2 [*Homo sapiens*]	R.FPSVSLQEASSFFQR.D	8928	26.87	865.43	2	1729.86	129
					R.HPPPPPFQNQQRPPR.R			896.97; 598.31; 448.98	2; 3; 4	1792.94	47
					R.HPQEQPLW.-			1034.50; 517.75	1; 2	1034.50	x
					R.QLSLPR.F			713.43; 357.21	1; 2	713.43	40
P3	2	0	gi55667085	PREDICTED: similar to pHL E1F1 isoform 2 [*Pan troglodytes*]	R.FPSVSLQEASSFFR.R	11317	32.09	801.40	2	1601.80	124
					R.HPPPPPFQNQQRPPR.R			896.97; 598.31; 448.98	2; 3; 4	1792.94	42
					R.HPQEQPLW.-			1034.50; 517.75	1; 2	1034.50	35
					R.QLSLPR.F			713.43; 357.21	1; 2	713.43	40
P4	4	2	gi154448886	proline-rich protein 4 isoform 2 [*Homo sapiens*]	R.FPSVSLQEASSFFQR.D	8384	32.84	865.43	2	1729.86	128
					R.HPPPPPFQNQQRPPR.R			896.97; 598.31; 448.98	2; 3; 4	1792.94	42
					R.HPQEQPLW.-			1034.50; 517.75	1; 2	1034.50	37
					R.QLSLPR.F			713.43; 357.21	1; 2	713.43	40
			gi55667085	PREDICTED: similar to pHL E1F1 isoform 2 [*Pan troglodytes*]	R.FPSVSLQEASSFFR.R	7302	32.09	801.40	2	1601.80	124
					R.HPPPPPFQNQQRPPR.R			896.97; 598.31; 448.98	2; 3; 4	1792.94	42
					R.HPQEQPLW.-			1034.50; 517.75	1; 2	1034.50	37
					R.QLSLPR.F			713.43; 357.21	1; 2	713.43	40

Table 4.10: (continued)

Group	#Volunteers		Accession	Protein	Peptides [AA-sequences]	In-solution LC-ESI-LTQ-Orbitrap-XL MS					
	Male	Female				Mascot score	SC %	m/z [Da]	Charge (+)	MH+ [Da]	Ion score
P5	7	13	gi1050983	pHL E1F1 [*Homo sapiens*]	R.FPSVSLQEASSFFR.R	9767	32.84	801.40	2	1601.80	124
					R.HPPPPPFQNQQRPPQR.G			961.00; 641.00; 481.00	2; 3; 4	1920.99	57
					R.HPQEQPLW.-			1034.50; 517.75	1; 2	1034.50	35
					R.QLSLPR.F			713.43; 357.21	1; 2	713.43	40
			gi55667085	PREDICTED: similar to pHL E1F1 isoform 2 [*Pan troglodytes*]	R.FPSVSLQEASSFFR.R	9613	32.09	801.40	2	1601.80	124
					R.HPPPPPFQNQQRPPR.R			896.97; 598.31; 448.98	2; 3; 4	1792.94	50
					R.HPQEQPLW.-			1034.50; 517.75	1; 2	1034.50	35
					R.QLSLPR.F			713.43; 357.21	1; 2	713.43	40
P6	6	5	gi1050983	pHL E1F1 [*Homo sapiens*]	R.FPSVSLQEASSFFR.R	14700	32.84	801.40	2	1601.80	124
					R.HPPPPPFQNQQRPPQR.G			961.00; 641.00; 481.00	2; 3; 4	1920.99	63
					R.HPQEQPLW.-			1034.50; 517.75	1; 2	1034.50	35
					R.QLSLPR.F			713.43; 357.21	1; 2	713.43	43
			gi154448886	proline-rich protein 4 isoform 2 [*Homo sapiens*]	R.FPSVSLQEASSFFQR.D	14579	32.84	865.43	2	1729.86	141
					R.HPPPPPFQNQQRPPR.R			896.97; 598.31; 448.98	2; 3; 4	1792.94	37
					R.HPQEQPLW.-			1034.50; 517.75	1; 2	1034.50	42
					R.QLSLPR.F			713.43; 357.21	1; 2	713.43	43
			gi55667085	PREDICTED: similar to pHL E1F1 isoform 2 [*Pan troglodytes*]	R.FPSVSLQEASSFFR.R	14365	32.09	801.40	2	1601.80	124
					R.HPPPPPFQNQQRPPR.R			896.97; 598.31; 448.98	2; 3; 4	1792.94	37
					R.HPQEQPLW.-			1034.50; 517.75	1; 2	1034.50	42
					R.QLSLPR.F			713.43; 357.21	1; 2	713.43	43

Note: The predicted protein similar to pHL E1F1 isoform 2 from *Pan troglodytes* database is designated as PRR4-N3 in this study.

5 DISCUSSION

5.1 Identification and verification of potential tear protein biomarker panels to distinguish DES subgroups

A total of 200 proteins were identified in the tear fluids from all four groups, suggesting the presence of a wealth of proteins in the tears. The total number of identified proteins in this study is higher than those previously identified by Zhou *et al* and Salvisberg *et al* with 93 and 185 proteins, respectively; but lesser than the 1543 proteins identified by Zhou *et al* **[49, 52, 155]**. This discrepancy can be attributed to the higher amount of proteins (400 µg) from four healthy subjects (3 females and 1 male, average age: 36 ± 14) utilized by Zhou *et al* for their analysis compared to the 50 µg per analysis employed in this study **[57]**. The similar approach could not be practically utilized in this study due the limited amount of proteins collected from the DES patients. On the other hand, most of the identified proteins mentioned in the literatures (**Table: 1.1**) did not conform to the MIAPE guidelines, especially the use of FDR of 1 % in their data presentations. Hence, the identifications are associated with differing or lower levels of confidence, which prevents the critical evaluation of the work.

Although as many as 200 proteins were successfully identified in this study, lacrimal gland secreted proteins composed of LYZ, LCN1, LTF and PIP make up as much as 60 % of the total tear proteome, and the top 20 proteins accountable for approximately 90 %. The rest of the approximately 10 % of the total tear proteome consisted of as many as 180 proteins. For the first time, this study demonstrated the degree of abundance of each tear protein utilizing iBAQ value in the DES subgroups and CTRL, by taking advantage of the state-of-the-art MaxQuant computational proteomics platform. Since the classification of degree of tear proteins abundance still remains indiscriminate, in this study, the tear samples were postulated as a major protein if iBAQ values are larger than 0.5 % and minor if lower than 0.5 %. This data highlights that any potential additional protein identifications will be in the minor abundance range.

In the discovery study, the proteomics strategy was successfully employed to identify and quantify large number of proteins to discover candidate protein biomarkers to distinguish the different DES subgroups. As many as 77 proteins were found to be significantly differentially expressed in DES subgroups compared to CTRL based on the LFQ analysis. Besides, 41 proteins were found to be associated to DES for the first time, as tabulated in **Table 4.3**. However, only 18 proteins were considered to be major proteins based on the iBAQ analysis. Subsequently, 13 major proteins were successfully verified employing the AIMS strategy in DES subgroups compared to CTRL, which composed of PRR4, ZG16B, SCGB2A1, DMBT1, PROL1, LACRT, ALDH3A1, ENO1, TF, S100A8, S100A9, PEBP1 and ORM1. These proteins play specific biological functions in the ocular surface and any alterations in these proteins could be used as potential indicators for the cause and/or effect of the specific DES.

Among the 13 differentially expressed proteins identified, PRR4, ZG16B and PROL1 were found to be slightly decreased in abundance in the DRYlip subgroup and to be most strongly decreased in both DRYaq and DRYaqlip subgroups. Similarly, drastic decrement in abundance of truncated PRR4 in DRYaq group was also demonstrated previously by other studies **[7, 47, 81, 106].** In addition, Boehm *et al* also demonstrated similar decrement profile of PRR4 in the DRYaqlip subgroup and Nichols *et al* in contact lens users associated with DES (DES_CL) **[48, 106]**. The decrement level of PRR4 was also widely documented in recent studies of dry eye associated with systemic diseases, namely Sjogren's syndrome (DRY_SS), Stevens-Johnson syndrome (DRY_SJS) and rheumatoid arthritis (DRY_RA) **[7, 8, 78].** It is also important to note that similar decrement patterns of PRR4 were documented in other systemic diseases, namely, thyroid-associated orbitopathy, diabetic proliferative retinopathy and multiple sclerosis **[79, 120, 121]**. These findings collectively attribute the decrement of PRR4 to the functional involvement of the lacrimal gland. Interestingly, even though the expression profiles of PRR4 were well documented to be associated with DES, the precise biological functions of PRR4 in tears are yet to be defined, which may have vital roles in the stability of the tear film and the protection of the ocular surface **[115-119]**.

Hitherto, the decrement of ZG16B protein was only demonstrated by Srinivasan *et al* in tears of symptomatic aqueous deficiency DES (DRY_MSDE) patients **[81]**. In addition, Salvisberg *et al* reported decrement of ZG16B in tears of patients with multiple sclerosis **[79]**. However, both studies did not verify the ZG16B expression profiles employing orthogonal methods,

mainly due to the absence of working antibodies. The precise biological function of ZG16B is also largely unknown in tears. Up till now, ZG16p is known as a secretory lectin protein that is proposed to play a regulatory role to promote "flushing out" of the granule content (e.g. enzymes/ proteins) during exocytosis in pancreatic acinar cells and in the intestinal goblet cells **[156, 157]**. Furthermore, this secreted protein have been found to play a crucial role in gene regulation and cancer metastasis; proposing a potential role of this protein in the maintenance of the inflammatory state in cancer tissue **[158-162].** It is important to highlight here that similar to the findings of this study, both ZG16B and PRR4 were also found to be distinctly decreased in abundance in the tear samples of patients with multiple sclerosis **[79]**. Their potential roles in regulatory, protection and inflammation associated to their significant reduction in tears of DES patients in this study as well as in other systemic diseases make both ZG16B and PRR4 promising and enticing candidates for future studies.

Next, similar to the findings of the present study, Srinivasan *et al* also documented decrement of PROL1 in the DRY_MSDE group **[81]**. The exact function of PROL1 is also still largely unknown. Recently, Dufour *et al* reported that the immunoreactive Opiorphin (QRFSR-peptide), a mature secretory peptide product of the PROL1 gene, is secreted primarily by lacrimal gland tears at the highest physiological rates (~200 ng/ml) in healthy volunteers **[163].** They suggested that the potential role of opiorphin is in modulating lacrimal fluid homeostasis by increasing enkephalin bioavailability in case of certain causes of epiphora (overflow of tears onto the face). The authors also proposed a paracrine and/or autocrine role of opiophin in the lacrimal system and at the ocular surface. These findings also collectively attribute the decrement of PROL1 to the functional involvement of the lacrimal gland.

The decreased abundance of SCGB2A1 and DMBT1 were successfully verified in DRYaq and DRYaqlip groups, meanwhile LACRT was only decreased in abundance in the DRYaqlip group. Similar decrement in abundance of SCGB2A1 in DRYaq group was also demonstrated by Soria *et al* and Srinivasan *et al* **[81, 107]**. On the contrary, increased abundance level of this protein was demonstrated by Boehm *et al* in DRYaq and DRYaqlip groups, and by Nichols *et al* in the DES_CL group **[48, 106]**. These divergences may well be due to differences in analytic and sample collection methods employed or specific patient details. SCGB2A1, a member of the uteroglobin family, is a protein of unknown function. Nevertheless, peptides derived from uteroglobin family are known to be among the most potent anti-inflammatory agents identified to date **[164].** Although normal expression

of SCGB2A1 has been described in secretory lacrimal glands, mucosal epithelia of breast and uterus, SCGB2A1 has been reported to be overexpressed in primary breast cancer tissues and in occult breast metastases, and is considered one of the most informative breast cancer markers to detect micrometastatic disease in the circulation and lymph nodes **[165-169]**. In addition, high differential expression of SCGB2A1 in multiple histological types of epithelial ovarian cancer was also demonstrated **[170]**. It is suggested that this protein may bind androgens, estramustine (a chemotherapeutic agent used for prostate cancer) and other steroids (may be under transcriptional regulation of steroid hormones) **[171].**

Next, DMBT1 was found for the first time to be significantly decreased in abundance in DRYaq and DRYaqlip subgroups in this study. It is well documented that this protein may play critical roles in the mucosal defense system, cellular immune defense and epithelial differentiation **[172-174]**. It displays a broad calcium-dependent binding spectrum against both gram-positive and gram-negative bacteria, suggesting a role in defense against bacterial pathogens **[175]**. Moreover, it binds to a range of poly-sulfated and poly-phosphorylated ligands which may explain its broad bacterial-binding specificity **[176]**. Interestingly, a study showed that DMBT1 interacts with pancreatic zymogens in a pH-dependent manner and may act as a Golgi cargo receptor in the regulated secretory pathway of the pancreatic acinar cell **[177]**.

Decrement abundance of LACRT was also documented in various studies associated with DES, namely in the DRYaq, DRY_SS, DRY_SJS, DRY_RA, DRY_MDE, DRY_MSDE and DRY_CL **[7, 48, 78, 81].** LACRT is an eye-specific growth factor that may play an imperative role in secretion and renewal of lacrimal and ocular surface epithelia **[178, 179]**. It is a secretory glycoprotein released apically from human lacrimal acinar cells and also appears to be a product of the meibomian gland **[4]**. It been shown that LACRT functions as autocrine/ paracrine enhancer of the lacrimal constitutive secretion, promoting sustained basal tearing, ductal cell mitogen and stimulator of corneal epithelial cells **[180, 181]**. Hence, LACRT can itself act as regulator of tear secretion and as factor for renewal of ocular epithelia. Down regulation of this protein can therefore contribute to the disease progression in terms of severity.

Among the 13 differentially expressed proteins identified, S100A8 and S100A9 were found to be increased in abundance in all the DES subgroups, and they discriminated best the DRYaq and DRYaqlip from the CTRL group. Decrement in abundance of S100A8 and

S100A9 were widely documented in various studies associated with DRYaq, DRYaqlip and DRY_SS **[47, 52, 78, 106, 107]**. These proteins are known to participate in inflammatory processes and Zhou *et al* reported that higher expression of these proteins were associated significantly with increased signs of dryness **[52]**. S100 proteins are identified to interact with other proteins to modulate a variety of biological functions such as cell migration, proliferation and differentiation. Furthermore, these proteins are correlated to various diseases such as cancer metastasis, sclerosis and pterygium, many of which involve in inflammation, innate immunity, tissue damage and wound healing **[182-184].**

The increased abundance of ENO1, ORM1, TF and PEBP1 were successfully verified in DRYaq and DRYaqlip groups, meanwhile ALDH3A1 was only increased in abundance in DRYaqlip group. Zhou *et al* demonstrated that the increment abundance of ENO1 in the tears was found to correctly identify a patient as belonging to the DRYaqlip group in 85 % of the time **[52]**. ENO1 is a key glycolytic enzyme expressed abundantly in most cells, and it was also found to be a cell surface protein on hematopoietic cells (neutrophils, B cells, T Cells, monocytes), epithelial cells and neuronal cells **[185]**. Recent studies indicate that it may play an important role in several disease processes, for example, in cancer and autoimmune disorders **[155, 185-188]**.

The similar increment of ORM1 protein was also documented in DRYaqlip and DRY_SS groups **[52, 78]**. ORM1 is a heavily glycosylated protein (45 %) with a molecular weight of 41−43 kDa and has also been classified as a member of the immunocalin family, a lipocalin subfamily that modulates immune and inflammatory responses **[189].** The synthesis is controlled by glucocorticoids, interleukin-1 and interleukin-6 and appears to function in modulating the activity of the immune system during the acute-phase reaction **[190]**.

Meanwhile, the similar increment of TF was only documented by Li *et al* in DRY_SS group **[78]**. TF is an iron binding transport protein which can bind two Fe^{3+} ions in association with the binding of an anion, usually bicarbonate and it is responsible for the transport of iron from sites of absorption and heme degradation to those of storage and utilization **[191-193]**. Its iron binding capacity yields anti-microbial properties by keeping required iron stores unavailable to pathogens and increase in TF levels are seen in conjunction with low iron levels and iron deficiency anemia.

PEBP1 was found for the first time significantly increased in abundance in DRYaq and DRYaqlip groups in this study. PEBP1 is an inhibitory modulator of Raf kinase protein and G-protein coupled receptor (GPCR) signalling cascade, as well as an activator of nuclear factor κB (NF-κB) **[194, 195].** Therefore, PEBP1 basically represents a novel effector of signal transduction pathways that control cellular growth, motility, apoptosis, genomic integrity and therapeutic resistance **[194]**. In addition, investigation of PEBP1 molecular structure showed that PEBP1 may act as a scaffold protein, facilitating the assembly of a multi-component protein complex **[194].** Besides, the disruption of PEBP1 has been reported to be related with a wide range of diseases, such as cancer, pancreatitis and Alzheimer's disease, making it a potential target for disease therapy **[194].**

Increment in abundance of ALDH3A1 was also documented in several studies of DRY_SS, DRY_MDE but has never been verified **[78, 81]**. ALDH3A1 is a corneal crystallin protein, highly expressed in epithelial cells and stromal keratocytes, but not in endothelial cells **[196]**. The expression of ALDH3A1 at levels beyond those needed for metabolism in the cornea has led to the suggestion that these proteins may have added roles in this ocular structure. An essential role for ALDH3A1 in the cornea is suggested by observation that diseased corneas, especially cataract development, are associated with decreased ALDH3A1 catalytic activity **[197, 198]**. Accumulating lines of evidence propose that ALDH3A1 mediate their effects by direct absorption of ultraviolet radiation (UV), metabolism of toxic aldehydes produced by UVR-induced lipid peroxidation and acting as antioxidants by scavenging directly UVR-induced free radicals or by producing the antioxidant NAD(P)H **[199-201]**.

The rest of the 63 differentially expressed proteins were not successfully verified, largely due to the low abundance of these proteins in tears and limitations of the AIMS strategy. However, similar expression profiles of the 35 of proteins from this list were already demonstrated in other studies associated with dry eye with/ without systemic diseases, as tabulated in **Table 4.3,** thereby, corroborating with the present results. This study also identified 42 novel proteins associated with DES, and this supports the relevance of the quantitative tear proteome comparison in order to identify new protein marker candidates for specific DES. The findings suggest that the development of DES is a complicated process involving proteins of multiple biological functions with participation of novel proteins. In this study, although 22 tear proteins were differentially expressed in DRYlip compared to CTRL, they were only differentially expressed in a lesser degree compared to DRYaq and DRYaqlip.

On the contrary, this study demonstrated that tear proteins in DRYaq and DRYaqlip patients compared to CTRL exhibited a marked increase in the number of differentially expressed proteins with 76 that are mainly involved in metabolic processes, immune response, inflammatory response and protease inhibition. It is hypothesized that the pathological mechanisms underlying DRYaq and DRYaqlip are driven by tear film instability which induces the activation of inflammatory cascade and subsequent release of inflammatory mediators and immune defense mechanisms. These host-defense mechanisms act in concert to maintain homeostasis of the tear film following the disease insult **[1]**. These diverse functions are bio-energetically expensive and require precise control of cellular metabolic pathways **[202].** Collectively, these results reveal for the first time that high numbers of metabolic enzymes are expressed, preferentially to fuel the cell fate decisions and effector functions of the aforementioned metabolic processes. A better understanding of the metabolic checkpoints that control these transitions might provide new insights for modulating immunity in infection and inflammatory disorders of the ocular surface.

In the sequence of novel marker identification, the validity of a candidate biomarker must be exhaustively tested. However, biomarker validation is a time-consuming and very costly task, mainly due to the complexity of multiplexed assays and multicenter clinical studies. Therefore, in the present study, we performed the AIMS analysis to screen prior to the further validation process in order to establish the validity and discriminative power of the identified candidate markers and also to determine the minimal quantity of tear to be used. It also remains to test the large number of invalidated candidate marker proteins found in the present study. Further characterization of these proteins could provide potential diagnostic markers and therapeutic targets that may lead to better outcomes for the DES patients.

5.2 Characterization of human reflex tear proteome in healthy volunteers

There are several major findings emerging from the current study that demonstrated that there are still significant differences in the basal and reflex tear proteome that have never been reported in the literature. A total of 52 proteins were identified from the tear samples of healthy volunteers collected employing the capillary method in this study. This result is in agreement with previous studies by Green-Church *et al* and Li *et al* employing similar sampling methods, which reported identification of 40 and 54 proteins, respectively **[58, 61]**. Remarkably, an increased abundance in PRR4 was demonstrated for the first time in reflex tears in all three experimental designs employed in the present study. This indicates that lacrimal gland-specific PRR4 represents the major expressed protein in reflex tears in an attempt to wash out irritants that come into contact with the eye. On one hand, the LFQ analysis by 1DE and LC-ESI-MS/MS demonstrated the overall increased abundance of PRR4, and on the other hand, the 2DE and LC-ESI-MS/MS analysis showed specific increased abundance of the highly acidic PRR4 spots. This finding highlights the importance of PRR4 regulation in the tears for the protection of the ocular surface, whereby its absence or modifications in the tears may contribute towards the pathogenesis of DES **[7, 8, 47, 48, 56]**. Besides increased abundance of PRR4, this study also corroborated with numerous reports that primary lacrimal proteins (e.g. LTF, LYZ and LCN1) remained essentially static in both basal and reflex tear samples **[108, 109, 112].** Hitherto, it was postulated that these primary lacrimal proteins are packaged and secreted *via* exocytosis in unison with lacrimal fluid in direct response to neural stimulation. However, in this study we demonstrated that PRR4 was expressed relatively in a higher abundance compared to the other abundant proteins.

It was also demonstrated for the first time that ZG16B was highly expressed in the reflex tears. However, the detailed function(s) of this ZG16B in tears, especially in reflex tears, remain to be elucidated. Two paralogs of ZG16B, the zymogen granule membrane protein 16 (ZG16p) and pancreatic adenocarcinoma up-regulated factor (PAUF) have recently been found to play a crucial role in gene regulation and cancer metastasis **[159-161]**. The crystal structures of ZG16B and ZG16p were also recently resolved and the overall structure of ZG16B is almost similar to that of ZG16p, motifs analogous to jacalin related mannose-binding type lectins **[158].** ZG16p is known as a secretory protein that interacts with glycosaminoglycans and the binding is considered to be pivotal for condensation-sorting of

pancreatic enzymes *via* activation of anion-cation channels in the zymogen granule membrane in pancreatic acinar cells **[203, 204]**. Therefore, it was proposed that this protein might play a regulatory role to promote "flushing out" of the granule content (e.g. enzymes/ proteins) during exocytosis in pancreatic acinar cells and in the intestinal goblet cells **[156, 157]**. It is therefore tempting to suggest that the ZG16B may potentially play a similar regulatory role as ZG16p in the lacrimal gland acinar cells to regulate the exocytosis of synthesized and enzymatically modified secretory proteins stored in the secretory granules, in direct response to neural stimulation. Recently, ZG16B as well as PRR4 were found significantly reduced in tear samples of multiple sclerosis patients **[79]**. Therefore, the increased abundance of both proteins in reflex tears, as shown in the current study, as well as their down regulation in tears of individuals with certain neurological diseases, highlight the importance of proper neurological stimulation on the acinar cells in lacrimal gland to express ZG16B and subsequently PRR4.

Stimulated lacrimal gland fluid secretion is dependent upon vasodilation with increased blood flow augmenting protein secretion **[42, 205].** The increased abundance of ALB in reflex tears is thus suggested to be derived from vascular leakage and inflammatory process **[112]**. The increased abundance of MSLN in reflex tears and its physiological role in ocular surface still remains largely unknown. Nevertheless, it was found in the endothelium, stroma and more intensely in the epithelium of the cornea, limbus and conjunctiva of the eye **[206]**. It is anticipated that there are interactions between MSLN and N-linked glycans of mucin 16 (MUC16) in corneal and conjunctival epithelium **[207, 208]**. Therefore, the increment of MSLN in reflex tears could be aimed to directly heighten the physiological functions of MUC16 in hydration, lubrication and epithelial barrier of the ocular surface **[207, 209, 210]**.

This study also showed decreased abundance of proteins involved in the mucosal immune defense during reflex tearing, which are the PIGR and IGHA1. Similar observation of down regulation of IGHA1 was well documented previously **[108, 109, 112]**. Moreover**,** PIGR plays crucial roles to protect IGHA1 from proteolytic degradation and mediates transcellular transport to the apical membrane, and is subsequently released into the extracellular space **[211-213].** It is interesting to note that unlike most abundant proteins that are expressed and secreted mainly *via* the exocytotic pathway in lacrimal gland that is regulated by neural stimulation, secretion of IGHA1 and PIGR are regulated by the rate of synthesis and constitutively secreted *via* the transcytotic pathway **[40, 41, 108, 109, 214-216]**. Therefore, it

is generally accepted that during reflex tearing, secretion of proteins by exocytosis exceeds the amount of proteins secreted *via* transcytosis, which leads to relatively low levels of IGHA1 and PIGR **[42, 112]**.

SCGB2A1 also showed decreased abundance in all the analysis, and decrement profile of SCGB2A1 was also observed in both DRYaq and DRYaqlip subgroups. The function of this uteroglobin protein in tears remains to be determined. CLU was found to be decreased in the reflex tears and this observation is associated with the occurrence of inflammatory factors **[217-219]**. On the other hand, the decreased abundance of cystatin spots in the 2DE gels of reflex tears was observed and subsequently AIMS analysis of the signature peptides of CST4 and CST1 confirmed the decreased expression. CST4 and CST1 are extracellular proteins and their role as proteinase inhibitors to prevent uncontrolled proteolysis and tissue damages is well established **[220]**. It is suggested that low levels of CST4 and CST1 might increase the level of tear protease and its activity, and their reduction is attributed to keratoconus, blepharitis and in reflex tearing as shown in this study **[54, 221-224]**.

In general, the findings of the current study provide evidence to the missing link of the most important increased abundance proteins, particularly PRR4 and ZG16B in reflex tears for the first time, which are hypothesized to be the key players in the protection of the ocular surface. Therefore, this study further highlights the importance of care during tear sampling to avoid initiation of reflex tearing, which will potentially result not only in low levels of IGHA1, but high levels of PRR4 and ZG16B. On the other hand, it remains to be elucidated the functional role(s) of ZG16B in acinar cells in the regulation of exocytosis of lacrimal-specific proteins, especially PRR4. In conclusion, this study has unraveled a novel aspect in reflex tearing, in which various key proteins were found to be differentially expressed, especially PRR4. These proteins are conjectured to possess vital functions in the protection of the ocular surface and would be instrumental for future studies of ocular-related pathology.

5.3 Characterization of Lacrimal Proline-Rich Protein 4 (PRR4) in Human Tear Proteome

The identification of PRR4-rich regions/ spots in-gel electrophoresis utilizing specific signature peptides generated from the MS systems has allowed further characterization of PRR4 in the tear proteome of healthy individuals. This study provides further evidence that PRR4 exists comparatively abundant in the tear fluid, which complements its detection in previous transcriptome studies on lacrimal gland **[113, 114]** and tear protein profiling **[49, 60, 61, 127].** In addition to the two existing PRR4 isoforms, a new variation designated as PRR4-N3 was also identified in this study. It is noteworthy that the combinations of specific signature peptides for PRR4 isoforms amongst the volunteers could be classified into six distinguished groups. Hence, this study ascertained the presence of inter-individual variability of PRR4 isoforms in tears of healthy individuals cause by point mutations **[225]**. Furthermore, pHL EIF1 was highly detected amongst the volunteers compared to PRR4-N3 and the least detected PRR4. Interestingly, the least distributed PRR4 isoform is the most deliberated isoform in the literatures **[6-8, 47-52, 56-61, 120, 121, 127, 223].** Thus, it was demonstrated that specific signature peptides are essential for exact identification of the PRR4 isoforms as well as the limitations in identifying some of these peptides employing MS approaches. To date, the lack of information about the characteristics and standardized designations for PRR4 isoforms has hindered complete understanding of the functions of PRR4 in tears. Therefore, to systematically simplify the PRR4 isoforms designations by adopting a similar naming convention to its ancillary name, the re-naming of PRR4 isoforms was proposed as PRR4 isoform 1 (PRR4-N1) (pHL E1F1:gi/1050983), PRR4 isoform 2 (PRR4-N2) (PRR4: Q16378: gi/ 154448886) and PRR4 isoform 3 (PRR4-N3) (pHL E1F1 isoform 2: gi/ 55667085), as depicted in **Figure 5.1**.

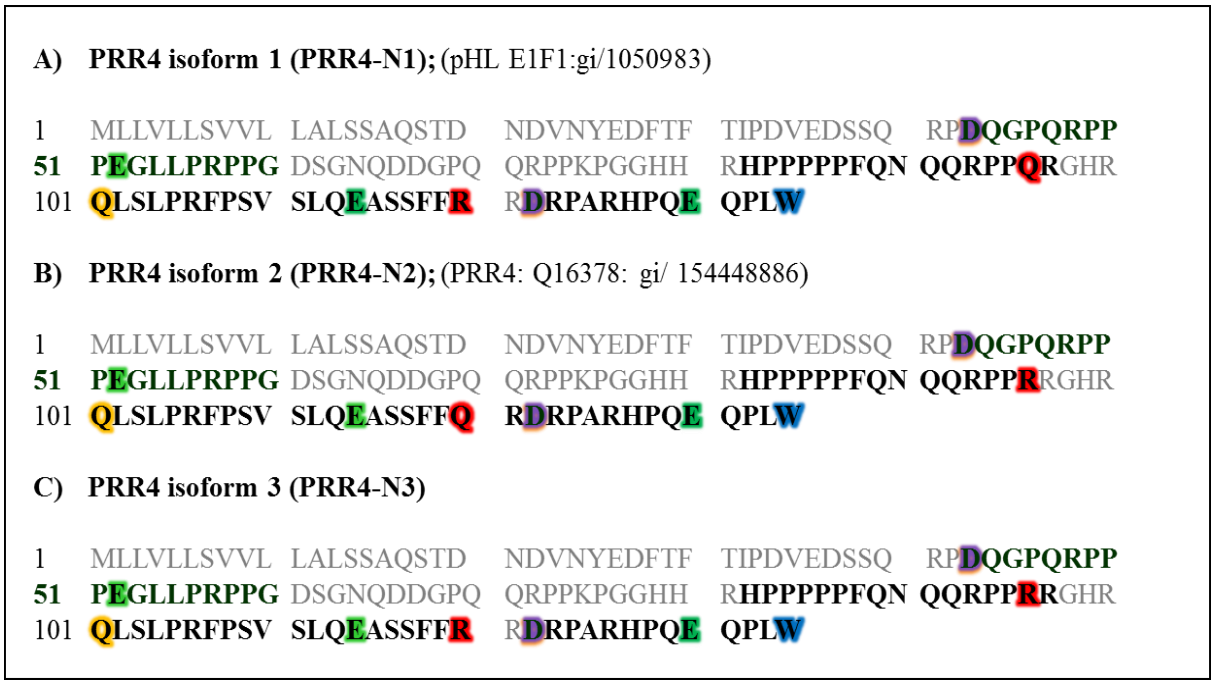

Figure 5.1: Schematic representation of isoforms and PTMs of PRR4.

The primary sequences of PRR4 isoforms according to the proposed designations are A) PRR4 isoform 1 (PRR4-N1) and B) PRR4 isoform 2 (PRR4-N2), and a new isoform C) PRR4 isoform 3 (PRR4-N3). The bold sequences were identified from LC-MALDI-MS/MS and LC-ESI-MS/MS analysis and the PRR4 isoforms were differentiated by the substitution of arginine (R) and glutamine (Q) at positions 96 and 120 as highlighted in red. Methylation at 3 glutamic acid residues (E)-52, 114 and 130 as highlighted in green, oxidation at one tryptophan residue (W)-134 as highlighted in blue, pyroglutamate formation at glutamine residue (Q)-101 and acetylation at aspartic acid residue at (D)-43 and 122 as highlighted in yellow were identified between the three PRR4 isoforms **[139]**.

In view of the fact that the volume of the tear sample is typically limited in a case study or a population-based study, the samples are pooled in most experiments and this will consequently hinder the detection and characterization of specific PRR4 isoforms. Therefore, we have successfully utilized a rapid and robust targeted data acquisition approach to identify the PRR4 isoforms in low volume tear samples. This targeted MS approach is advantageous since PRR4 isoform-specific peptides could be precisely detected in a single MS run. This essential information of the PRR4 isoforms and their signature peptides could be potentially utilized for further qualitative analysis on MS instruments (e.g. LTQ Orbitrap series) or absolute protein quantification analysis by targeted MS-based strategy [e.g. multiple-reaction-monitoring mass spectrometry (MRM-MS)] in future studies of pathological tear

samples, where isoforms and PTMs need to be probed. Absolute quantification analysis *via* targeted MS-based strategy has recently been used in proteomics for quantification of selected peptides in complex mixtures, where specific isoforms cannot be detected by classical antibody-based methods **[226-230]**. Hitherto, two of the PRR4 peptides were successfully used to quantify the amount of PRR4 protein deposited on daily wear silicone hydrogel lenses by applying the MRM-MS approach **[231]**. The exact functions of the PRR4 and the existence of the variable isoforms caused by point mutations are yet to be explored. Establishments of techniques to identify PRR4 isoforms as presented herein is the first important step for further quantifications of the protein in the disease state, followed by determination of the functional consequences. Protein isoforms can play important roles in various biological processes and can potentially be used as biomarkers or therapeutic targets/ mediators **[232-237]**. For example, studies by Shokeer and Mannervik demonstrated that one of the factors for new functions development in an enzyme is through point mutation **[238]**.

It is evident from the current 2DE investigation that PRR4 in tears exists in broad polymorphisms. The other abundant proteins distributions visualized in 2DE in this study are in agreement with findings documented in the literature **[7, 8, 51, 53, 54, 58, 239-242].** Four types of modifications were identified in several PRR4 spots in 2DE, which are methylation, acetylation, oxidation and pyroglutamate formation. The O-methylation of PRR4 isoforms on three glutamic acid sites was identified in this study. Protein methylation in PRR4 can potentially induce significant changes in protein structure and function due to the three major properties, which are neutralization of the negative charge, increase in size and hydrophobicity **[243]**. Protein structure is influenced to a large extent by the charge state of groups on the side chains of several amino acids, and modifications can alter diverse protein properties, which may potentially play a critical role in cellular regulation **[243].** On the other hand, the oxidation of PRR4 *in vivo* by oxidative stress may lead to a loss of protein function. Oxygen centered reactive species can cause specific structural modifications in amino acids and perturb the properties of the proteins, such as conformation, catalytic activity, susceptibility to proteolysis or intracellular location **[244-248]**. In the current study, only one N-terminal of glutamine in the PRR4 isoforms was found modified to pyroglutamate by glutamine cyclase during protein synthesis. Similar modification was also detected in PRR4 by Hayakawa *et al* as naturally occurring N-terminal pyroglutamic peptides **[149]**. As of now, the role of pyroglutamic acid is poorly understood and the biological relevance in PRR4 is unknown. The N-terminal pyroglutamate structure is known to provide resistance to proteins

from degradation by amino peptidases; for example, structural proteins like fibrin, fibrinogen and collagen-like proteins have N-terminal pyroglutamate that protects them from degradation **[249]**. In addition to its effect on the stability of proteins, the N-terminal pyroglutamate structure can have an important role in the functionality of the protein or peptide, and may be necessary for proper cellular activity **[250-252]**. Until now, the N-terminal acetylation is hypothesized to be involved in mediating protein degradation, prevention of translocation and promotes protein-protein interactions **[253-257].** These examples clearly demonstrate that N-terminal acetylation, as well as the aforementioned modifications in PRR4, promote a variety of biological functions that cannot be predicted from the primary amino acid sequences. Therefore, the fundamental characteristics of PRR4 presented herein will facilitate further investigation on the functional consequences of these modifications in the maintenance of the normal ocular surface system**.** Recent scientific evidence is signifying that the differentiation and quantification of isoforms/ PTMs or the "proteoform" of the proteins could improve insights into disease diagnosis and management **[234, 258].**

In conclusion, the findings of this investigation have demonstrated that highly abundant PRR4 has developed intricate mechanisms of modification, both to increase the diversity of its functions and to regulate various biological activities. However, it remains to be determined how these modifications can affect its activity, localization in the tear layer, protein stability and the ability to form a complex with other molecules for signaling events that orchestrate the biological functions in the ocular system. Furthermore, investigation of these modification patterns in different ophthalmopathologies will provide important biological information towards further understanding of its key role in pathophysiological processes.

6 CONCLUSION

In gist, there are several major findings emerging from the current study. First, several important differential expression of proteins that were never explored extensively in the ocular system were identified. In the discovery study to distinguish the different DES subgroups, 79 potential protein biomarkers were identified. Amongst these proteins, 13 highly differentially expressed proteins were verified by targeted MS analysis. Hence, utilization of multiple tear biomarkers considering multiple biological functional characteristics (i.e. secretion deficiency, metabolic processes, immune response, inflammatory response and protease inhibition) will result in significant improvement of DES diagnostic accuracy. Among the differential proteins, PRR4, ZG16B, SCGB2A1, DMBT1, PROL1, LACRT, ALDH3A1, ENO1, TF, S100A8, S100A9, PEBP1 and ORM1 were verified to be significantly differentially expressed in abundance in DES subgroups, and thus, are highly regarded as potential biomarkers for the pathology.

Second, the results of this study successfully demonstrated that the highly abundant lacrimal gland-specific PRR4 and ZG16B represent the major increased proteins in reflex tears for the first time. This finding highlights the significant regulation of these proteins in tears for the protection of the ocular surface, whereby its deficiency in tears may contribute towards the pathogenesis of DES.

Third, PRR4 proteoforms were extensively characterized in healthy human tears employing the MS system, which resulted in identification of a new PRR4 isoform designated as PRR4-N3. In this study, designation of PRR4 isoforms was systematically simplified as PRR4-N1, PRR4-N2 and PRR4-N3. In addition, combinations of four types of PTMs which are methylation, acetylation, oxidation and pyroglutamate formation were identified for PRR4. The exact functions of the PRR4 and the existence of the variable isoforms and PTMs remain to be explored. To date, the lack of information about the characteristics and standardized designations for PRR4 isoforms has hindered complete understanding of the functions of PRR4 in tears. Therefore, the characteristic profiles of PRR4 elucidated in this study will contribute to the existing body of knowledge and open new avenues for in-depth functional investigation.

Fourth, a rapid and robust targeted data acquisition approach of in-solution digestion based LC-ESI-MS/MS strategy was optimized and developed to relatively quantify proteins in individual tear samples. In view of the fact that tear volume is typically limited in a case

study or a population-based study, the samples are pooled in most experiments and this will consequently hinder the detection and characterization of specific protein isoforms (e.g. PRR4-N1/N2/N3, CST4/CST1, IgA1/2 etc.). However, with the targeted approach employed, only small amounts of tear samples are required and this targeted MS strategy was instrumental for quantifying proteins that cannot be effectively detected by classical antibody-based methods. Additionally, this targeted MS approach is advantageous since multiple protein isoform-specific peptides could be precisely detected in a single MS run. This approach will enable elucidation of protein isoforms regulation, which might have important roles in the various biological processes and can potentially be used as biomarkers or therapeutic targets/ mediators.

In conclusion, this study had identified the major protein biomarkers for specific DES subgroups and further characterized the intricate proteome regulation during reflex tearing, especially the potential role of PRR4 proteoforms, which may be the key player in the protection and maintenance of dynamic balance of the ocular surface. The outcomes of the identification and characterization of these protein biomarkers in this study, when extrapolated to clinical application, can provide invaluable hints on development of specific diagnostic tool for clinical tests and are of great importance for the prognostic usage for improved clinical management of the disease. It is important to highlight here that these protein biomarker panels could be potentially developed for topical protein therapy as effective medical treatments for DES. To date, there are no effective protein therapies available for DES due to the limited major biomarkers identified. The identification of the major deficient proteins in DES in this study, especially PRR4, could be applied as biotherapeutics. Developments of topical eye drops for DES with these recombinant proteins may physiologically rescue the ocular surface when a deficiency is detected. In succession, insights into the characterized PRR4 proteoforms regulations and PRR4-mediated protein interactions, which remain to be elucidated, are proposed to be explored for further understanding of their importance in DES pathogenesis, diagnosis and possible treatment options.

7 REFERENCES

[1] DEWS, The definition and classification of dry eye disease: report of the Definition and Classification Subcommittee of the International Dry Eye WorkShop (2007). *Ocul Surf* 2007, *5*, 75-92.

[2] Herber, S., Grus, F. H., Sabuncuo, P., Augustin, A. J., Two-dimensional analysis of tear protein patterns of diabetic patients. *Electrophoresis* 2001, *22*, 1838-1844.

[3] Tomosugi, N., Kitagawa, K., Takahashi, N., Sugai, S., Ishikawa, I., Diagnostic potential of tear proteomic patterns in Sjögren's syndrome. *Journal of proteome research* 2005, *4*, 820-825.

[4] Tsai, P. S., Evans, J. E., Green, K. M., Sullivan, R. M., *et al.*, Proteomic analysis of human meibomian gland secretions. *The British journal of ophthalmology* 2006, *90*, 372-377.

[5] Li, K., Liu, X., Chen, Z., Huang, Q., Wu, K., Quantification of tear proteins and sPLA2-IIa alteration in patients with allergic conjunctivitis. *Molecular vision* 2010, *16*, 2084.

[6] Zhou, L., Beuerman, R. W., Ang, L. P., Chan, C. M., *et al.*, Elevation of human alpha-defensins and S100 calcium-binding proteins A8 and A9 in tear fluid of patients with pterygium. *Investigative ophthalmology & visual science* 2009, *50*, 2077-2086.

[7] Aluru, S. V., Agarwal, S., Srinivasan, B., Iyer, G. K., *et al.*, Lacrimal proline rich 4 (LPRR4) protein in the tear fluid is a potential biomarker of dry eye syndrome. *PloS one* 2012, *7*, e51979.

[8] Saijyothi, A. V., Angayarkanni, N., Syama, C., Utpal, T., *et al.*, Two dimensional electrophoretic analysis of human tears: collection method in dry eye syndrome. *Electrophoresis* 2010, *31*, 3420-3427.

[9] Schein, O. D., Munoz, B., Tielsch, J. M., Bandeen-Roche, K., West, S., Prevalence of dry eye among the elderly. *American journal of ophthalmology* 1997, *124*, 723-728.

[10] Jie, Y., Xu, L., Wu, Y., Jonas, J., Prevalence of dry eye among adult Chinese in the Beijing Eye Study. *Eye* 2008, *23*, 688-693.

[11] Guo, B., Lu, P., Chen, X., Zhang, W., Chen, R., Prevalence of dry eye disease in Mongolians at high altitude in China: the Henan eye study. *Ophthalmic epidemiology* 2010, *17*, 234-241.

[12] McCarty, C. A., Bansal, A. K., Livingston, P. M., Stanislavsky, Y. L., Taylor, H. R., The epidemiology of dry eye in Melbourne, Australia. *Ophthalmology* 1998, *105*, 1114-1119.

[13] Moss, S. E., Klein, R., Klein, B. E., Prevalence of and risk factors for dry eye syndrome. *Archives of ophthalmology* 2000, *118*, 1264-1268.

[14] Lee, A., Lee, J., Saw, S., Gazzard, G., *et al.*, Prevalence and risk factors associated with dry eye symptoms: a population based study in Indonesia. *British Journal of Ophthalmology* 2002, *86*, 1347-1351.

[15] Viso, E., Rodriguez-Ares, M. T., Gude, F., Prevalence of and associated factors for dry eye in a Spanish adult population (the Salnes Eye Study). *Ophthalmic epidemiology* 2009, *16*, 15-21.

[16] Lekhanont, K., Rojanaporn, D., Chuck, R. S., Vongthongsri, A., Prevalence of dry eye in Bangkok, Thailand. *Cornea* 2006, *25*, 1162-1167.

[17] Chia, E. M., Mitchell, P., Rochtchina, E., Lee, A. J., *et al.*, Prevalence and associations of dry eye syndrome in an older population: the Blue Mountains Eye Study. *Clinical & experimental ophthalmology* 2003, *31*, 229-232.

[18] Lu, P., Chen, X., Liu, X., Yu, L., *et al.*, Dry eye syndrome in elderly Tibetans at high altitude: a population-based study in China. *Cornea* 2008, *27*, 545-551.

[19] Hashemi, H., Khabazkhoob, M., Kheirkhah, A., Emamian, M. H., *et al.*, Prevalence of dry eye syndrome in an adult population. *Clin Experiment Ophthalmol* 2014, *42*, 242-248.

[20] Yu, J., Asche, C. V., Fairchild, C. J., The economic burden of dry eye disease in the United States: a decision tree analysis. *Cornea* 2011, *30*, 379-387.

[21] Waduthantri, S., Yong, S. S., Tan, C. H., Shen, L., *et al.*, Cost of dry eye treatment in an Asian clinic setting. *PloS one* 2012, *7*, e37711.

[22] Lemp, M. A., Foulks, G. N., The definition and classification of dry eye disease. *The Ocular Surface* 2007, *5*, 75-92.

[23] Lemp, A., Sullivan, B. D., Crews, L. A., Biomarkers in dry eye disease. *Eur Ophthal Rev* 2012, *6*, 157-163.

[24] Gilbard, J. P., Rossi, S. R., *Lacrimal Gland, Tear Film, and Dry Eye Syndromes*, Springer 1994, pp. 529-533.

[25] Lemp, M. A., Bron, A. J., Baudouin, C., del Castillo, J. M. B., *et al.*, Tear osmolarity in the diagnosis and management of dry eye disease. *American journal of ophthalmology* 2011, *151*, 792-798. e791.

[26] Liu, H., Begley, C., Chen, M., Bradley, A., *et al.*, A link between tear instability and hyperosmolarity in dry eye. *Investigative ophthalmology & visual science* 2009, *50*, 3671-3679.

[27] Johnson, M. E., Murphy, P. J., Changes in the tear film and ocular surface from dry eye syndrome. *Progress in retinal and eye research* 2004, *23*, 449-474.

[28] Acera, A., Rocha, G., Vecino, E., Lema, I., Durán, J. A., Inflammatory markers in the tears of patients with ocular surface disease. *Ophthalmic research* 2008, *40*, 315.

[29] Luo, L., Li, D.-Q., Corrales, R. M., Pflugfelder, S. C., Hyperosmolar saline is a proinflammatory stress on the mouse ocular surface. *Eye & contact lens* 2005, *31*, 186-193.

[30] Luo, L., Li, D.-Q., Doshi, A., Farley, W., *et al.*, Experimental dry eye stimulates production of inflammatory cytokines and MMP-9 and activates MAPK signaling pathways on the ocular surface. *Investigative ophthalmology & visual science* 2004, *45*, 4293-4301.

[31] Zierhut, M., Dana, M. R., Stern, M. E., Sullivan, D. A., Immunology of the lacrimal gland and ocular tear film. *Trends in immunology* 2002, *23*, 333-335.

[32] Bron, A. J., Diagnosis of dry eye. *Survey of ophthalmology* 2001, *45*, S221-S226.

[33] Nichols, K. K., Nichols, J. J., Mitchell, G. L., The lack of association between signs and symptoms in patients with dry eye disease. *Cornea* 2004, *23*, 762-770.

[34] Lemp, A., Report of the National Eye Institute/Industry Workshop on clinical trials in dry eyes. *Eye & Contact Lens* 1995, *21*, 221-232.

[35] Janssen, P., Van Bijsterveld, O., Tear fluid proteins in Sjogren's syndrome. *Scandinavian journal of rheumatology. Supplement* 1985, *61*, 224-227.

[36] Mackie, I., Seal, D., Confirmatory tests for the dry eye of Sjogren's syndrome. *Scandinavian journal of rheumatology. Supplement* 1985, *61*, 220-223.

[37] Goren, M. B., Goren, S. B., Diagnostic tests in patients with symptoms of keratoconjunctivitis sicca. *American journal of ophthalmology* 1988, *106*, 570-574.

[38] McCollum, C. J., Foulks, G. N., Bodner, B., Shepard, J., *et al.*, Rapid assay of lactoferrin in keratoconjunctivitis sicca. *Cornea* 1994, *13*, 505-508.

[39] Boersma, H., Van Bijsterveld, O., The lactoferrin test for the diagnosis of keratoconjunctivitis sicca in clinical practice. *Annals of ophthalmology* 1987, *19*, 152-154.

[40] Allansmith, M. R., Gillette, T. E., Secretory component in human ocular tissues. *Am J Ophthalmol* 1980, *89*, 353-361.

[41] Dartt, D. A., Signal transduction and control of lacrimal gland protein secretion: a review. *Current eye research* 1989, *8*, 619-636.

[42] Dartt, D. A., Neural regulation of lacrimal gland secretory processes: relevance in dry eye diseases. *Prog Retin Eye Res* 2009, *28*, 155-177.

[43] Butovich, I. A., Tear film lipids. *Experimental eye research* 2013, *117*, 4-27.

[44] Bron, A. J., Tiffany, J. M., Gouveia, S. M., Yokoi, N., Voon, L. W., Functional aspects of the tear film lipid layer. *Exp Eye Res* 2004, *78*, 347-360.

[45] Rolando, M., Zierhut, M., The ocular surface and tear film and their dysfunction in dry eye disease. *Surv Ophthalmol* 2001, *45 Suppl 2*, S203-210.

[46] Stern, M. E., Beuerman, R. W., Fox, R. I., Gao, J., *et al.*, The pathology of dry eye: the interaction between the ocular surface and lacrimal glands. *Cornea* 1998, *17*, 584-589.

[47] Grus, F. H., Podust, V. N., Bruns, K., Lackner, K., *et al.*, SELDI-TOF-MS ProteinChip array profiling of tears from patients with dry eye. *Investigative ophthalmology & visual science* 2005, *46*, 863-876.

[48] Nichols, J. J., Green-Church, K. B., Mass spectrometry-based proteomic analyses in contact lens-related dry eye. *Cornea* 2009, *28*, 1109-1117.

[49] Zhou, L., Beuerman, R. W., Tear analysis in ocular surface diseases. *Prog Retin Eye Res* 2012, *31*, 527-550.

[50] Funke, S., Azimi, D., Wolters, D., Grus, F. H., Pfeiffer, N., Longitudinal analysis of taurine induced effects on the tear proteome of contact lens wearers and dry eye patients using a RP-RP-Capillary-HPLC-MALDI TOF/TOF MS approach. *Journal of proteomics* 2012, *75*, 3177-3190.

[51] Lema, I., Brea, D., Rodriguez-Gonzalez, R., Diez-Feijoo, E., Sobrino, T., Proteomic analysis of the tear film in patients with keratoconus. *Mol Vis* 2010, *16*, 2055-2061.

[52] Zhou, L., Beuerman, R. W., Chan, C. M., Zhao, S. Z., *et al.*, Identification of tear fluid biomarkers in dry eye syndrome using iTRAQ quantitative proteomics. *J Proteome Res* 2009, *8*, 4889-4905.

[53] Ananthi, S., Chitra, T., Bini, R., Prajna, N. V., *et al.*, Comparative analysis of the tear protein profile in mycotic keratitis patients. *Mol Vis* 2008, *14*, 500-507.

[54] Koo, B. S., Lee, D. Y., Ha, H. S., Kim, J. C., Kim, C. W., Comparative analysis of the tear protein expression in blepharitis patients using two-dimensional electrophoresis. *J Proteome Res* 2005, *4*, 719-724.

[55] Herber, S., Grus, F. H., Sabuncuo, P., Augustin, A. J., Two-dimensional analysis of tear protein patterns of diabetic patients. *Electrophoresis* 2001, *22*, 1838-1844.

[56] Boehm, N., Funke, S., Wiegand, M., Wehrwein, N., *et al.*, Alterations in the tear proteome of dry eye patients--a matter of the clinical phenotype. *Investigative ophthalmology & visual science* 2013, *54*, 2385-2392.

[57] Zhou, L., Zhao, S. Z., Koh, S. K., Chen, L., *et al.*, In-depth analysis of the human tear proteome. *Journal of proteomics* 2012, *75*, 3877-3885.

[58] Green-Church, K. B., Nichols, K. K., Kleinholz, N. M., Zhang, L., Nichols, J. J., Investigation of the human tear film proteome using multiple proteomic approaches. *Mol Vis* 2008, *14*, 456-470.

[59] de Souza, G. A., Godoy, L. M., Mann, M., Identification of 491 proteins in the tear fluid proteome reveals a large number of proteases and protease inhibitors. *Genome biology* 2006, *7*, R72.

[60] Zhou, L., Beuerman, R. W., Foo, Y., Liu, S., *et al.*, Characterisation of human tear proteins using high-resolution mass spectrometry. *Annals of the Academy of Medicine, Singapore* 2006, *35*, 400-407.

[61] Li, N., Wang, N., Zheng, J., Liu, X. M., *et al.*, Characterization of human tear proteome using multiple proteomic analysis techniques. *J Proteome Res* 2005, *4*, 2052-2061.

[62] Sack, R. A., Sathe, S., Hackworth, L. A., Willcox, M. D., *et al.*, The effect of eye closure on protein and complement deposition on Group IV hydrogel contact lenses: relationship to tear flow dynamics. *Current eye research* 1996, *15*, 1092-1100.

[63] McGill, J., Liakos, G., Goulding, N., Seal, D., Normal tear protein profiles and age-related changes. *British journal of ophthalmology* 1984, *68*, 316-320.

[64] Kijlstra, A., Polak, B., Luyendijk, L., Transient decrease of secretory IgA in tears during rigid gas permeable contact lens wear. *Current eye research* 1992, *11*, 123-126.

[65] Zhang, Z., Wu, S., Stenoien, D. L., Paša-Tolic, L., High-throughput proteomics. *Annual Review of Analytical Chemistry* 2014, *7*, 427-454.

[66] Szabo, Z., Janaky, T., Challenges and developments in protein identification using mass spectrometry. *TrAC Trends in Analytical Chemistry* 2015.

[67] Ong, S.-E., Foster, L. J., Mann, M., Mass spectrometric-based approaches in quantitative proteomics. *Methods* 2003, *29*, 124-130.

[68] Nahnsen, S., Bielow, C., Reinert, K., Kohlbacher, O., Tools for label-free peptide quantification. *Molecular & Cellular Proteomics* 2013, *12*, 549-556.

[69] Bantscheff, M., Lemeer, S., Savitski, M. M., Kuster, B., Quantitative mass spectrometry in proteomics: critical review update from 2007 to the present. *Analytical and bioanalytical chemistry* 2012, *404*, 939-965.

[70] Cox, J., Mann, M., MaxQuant enables high peptide identification rates, individualized p.p.b.-range mass accuracies and proteome-wide protein quantification. *Nat Biotechnol* 2008, *26*, 1367-1372.

[71] Maher, S., Jjunju, F. P., Taylor, S., Colloquium: 100 years of mass spectrometry: Perspectives and future trends. *Reviews of Modern Physics* 2015, *87*, 113.

[72] Fenn, J. B., Shamamian, V., *PROCEEDINGS OF THE ANNUAL TECHNICAL CONFERENCE-SOCIETY OF VACUUM COATERS* 2004, p. 3.

[73] Fenn, J. B., Mann, M., Meng, C. K., Wong, S. F., Whitehouse, C. M., Electrospray ionization for mass spectrometry of large biomolecules. *Science* 1989, *246*, 64-71.

[74] Tanaka, K., The origin of macromolecule ionization by laser irradiation (Nobel lecture). *Angewandte Chemie International Edition* 2003, *42*, 3860-3870.

[75] Tanaka, K., Waki, H., Ido, Y., Akita, S., *et al.*, Protein and polymer analyses up to m/z 100 000 by laser ionization time? of? flight mass spectrometry. *Rapid communications in mass spectrometry* 1988, *2*, 151-153.

[76] Karas, M., Hillenkamp, F., Laser desorption ionization of proteins with molecular masses exceeding 10,000 daltons. *Analytical chemistry* 1988, *60*, 2299-2301.

[77] Hutchens, T. W., Yip, T. T., New desorption strategies for the mass spectrometric analysis of macromolecules. *Rapid Communications in Mass Spectrometry* 1993, *7*, 576-580.

[78] Li, B., Sheng, M., Li, J., Yan, G., *et al.*, Tear proteomic analysis of Sjögren syndrome patients with dry eye syndrome by two-dimensional-nano-liquid chromatography coupled with tandem mass spectrometry. *Scientific reports* 2014, *4*.

[79] Salvisberg, C., Tajouri, N., Hainard, A., Burkhard, P. R., *et al.*, Exploring the human tear fluid: discovery of new biomarkers in multiple sclerosis. *Proteomics. Clinical applications* 2014, *8*, 185-194.

[80] Leonardi, A., Palmigiano, A., Mazzola, E., Messina, A., *et al.*, Identification of human tear fluid biomarkers in vernal keratoconjunctivitis using iTRAQ quantitative proteomics. *Allergy* 2014, *69*, 254-260.

[81] Srinivasan, S., Thangavelu, M., Zhang, L., Green, K. B., Nichols, K. K., iTRAQ quantitative proteomics in the analysis of tears in dry eye patients. *Investigative ophthalmology & visual science* 2012, *53*, 5052-5059.

[82] Guilhaus, M., Principles and instrumentation in time-of-flight mass spectrometry. *J. Mass Spectrom* 1995, *30*, 1519-1532.

[83] Morris, H. R., Paxton, T., Dell, A., Langhorne, J., *et al.*, High sensitivity collisionally-activated decomposition tandem mass spectrometry on a novel quadrupole/orthogonal-acceleration time-of-flight mass spectrometer. *Rapid Communications in Mass Spectrometry* 1996, *10*, 889-896.

[84] Makarov, A., *Proceedings of the 48th ASMS conference on mass spectrometry and allied topics, Dallas, TX* 1999.

[85] Hu, Q., Noll, R. J., Li, H., Makarov, A., *et al.*, The Orbitrap: a new mass spectrometer. *Journal of mass spectrometry* 2005, *40*, 430-443.

[86] Zubarev, R. A., Makarov, A., Orbitrap mass spectrometry. *Analytical chemistry* 2013, *85*, 5288-5296.

[87] Carvalho, A. S., Penque, D., Matthiesen, R., Bottom up proteomics data analysis strategies to explore protein modifications and genomic variants. *Proteomics* 2015.

[88] Catherman, A. D., Skinner, O. S., Kelleher, N. L., Top down proteomics: facts and perspectives. *Biochemical and biophysical research communications* 2014, *445*, 683-693.

[89] Shi, Y., Xiang, R., Horváth, C., Wilkins, J. A., The role of liquid chromatography in proteomics. *Journal of Chromatography A* 2004, *1053*, 27-36.

[90] Ishihama, Y., Proteomic LC–MS systems using nanoscale liquid chromatography with tandem mass spectrometry. *Journal of Chromatography A* 2005, *1067*, 73-83.

[91] Shen, Y., Zhao, R., Belov, M. E., Conrads, T. P., *et al.*, Packed capillary reversed-phase liquid chromatography with high-performance electrospray ionization Fourier transform ion cyclotron resonance mass spectrometry for proteomics. *Analytical chemistry* 2001, *73*, 1766-1775.

[92] Lau, K. W., Jones, A. R., Swainston, N., Siepen, J. A., Hubbard, S. J., Capture and analysis of quantitative proteomic data. *Proteomics* 2007, *7*, 2787-2799.

[93] Hessling, B., Büttner, K., Hecker, M., Becher, D., Global relative quantification with LC-MALDI-cross-validation with LTQ-Orbitrap proves reliability and reveals complementary ionization preferences. *Molecular & Cellular Proteomics* 2013, mcp. M112. 023457.

[94] Marouga, R., David, S., Hawkins, E., The development of the DIGE system: 2D fluorescence difference gel analysis technology. *Analytical and bioanalytical chemistry* 2005, *382*, 669-678.

[95] Minden, J., Comparative proteomics and difference gel electrophoresis. *Biotechniques* 2007, *43*, 739.

[96] Ong, S.-E., Blagoev, B., Kratchmarova, I., Kristensen, D. B., *et al.*, Stable isotope labeling by amino acids in cell culture, SILAC, as a simple and accurate approach to expression proteomics. *Molecular & cellular proteomics* 2002, *1*, 376-386.

[97] Gygi, S. P., Rist, B., Gerber, S. A., Turecek, F., *et al.*, Quantitative analysis of complex protein mixtures using isotope-coded affinity tags. *Nature biotechnology* 1999, *17*, 994-999.

[98] Gygi, S. P., Rist, B., Griffin, T. J., Eng, J., Aebersold, R., Proteome analysis of low-abundance proteins using multidimensional chromatography and isotope-coded affinity tags. *Journal of proteome research* 2002, *1*, 47-54.

[99] Weisser, H., Nahnsen, S., Grossmann, J., Nilse, L., *et al.*, An automated pipeline for high-throughput label-free quantitative proteomics. *Journal of proteome research* 2013, *12*, 1628-1644.

[100] Bantscheff, M., Schirle, M., Sweetman, G., Rick, J., Kuster, B., Quantitative mass spectrometry in proteomics: a critical review. *Analytical and bioanalytical chemistry* 2007, *389*, 1017-1031.

[101] Matzke, M. M., Brown, J. N., Gritsenko, M. A., Metz, T. O., *et al.*, A comparative analysis of computational approaches to relative protein quantification using peptide peak intensities in label-free LC-MS proteomics experiments. *Proteomics* 2013, *13*, 493-503.

[102] Cox, J., Hein, M. Y., Luber, C. A., Paron, I., *et al.*, MaxLFQ allows accurate proteome-wide label-free quantification by delayed normalization and maximal peptide ratio extraction. *Molecular & Cellular Proteomics* 2014, mcp. M113. 031591.

[103] Cox, J., Neuhauser, N., Michalski, A., Scheltema, R. A., *et al.*, Andromeda: a peptide search engine integrated into the MaxQuant environment. *Journal of proteome research* 2011, *10*, 1794-1805.

[104] Posa, A., Bräuer, L., Schicht, M., Garreis, F., *et al.*, Schirmer strip vs. capillary tube method: non-invasive methods of obtaining proteins from tear fluid. *Annals of Anatomy-Anatomischer Anzeiger* 2013, *195*, 137-142.

[105] Pieragostino, D., D'Alessandro, M., di Ioia, M., Di Ilio, C., *et al.*, Unraveling the molecular repertoire of tears as a source of biomarkers: Beyond ocular diseases. *PROTEOMICS-Clinical Applications* 2015.

[106] Boehm, N., Funke, S., Wiegand, M., Wehrwein, N., *et al.*, Alterations in the tear proteome of dry-eye patients - a matter of the clinical phenotype. *Investigative ophthalmology & visual science* 2013.

[107] Soria, J., Duran, J. A., Etxebarria, J., Merayo, J., *et al.*, Tear proteome and protein network analyses reveal a novel pentamarker panel for tear film characterization in dry eye and meibomian gland dysfunction. *Journal of proteomics* 2013, *78*, 94-112.

[108] Fullard, R. J., Snyder, C., Protein levels in nonstimulated and stimulated tears of normal human subjects. *Investigative ophthalmology & visual science* 1990, *31*, 1119-1126.

[109] Fullard, R. J., Tucker, D. L., Changes in human tear protein levels with progressively increasing stimulus. *Investigative ophthalmology & visual science* 1991, *32*, 2290-2301.

[110] Snyder, C., Fullard, R. J., Clinical profiles of non dry eye patients and correlations with tear protein levels. *International ophthalmology* 1991, *15*, 383-389.

[111] Sonoda, S., Uchino, E., Nakao, K., Sakamoto, T., Inflammatory cytokine of basal and reflex tears analysed by multicytokine assay. *The British journal of ophthalmology* 2006, *90*, 120-122.

[112] Sack, R. A., Tan, K. O., Tan, A., Diurnal tear cycle: evidence for a nocturnal inflammatory constitutive tear fluid. *Investigative ophthalmology & visual science* 1992, *33*, 626-640.

[113] Dickinson, D. P., Thiesse, M., A major human lacrimal gland mRNA encodes a new proline-rich protein family member. *Investigative ophthalmology & visual science* 1995, *36*, 2020-2031.

[114] Ozyildirim, A. M., Wistow, G. J., Gao, J., Wang, J., *et al.*, The lacrimal gland transcriptome is an unusually rich source of rare and poorly characterized gene transcripts. *Investigative ophthalmology & visual science* 2005, *46*, 1572-1580.

[115] Boze, H., Marlin, T., Durand, D., Perez, J., *et al.*, Proline-rich salivary proteins have extended conformations. *Biophysical journal* 2010, *99*, 656-665.

[116] Ligtenberg, A. J., Walgreen-Weterings, E., Veerman, E. C., de Soet, J. J., *et al.*, Influence of saliva on aggregation and adherence of Streptococcus gordonii HG 222. *Infection and immunity* 1992, *60*, 3878-3884.

[117] Gibbons, R. J., Bacterial adhesion to oral tissues: a model for infectious diseases. *Journal of dental research* 1989, *68*, 750-760.

[118] Hatton, M. N., Loomis, R. E., Levine, M. J., Tabak, L. A., Masticatory lubrication. The role of carbohydrate in the lubricating property of a salivary glycoprotein-albumin complex. *The Biochemical journal* 1985, *230*, 817-820.

[119] Fábián, T. K., Hermann, P., Beck, A., Fejérdy, P., Fábián, G., Salivary defense proteins: their network and role in innate and acquired oral immunity. *International journal of molecular sciences* 2012, *13*, 4295-4320.

[120] Matheis, N., Okrojek, R., Grus, F. H., Kahaly, G. J., Proteomics of tear fluid in thyroid-associated orbitopathy. *Thyroid : official journal of the American Thyroid Association* 2012, *22*, 1039-1045.

[121] Csosz, E., Boross, P., Csutak, A., Berta, A., *et al.*, Quantitative analysis of proteins in the tear fluid of patients with diabetic retinopathy. *Journal of proteomics* 2012, *75*, 2196-2204.

[122] Acera, A., Vecino, E., Rodriguez-Agirretxe, I., Aloria, K., *et al.*, Changes in tear protein profile in keratoconus disease. *Eye (London, England)* 2011, *25*, 1225-1233.

[123] Fischer, A. J., Goss, K. L., Scheetz, T. E., Wohlford-Lenane, C. L., *et al.*, Differential gene expression in human conducting airway surface epithelia and submucosal glands. *American journal of respiratory cell and molecular biology* 2009, *40*, 189-199.

[124] Lamkin, M. S., Arancillo, A. A., Oppenheim, F. G., Temporal and compositional characteristics of salivary protein adsorption to hydroxyapatite. *Journal of dental research* 1996, *75*, 803-808.

[125] Casado, B., Iadarola, P., Pannell, L. K., Luisetti, M., *et al.*, Protein expression in sputum of smokers and chronic obstructive pulmonary disease patients: a pilot study by CapLC-ESI-Q-TOF. *J Proteome Res* 2007, *6*, 4615-4623.

[126] Zinovyeva, M. V., Monastyrskaya, G. S., Kopantzev, E. P., Vinogradova, T. V., *et al.*, Identification of some human genes oppositely regulated during esophageal squamous cell carcinoma formation and human embryonic esophagus development. *Diseases of the esophagus : official journal of the International Society for Diseases of the Esophagus / I.S.D.E* 2010, *23*, 260-270.

[127] Fung, K. Y., Morris, C., Sathe, S., Sack, R., Duncan, M. W., Characterization of the in vivo forms of lacrimal-specific proline-rich proteins in human tear fluid. *Proteomics* 2004, *4*, 3953-3959.

[128] Gipson, I. K., Research in dry eye: report of the Research Subcommittee of the International Dry Eye WorkShop (2007). *The Ocular Surface* 2007, *5*, 179-193.

[129] Grus, F. H., Augustin, A. J., Analysis of tear protein patterns by a neural network as a diagnostical tool for the detection of dry eyes. *From Genome to Proteome: Advances in the Practice and Application of Proteomics*, 295-300.

[130] Grus, F. H. A., A. J, High performance liquid chromatography analysis of tear protein patterns in diabetic and non-diabetic dry-eye patients *European Journal of Ophthalmology* 2001, *11*.

[131] Versura, P., Nanni, P., Bavelloni, A., Blalock, W. L., *et al.*, Tear proteomics in evaporative dry eye disease. *Eye (London, England)* 2010, *24*, 1396-1402.

[132] Craig, J. P., Tomlinson, A., Importance of the lipid layer in human tear film stability and evaporation. *Optometry & Vision Science* 1997, *74*, 8-13.

[133] Maïssa, C., Guillon, M., Tear film dynamics and lipid layer characteristics—Effect of age and gender. *Contact Lens and Anterior Eye* 2010, *33*, 176-182.

[134] Tong, L., Chaurasia, S. S., Mehta, J. S., Beuerman, R. W., Screening for meibomian gland disease: its relation to dry eye subtypes and symptoms in a tertiary referral clinic in singapore. *Investigative ophthalmology & visual science* 2010, *51*, 3449-3454.

[135] Foulks, G. N., Bron, A. J., Meibomian gland dysfunction: a clinical scheme for description, diagnosis, classification, and grading. *The ocular surface* 2003, *1*, 107-126.

[136] Taylor, C. F., Paton, N. W., Lilley, K. S., Binz, P.-A., *et al.*, The minimum information about a proteomics experiment (MIAPE). *Nature biotechnology* 2007, *25*, 887-893.

[137] Martínez-Bartolomé, S., Binz, P.-A., Albar, J. P., *Plant Proteomics*, Springer 2014, pp. 765-780.

[138] Shevchenko, A., Tomas, H., Havlis, J., Olsen, J. V., Mann, M., In-gel digestion for mass spectrometric characterization of proteins and proteomes. *Nature protocols* 2006, *1*, 2856-2860.

[139] Perumal, N., Funke, S., Pfeiffer, N., Grus, F. H., Characterization of Lacrimal Proline-Rich Protein 4 (PRR4) in Human Tear Proteome. *Proteomics* 2014.

[140] Olsen, J. V., de Godoy, L. M., Li, G., Macek, B., *et al.*, Parts per million mass accuracy on an Orbitrap mass spectrometer via lock mass injection into a C-trap. *Molecular & cellular proteomics : MCP* 2005, *4*, 2010-2021.

[141] Luber, C. A., Cox, J., Lauterbach, H., Fancke, B., *et al.*, Quantitative proteomics reveals subset-specific viral recognition in dendritic cells. *Immunity* 2010, *32*, 279-289.

[142] Schwanhäusser, B., Busse, D., Li, N., Dittmar, G., *et al.*, Global quantification of mammalian gene expression control. *Nature* 2011, *473*, 337-342.

[143] Lu, P., Vogel, C., Wang, R., Yao, X., Marcotte, E. M., Absolute protein expression profiling estimates the relative contributions of transcriptional and translational regulation. *Nature biotechnology* 2006, *25*, 117-124.

[144] Malmström, J., Beck, M., Schmidt, A., Lange, V., *et al.*, Proteome-wide cellular protein concentrations of the human pathogen Leptospira interrogans. *Nature* 2009, *460*, 762-765.

[145] Jaffe, J. D., Keshishian, H., Chang, B., Addona, T. A., *et al.*, Accurate Inclusion Mass Screening A Bridge from Unbiased Discovery to Targeted Assay Development for Biomarker Verification. *Molecular & Cellular Proteomics* 2008, *7*, 1952-1962.

[146] Savitski, M. M., Fischer, F., Mathieson, T., Sweetman, G., *et al.*, Targeted data acquisition for improved reproducibility and robustness of proteomic mass spectrometry assays. *Journal of the American Society for Mass Spectrometry* 2010, *21*, 1668-1679.

[147] Rifai, N., Gillette, M. A., Carr, S. A., Protein biomarker discovery and validation: the long and uncertain path to clinical utility. *Nature biotechnology* 2006, *24*, 971-983.

[148] Blais, D. R., Vascotto, S. G., Griffith, M., Altosaar, I., LBP and CD14 secreted in tears by the lacrimal glands modulate the LPS response of corneal epithelial cells. *Investigative ophthalmology & visual science* 2005, *46*, 4235-4244.

[149] Hayakawa, E., Landuyt, B., Baggerman, G., Cuyvers, R., *et al.*, Peptidomic analysis of human reflex tear fluid. *Peptides* 2013, *42*, 63-69.

[150] Schneider, C. A., Rasband, W. S., Eliceiri, K. W., NIH Image to ImageJ: 25 years of image analysis. *Nature methods* 2012, *9*, 671-675.

[151] Ma, B., Zhang, K., Hendrie, C., Liang, C., *et al.*, PEAKS: powerful software for peptide de novo sequencing by tandem mass spectrometry. *Rapid communications in mass spectrometry : RCM* 2003, *17*, 2337-2342.

[152] Han, X., He, L., Xin, L., Shan, B., Ma, B., PeaksPTM: Mass spectrometry-based identification of peptides with unspecified modifications. *J Proteome Res* 2011, *10*, 2930-2936.

[153] Ohashi, Y., Ishida, R., Kojima, T., Goto, E., *et al.*, Abnormal protein profiles in tears with dry eye syndrome. *American journal of ophthalmology* 2003, *136*, 291-299.

[154] Issaq, H., Veenstra, T., Two-dimensional polyacrylamide gel electrophoresis (2D-PAGE): advances and perspectives. *Biotechniques* 2008, *44*, 697-698, 700.

[155] Zhou, W., Capello, M., Fredolini, C., Piemonti, L., *et al.*, Mass spectrometry analysis of the post-translational modifications of α-enolase from pancreatic ductal adenocarcinoma cells. *Journal of proteome research* 2010, *9*, 2929-2936.

[156] De Lisle, R. C., Hopfer, U., Electrolyte permeabilities of pancreatic zymogen granules: implications for pancreatic secretion. *The American journal of physiology* 1986, *250*, G489-496.

[157] Guo, X. W., Merlin, D., Laboisse, C., Hopfer, U., Purinergic agonists, but not cAMP, stimulate coupled granule fusion and Cl- conductance in HT29-Cl.16E. *The American journal of physiology* 1997, *273*, C804-809.

[158] Kanagawa, M., Satoh, T., Ikeda, A., Nakano, Y., *et al.*, Crystal structures of human secretory proteins ZG16p and ZG16b reveal a Jacalin-related beta-prism fold. *Biochemical and biophysical research communications* 2011, *404*, 201-205.

[159] Neuschwander-Tetri, B. A., Fimmel, C. J., Kladney, R. D., Wells, L. D., Talkad, V., Differential expression of the trypsin inhibitor SPINK3 mRNA and the mouse ortholog of secretory granule protein ZG-16p mRNA in the mouse pancreas after repetitive injury. *Pancreas* 2004, *28*, e104-111.

[160] Kim, S. A., Lee, Y., Jung, D. E., Park, K. H., *et al.*, Pancreatic adenocarcinoma up-regulated factor (PAUF), a novel up-regulated secretory protein in pancreatic ductal adenocarcinoma. *Cancer science* 2009, *100*, 828-836.

[161] Lee, Y., Kim, S. J., Park, H. D., Park, E. H., *et al.*, PAUF functions in the metastasis of human pancreatic cancer cells and upregulates CXCR4 expression. *Oncogene* 2010, *29*, 56-67.

[162] Barderas, R., Mendes, M., Torres, S., Bartolomé, R. A., *et al.*, In-depth characterization of the secretome of colorectal cancer metastatic cells identifies key proteins in cell adhesion, migration, and invasion. *Molecular & Cellular Proteomics* 2013, *12*, 1602-1620.

[163] Dufour, E., Villard-Saussine, S., Mellon, V., Leandri, R., *et al.*, Opiorphin secretion pattern in healthy volunteers: gender difference and organ specificity. *Biochem Anal Biochem* 2013, *2*, 2-11.

[164] Benson, M., Carlsson, L., Adner, M., Jernås, M., *et al.*, Gene profiling reveals increased expression of uteroglobin and other anti-inflammatory genes in glucocorticoid-treated nasal polyps. *Journal of allergy and clinical immunology* 2004, *113*, 1137-1143.

[165] Aihara, T., Fujiwara, Y., Ooka, M., Sakita, I., *et al.*, Mammaglobin B as a novel marker for detection of breast cancer micrometastases in axillary lymph nodes by reverse transcription-polymerase chain reaction. *Breast cancer research and treatment* 1999, *58*, 137-140.

[166] O'Brien, N., Maguire, T. M., O'Donovan, N., Lynch, N., *et al.*, Mammaglobin a: a promising marker for breast cancer. *Clinical chemistry* 2002, *48*, 1362-1364.

[167] Mercatali, L., Valenti, V., Calistri, D., Calpona, S., *et al.*, RT-PCR determination of maspin and mammaglobin B in peripheral blood of healthy donors and breast cancer patients. *Annals of oncology* 2006, *17*, 424-428.

[168] Ooka, M., Sakita, I., Fujiwara, Y., Tamaki, Y., *et al.*, Selection of mRNA markers for detection of lymph node micrometastases in breast cancer patients. *Oncology reports* 2000, *7*, 561-567.

[169] Nissan, A., Jager, D., Roystacher, M., Prus, D., *et al.*, Multimarker RT–PCR assay for the detection of minimal residual disease in sentinel lymph nodes of breast cancer patients. *British journal of cancer* 2006, *94*, 681-685.

[170] Bellone, S., Tassi, R., Betti, M., English, D., *et al.*, Mammaglobin B (SCGB2A1) is a novel tumour antigen highly differentially expressed in all major histological types of ovarian cancer: implications for ovarian cancer immunotherapy. *British journal of cancer* 2013, *109*, 462-471.

[171] Xiao, F., Mirwald, A., Papaioannou, M., Baniahmad, A., Klug, J. r., Secretoglobin 2A1 is under selective androgen control mediated by a peculiar binding site for Sp family transcription factors. *Molecular Endocrinology* 2005, *19*, 2964-2978.

[172] Prakobphol, A., Xu, F., Hoang, V. M., Larsson, T., *et al.*, Salivary agglutinin, which binds streptococcus mutansand helicobacter pylori, is the lung scavenger receptor

cysteine-rich protein gp-340. *Journal of Biological Chemistry* 2000, *275*, 39860-39866.

[173] Mollenhauer, J., Herbertz, S., Helmke, B., Kollender, G., *et al.*, Deleted in Malignant Brain Tumors 1 is a versatile mucin-like molecule likely to play a differential role in digestive tract cancer. *Cancer research* 2001, *61*, 8880-8886.

[174] Mollenhauer, J., End, C., Renner, M., Lyer, S., Poustka, A., DMBT1 as an archetypal link between infection, inflammation, and cancer. *Inmunologia* 2007, *26*, 193-209.

[175] Rosenstiel, P., Sina, C., End, C., Renner, M., *et al.*, Regulation of DMBT1 via NOD2 and TLR4 in intestinal epithelial cells modulates bacterial recognition and invasion. *The Journal of Immunology* 2007, *178*, 8203-8211.

[176] End, C., Bikker, F., Renner, M., Bergmann, G., *et al.*, DMBT1 functions as pattern-recognition molecule for poly-sulfated and poly-phosphorylated ligands. *European journal of immunology* 2009, *39*, 833-842.

[177] De Lisle, R. C., Ziemer, D., Processing of pro-Muclin and divergent trafficking of its products to zymogen granules and the apical plasma membrane of pancreatic acinar cells. *European journal of cell biology* 2000, *79*, 892-904.

[178] McKown, R. L., Wang, N., Raab, R. W., Karnati, R., *et al.*, Lacritin and other new proteins of the lacrimal functional unit. *Experimental eye research* 2009, *88*, 848-858.

[179] Karnati, R., Laurie, D. E., Laurie, G. W., Lacritin and the tear proteome as natural replacement therapy for dry eye. *Experimental eye research* 2013, *117*, 39-52.

[180] Sanghi, S., Kumar, R., Lumsden, A., Dickinson, D., *et al.*, cDNA and genomic cloning of lacritin, a novel secretion enhancing factor from the human lacrimal gland. *Journal of molecular biology* 2001, *310*, 127-139.

[181] Samudre, S., Lattanzio, F. A., Lossen, V., Hosseini, A., *et al.*, Lacritin, a novel human tear glycoprotein, promotes sustained basal tearing and is well tolerated. *Investigative ophthalmology & visual science* 2011, *52*, 6265-6270.

[182] Heizmann, C. W., Fritz, G., Schafer, B., S100 proteins: structure, functions and pathology. *Front Biosci* 2002, *7*, 1356-1368.

[183] Riau, A. K., Wong, T. T., Beuerman, R. W., Tong, L., Calcium-binding S100 protein expression in pterygium. *Molecular vision* 2009, *15*, 335.

[184] McKiernan, E., McDermott, E. W., Evoy, D., Crown, J., Duffy, M. J., The role of S100 genes in breast cancer progression. *Tumor Biology* 2011, *32*, 441-450.

[185] Pancholi, V., Multifunctional α-enolase: its role in diseases. *Cellular and Molecular Life Sciences CMLS* 2001, *58*, 902-920.

[186] Li, J., Qin, J., Zhang, H., Shan, Z., Teng, W., OR12-2: Direct Identification of Alpha-Enolase As an Autoantigen in the Pathogenesis of Autoimmune Thyroiditis. 2014.

[187] Capello, M., Principe, M., Chattaragada, M. S., Riganti, C., *et al.*, Can the moonlighting glycolytic enzyme {alpha}-enolase be a therapeutic target in pancreatic cancer. *Cancer Research* 2013, *73*, 1889.

[188] Díaz-Ramos, À., Roig-Borrellas, A., García-Melero, A., López-Alemany, R., α-Enolase, a multifunctional protein: its role on pathophysiological situations. *BioMed Research International* 2012, *2012*.

[189] Hochepied, T., Berger, F. G., Baumann, H., Libert, C., α 1-Acid glycoprotein: an acute phase protein with inflammatory and immunomodulating properties. *Cytokine & growth factor reviews* 2003, *14*, 25-34.

[190] Taguchi, K., Nishi, K., Chuang, V. T. G., Maruyama, T., Otagiri, M., Molecular Aspects of Human Alpha-1 Acid Glycoprotein—Structure and Function. *Immunology, Allergology and Rheumatology»" Acute Phase Proteins* 2013, 139-162.

[191] CRICHTON, R. R., CHARLOTEAUX-WAUTERS, M., Iron transport and storage. *European Journal of Biochemistry* 1987, *164*, 485-506.

[192] Chasteen, N. D., Human serotransferrin: structure and function. *Coordination Chemistry Reviews* 1977, *22*, 1-36.

[193] Castellano, A., Barteri, M., Castagnola, M., Bianconi, A., *et al.*, Structure-function relationship in the serotransferrin: the role of the pH on the conformational change and the metal ions release. *Biochemical and biophysical research communications* 1994, *198*, 646-652.

[194] Al-Mulla, F., Bitar, M. S., Taqi, Z., Yeung, K. C., RKIP: much more than Raf kinase inhibitory protein. *Journal of cellular physiology* 2013, *228*, 1688-1702.

[195] Yeung, K., Seitz, T., Li, S., Janosch, P., *et al.*, Suppression of Raf-1 kinase activity and MAP kinase signalling by RKIP. *nature* 1999, *401*, 173-177.

[196] Pappa, A., Estey, T., Manzer, R., Brown, D., Vasiliou, V., Human aldehyde dehydrogenase 3A1 (ALDH3A1): biochemical characterization and immunohistochemical localization in the cornea. *Biochem. J* 2003, *376*, 615-623.

[197] Gondhowiardjo, T. D., van Haeringen, N. J., Völker-Dieben, H. J., Beekhuis, H. W., *et al.*, Analysis of corneal aldehyde dehydrogenase patterns in pathologic corneas. *Cornea* 1993, *12*, 146-154.

[198] Lassen, N., Bateman, J. B., Estey, T., Kuszak, J. R., *et al.*, Multiple and Additive Functions of ALDH3A1 and ALDH1A1 CATARACT PHENOTYPE AND OCULAR OXIDATIVE DAMAGE IN Aldh3a1 (-/-)/Aldh1a1 (-/-) KNOCK-OUT MICE. *Journal of Biological Chemistry* 2007, *282*, 25668-25676.

[199] Kolozsvári, L., Nógrádi, A., Hopp, B., Bor, Z., UV absorbance of the human cornea in the 240-to 400-nm range. *Investigative ophthalmology & visual science* 2002, *43*, 2165-2168.

[200] Estey, T., Piatigorsky, J., Lassen, N., Vasiliou, V., ALDH3A1: a corneal crystallin with diverse functions. *Experimental eye research* 2007, *84*, 3-12.

[201] Chen, Y., Thompson, D. C., Koppaka, V., Jester, J. V., Vasiliou, V., Ocular aldehyde dehydrogenases: Protection against ultraviolet damage and maintenance of transparency for vision. *Progress in retinal and eye research* 2013, *33*, 28-39.

[202] Ganeshan, K., Chawla, A., Metabolic regulation of immune responses. *Annual review of immunology* 2014, *32*, 609-634.

[203] Braun, M., Thevenod, F., Photoaffinity labeling and purification of ZG-16p, a high-affinity dihydropyridine binding protein of rat pancreatic zymogen granule membranes that regulates a K(+)-selective conductance. *Molecular pharmacology* 2000, *57*, 308-316.

[204] Thevenod, F., Ion channels in secretory granules of the pancreas and their role in exocytosis and release of secretory proteins. *American journal of physiology. Cell physiology* 2002, *283*, C651-672.

[205] Botelho, S. Y., Martinez, E. V., Pholpramool, C., Prooyen, H. C., *et al.*, Modification of stimulated lacrimal gland flow by sympathetic nerve impulses in rabbit. *The American journal of physiology* 1976, *230*, 80-84.

[206] Jirsova, K., Neuwirth, A., Kalasova, S., Vesela, V., Merjava, S., Mesothelial proteins are expressed in the human cornea. *Exp Eye Res* 2010, *91*, 623-629.

[207] Argueso, P., Glycobiology of the ocular surface: mucins and lectins. *Japanese journal of ophthalmology* 2013, *57*, 150-155.

[208] Blalock, T. D., Spurr-Michaud, S. J., Tisdale, A. S., Gipson, I. K., Release of membrane-associated mucins from ocular surface epithelia. *Investigative ophthalmology & visual science* 2008, *49*, 1864-1871.

[209] Gipson, I. K., Distribution of mucins at the ocular surface. *Exp Eye Res* 2004, *78*, 379-388.

[210] Hodges, R. R., Dartt, D. A., Tear film mucins: front line defenders of the ocular surface; comparison with airway and gastrointestinal tract mucins. *Exp Eye Res* 2013, *117*, 62-78.

[211] Rojas, R., Apodaca, G., Immunoglobulin transport across polarized epithelial cells. *Nature reviews. Molecular cell biology* 2002, *3*, 944-955.

[212] Phalipon, A., Corthesy, B., Novel functions of the polymeric Ig receptor: well beyond transport of immunoglobulins. *Trends Immunol* 2003, *24*, 55-58.

[213] Kaetzel, C. S., The polymeric immunoglobulin receptor: bridging innate and adaptive immune responses at mucosal surfaces. *Immunological reviews* 2005, *206*, 83-99.

[214] Xu, S., Ma, L., Evans, E., Okamoto, C. T., Hamm-Alvarez, S. F., Polymeric immunoglobulin receptor traffics through two distinct apically targeted pathways in primary lacrimal gland acinar cells. *Journal of cell science* 2013, *126*, 2704-2717.

[215] Evans, E., Zhang, W., Jerdeva, G., Chen, C. Y., *et al.*, Direct interaction between Rab3D and the polymeric immunoglobulin receptor and trafficking through regulated secretory vesicles in lacrimal gland acinar cells. *American journal of physiology. Cell physiology* 2008, *294*, C662-674.

[216] Stolze, H., Sommer, H., Effect of different secretagogues on rabbit lacrimal gland protein secretion. *The Preocular Tear Film in Health, Disease and Contact Lens Wear* 1986, 409-415.

[217] Newkirk, M. M., Apostolakos, P., Neville, C., Fortin, P. R., Systemic lupus erythematosus, a disease associated with low levels of clusterin/apoJ, an antiinflammatory protein. *The Journal of rheumatology* 1999, *26*, 597-603.

[218] Hogasen, K., Mollnes, T. E., Harboe, M., Gotze, O., *et al.*, Terminal complement pathway activation and low lysis inhibitors in rheumatoid arthritis synovial fluid. *The Journal of rheumatology* 1995, *22*, 24-28.

[219] Nakamura, T., Nishida, K., Dota, A., Kinoshita, S., Changes in conjunctival clusterin expression in severe ocular surface disease. *Investigative ophthalmology & visual science* 2002, *43*, 1702-1707.

[220] Barka, T., Asbell, P. A., van der Noen, H., Prasad, A., Cystatins in human tear fluid. *Current eye research* 1991, *10*, 25-34.

[221] Levin, L. A., Avery, R., Shore, J. W., Woog, J. J., Baker, A. S., The spectrum of orbital aspergillosis: a clinicopathological review. *Surv Ophthalmol* 1996, *41*, 142-154.

[222] ter Rahe, B. S., van Haeringen, N. J., Cystatins in tears of patients with different corneal conditions. *Ophthalmologica. Journal international d'ophtalmologie. International journal of ophthalmology. Zeitschrift fur Augenheilkunde* 1998, *212*, 34-36.

[223] Acera, A., Suarez, T., Rodriguez-Agirretxe, I., Vecino, E., Duran, J. A., Changes in tear protein profile in patients with conjunctivochalasis. *Cornea* 2011, *30*, 42-49.

[224] Balasubramanian, S. A., Wasinger, V. C., Pye, D. C., Willcox, M. D., Preliminary identification of differentially expressed tear proteins in keratoconus. *Mol Vis* 2013, *19*, 2124-2134.

[225] Bennick, A., Structural and genetic aspects of proline-rich proteins. *Journal of dental research* 1987, *66*, 457-461.

[226] Lange, V., Picotti, P., Domon, B., Aebersold, R., Selected reaction monitoring for quantitative proteomics: a tutorial. *Molecular systems biology* 2008, *4*, 222.

[227] Kitteringham, N. R., Jenkins, R. E., Lane, C. S., Elliott, V. L., Park, B. K., Multiple reaction monitoring for quantitative biomarker analysis in proteomics and metabolomics. *Journal of chromatography. B, Analytical technologies in the biomedical and life sciences* 2009, *877*, 1229-1239.

[228] Malmstrom, L., Malmstrom, J., Selevsek, N., Rosenberger, G., Aebersold, R., Automated workflow for large-scale selected reaction monitoring experiments. *J Proteome Res* 2012, *11*, 1644-1653.

[229] Sung, H. J., Jeon, S. A., Ahn, J. M., Seul, K. J., *et al.*, Large-scale isotype-specific quantification of Serum amyloid A 1/2 by multiple reaction monitoring in crude sera. *Journal of proteomics* 2012, *75*, 2170-2180.

[230] Wu, J., Pungaliya, P., Kraynov, E., Bates, B., Identification and quantification of osteopontin splice variants in the plasma of lung cancer patients using immunoaffinity capture and targeted mass spectrometry. *Biomarkers : biochemical indicators of exposure, response, and susceptibility to chemicals* 2012, *17*, 125-133.

[231] Omali, N. B., Zhao, Z., Zhu, H., Tilia, D., Willcox, M. D., Quantification of individual proteins in silicone hydrogel contact lens deposits. *Mol Vis* 2013, *19*, 390-399.

[232] Blencowe, B. J., Alternative splicing: new insights from global analyses. *Cell* 2006, *126*, 37-47.

[233] Matlin, A. J., Clark, F., Smith, C. W., Understanding alternative splicing: towards a cellular code. *Nature reviews. Molecular cell biology* 2005, *6*, 386-398.

[234] Stastna, M., Van Eyk, J. E., Analysis of protein isoforms: can we do it better? *Proteomics* 2012, *12*, 2937-2948.

[235] Yi, Q., Tang, L., Alternative spliced variants as biomarkers of colorectal cancer. *Current drug metabolism* 2011, *12*, 966-974.

[236] Hilmi, C., Guyot, M., Pages, G., VEGF spliced variants: possible role of anti-angiogenesis therapy. *Journal of nucleic acids* 2012, *2012*, 162692.

[237] Blair, C. A., Zi, X., Potential molecular targeting of splice variants for cancer treatment. *Indian journal of experimental biology* 2011, *49*, 836-839.

[238] Shokeer, A., Mannervik, B., Minor modifications of the C-terminal helix reschedule the favored chemical reactions catalyzed by theta class glutathione transferase T1-1. *The Journal of biological chemistry* 2010, *285*, 5639-5645.

[239] You, J., Fitzgerald, A., Cozzi, P. J., Zhao, Z., *et al.*, Post-translation modification of proteins in tears. *Electrophoresis* 2010, *31*, 1853-1861.

[240] Ananthi, S., Santhosh, R. S., Nila, M. V., Prajna, N. V., *et al.*, Comparative proteomics of human male and female tears by two-dimensional electrophoresis. *Exp Eye Res* 2011, *92*, 454-463.

[241] Chu, C. Y., Poon, C. W., Pong, C. F., Pang, C. P., Wang, C. C., Human normal tear proteome. *Graefe's archive for clinical and experimental ophthalmology = Albrecht von Graefes Archiv fur klinische und experimentelle Ophthalmologie* 2009, *247*, 725-727.

[242] Molloy, M. P., Bolis, S., Herbert, B. R., Ou, K., *et al.*, Establishment of the human reflex tear two-dimensional polyacrylamide gel electrophoresis reference map: new proteins of potential diagnostic value. *Electrophoresis* 1997, *18*, 2811-2815.

[243] Sprung, R., Chen, Y., Zhang, K., Cheng, D., *et al.*, Identification and validation of eukaryotic aspartate and glutamate methylation in proteins. *J Proteome Res* 2008, *7*, 1001-1006.

[244] Stadtman, E. R., Berlett, B. S., Reactive oxygen-mediated protein oxidation in aging and disease. *Drug metabolism reviews* 1998, *30*, 225-243.

[245] Bregere, C., Rebrin, I., Sohal, R. S., Detection and characterization of in vivo nitration and oxidation of tryptophan residues in proteins. *Methods in enzymology* 2008, *441*, 339-349.

[246] Takamoto, K., Chance, M. R., Radiolytic protein footprinting with mass spectrometry to probe the structure of macromolecular complexes. *Annual review of biophysics and biomolecular structure* 2006, *35*, 251-276.

[247] Alvarez, B., Radi, R., Peroxynitrite reactivity with amino acids and proteins. *Amino acids* 2003, *25*, 295-311.

[248] Davies, M. J., Truscott, R. J., Photo-oxidation of proteins and its role in cataractogenesis. *Journal of photochemistry and photobiology. B, Biology* 2001, *63*, 114-125.

[249] Fietzek, P. P., Breitkreutz, D., Kuhn, K., Amino acid sequence of the amino-terminal region of calf skin collagen. *Biochimica et biophysica acta* 1974, *365*, 305-310.

[250] Kumar, A., Bachhawat, A. K., Pyroglutamic acid: throwing light on a lightly studied metabolite. *Curr. Sci* 2012, *102*, 288-297.

[251] Hinke, S. A., Pospisilik, J. A., Demuth, H. U., Mannhart, S., *et al.*, Dipeptidyl peptidase IV (DPIV/CD26) degradation of glucagon. Characterization of glucagon degradation products and DPIV-resistant analogs. *The Journal of biological chemistry* 2000, *275*, 3827-3834.

[252] Van Coillie, E., Proost, P., Van Aelst, I., Struyf, S., *et al.*, Functional comparison of two human monocyte chemotactic protein-2 isoforms, role of the amino-terminal pyroglutamic acid and processing by CD26/dipeptidyl peptidase IV. *Biochemistry* 1998, *37*, 12672-12680.

[253] Hwang, C. S., Shemorry, A., Varshavsky, A., N-terminal acetylation of cellular proteins creates specific degradation signals. *Science* 2010, *327*, 973-977.

[254] Forte, G. M., Pool, M. R., Stirling, C. J., N-terminal acetylation inhibits protein targeting to the endoplasmic reticulum. *PLoS biology* 2011, *9*, e1001073.

[255] Coulton, A. T., East, D. A., Galinska-Rakoczy, A., Lehman, W., Mulvihill, D. P., The recruitment of acetylated and unacetylated tropomyosin to distinct actin polymers permits the discrete regulation of specific myosins in fission yeast. *Journal of cell science* 2010, *123*, 3235-3243.

[256] Arnesen, T., Towards a functional understanding of protein N-terminal acetylation. *PLoS biology* 2011, *9*, e1001074.

[257] Hollebeke, J., Van Damme, P., Gevaert, K., N-terminal acetylation and other functions of Nalpha-acetyltransferases. *Biological chemistry* 2012, *393*, 291-298.

[258] Smith, L. M., Kelleher, N. L., Consortium for Top Down, P., Proteoform: a single term describing protein complexity. *Nature methods* 2013, *10*, 186-187.

8 APPENDIX 1

List of proteins identified in this study

	Gene names	Protein IDs	Protein names	Schirmer strip	Capillary tube
1	A2M	P01023	Alpha-2-macroglobulin	x	
2	ABHD14B	B4DQI4	Alpha/beta hydrolase domain-containing protein 14B	x	
3	ABRACL	Q5SZC9	Costars family protein ABRACL	x	
4	ACTA1	Q5T8M8	Actin, alpha skeletal muscle	x	
5	ACTB	P60709	Actin, cytoplasmic 1	x	
6	ACTBL2	Q562R1	Beta-actin-like protein 2	x	
7	ACTN4	O43707	Alpha-actinin-4	x	
8	ADH7	C9JP14	Alcohol dehydrogenase class 4 mu/sigma chain	x	
9	AGR2	C9J3E2	Anterior gradient protein 2 homolog	x	
10	AGT	P01019	Angiotensinogen	x	
11	AHSG	P02765	Alpha-2-HS-glycoprotein	x	
12	AKR1A1	P14550	Alcohol dehydrogenase [NADP(+)]	x	
13	AKR1C1	Q04828	Aldo-keto reductase family 1 member C1	x	
14	ALB	P02768	Serum albumin	x	x
15	ALDH1A1	P00352	Retinal dehydrogenase 1	x	
16	ALDH3A1	C9JMC5	Aldehyde dehydrogenase, dimeric NADP-preferring	x	
17	ALDOA	P04075	Fructose-bisphosphate aldolase A	x	
18	ALDOC	P09972	Fructose-bisphosphate aldolase	x	
19	ANXA1	P04083	Annexin A1	x	
20	ANXA2	P07355	Annexin A2	x	
21	ANXA3	P12429	Annexin A3	x	
22	ANXA4	Q6P452	Annexin	x	
23	ANXA5	P08758	Annexin A5	x	
24	APOA1	P0DM91	Apolipoprotein A-I		x
25	APOH	P02749	Beta-2-glycoprotein 1	x	
26	ARHGDIA	P52565	Rho GDP-dissociation inhibitor 1	x	
27	ARHGDIB	P52566	Rho GDP-dissociation inhibitor 2	x	
28	ASS1	P00966	Argininosuccinate synthase	x	
29	AZGP1	P25311	Zinc-alpha-2-glycoprotein	x	x
30	B2M	P61769	Beta-2-microglobulin	x	x
31	BLVRB	P30043	Flavin reductase (NADPH)	x	
32	C3	P01024	Complement C3	x	
33	CAP1	Q5T0R7	Adenylyl cyclase-associated protein 1	x	
34	CAPN1	P07384	Calpain-1 catalytic subunit	x	
35	CCDC171	Q6TFL3	Coiled-coil domain-containing protein 171	x	
36	CFH	P08603	Complement factor H	x	
37	CFL1	P23528	Cofilin-1	x	
38	CHI3L2	Q15782	Chitinase-3-like protein 2	x	
39	CLIC1	O00299	Chloride intracellular channel protein 1	x	
40	CLU	P10909	Clusterin	x	x
41	CNDP2	Q96KP4	Cytosolic non-specific dipeptidase	x	
42	CP	P00450	Ceruloplasmin	x	x
43	CST1	P01037	Cystatin-SN	x	x

44	CST3	P01034	Cystatin-C	x	
45	CST4	P01036	Cystatin-S	x	x
46	CSTA	P01040	Cystatin-A	x	
47	CSTB	P04080	Cystatin-B	x	
48	CTSB	P07858	Cathepsin B	x	
49	DDT	P30046	D-dopachrome decarboxylase	x	
50	DMBT1	Q9UGM3	Deleted in malignant brain tumors 1 protein	x	x
51	DPP3	Q9NY33	Dipeptidyl peptidase 3	x	
52	DPP7	Q9UHL4	Dipeptidyl peptidase 2	x	
53	NUP93	Q7ZU29	Nuclear pore complex protein Nup93		x
54	EEF1A1P5	Q5VTE0	Putative elongation factor 1-alpha-like 3	x	
55	ENO1	P06733	Alpha-enolase	x	
56	EZR	P15311	Ezrin	x	
57	FABP5	Q01469	Fatty acid-binding protein, epidermal	x	
58	FBP1	P09467	Fructose-1,6-bisphosphatase 1	x	
59	FNTA	P49354	Protein farnesyltransferase	x	
60	GAPDH	P04406	Glyceraldehyde-3-phosphate dehydrogenase	x	
61	GC	P02774	Vitamin D-binding protein	x	
62	GCHFR	P30047	GTP cyclohydrolase 1 feedback regulatory protein	x	
63	GDI2	P50395	Rab GDP dissociation inhibitor beta	x	
64	GLOD4	B7Z403	Glyoxalase domain-containing protein 4	x	
65	GLUL	P15104	Glutamine synthetase	x	
66	GPI	P06744	Glucose-6-phosphate isomerase	x	
67	GPX1	P07203	Glutathione peroxidase 1	x	
68	GSN	P06396	Gelsolin	x	
69	GSR	P00390	Glutathione reductase, mitochondrial	x	
70	GSTA2	P09210	Glutathione S-transferase A2	x	
71	GSTP1	P09211	Glutathione S-transferase P	x	
72	HP	P00738	Haptoglobin	x	x
73	HPX	P02790	Hemopexin	x	
74	HSPA1A	P08107	Heat shock 70 kDa protein 1A/1B	x	
75	HSPB1	P04792	Heat shock protein beta-1	x	
76	HSPG2	P98160	Basement membrane-specific heparan sulfate proteoglycan core protein	x	x
77	HV102	P01743	Ig heavy chain V-I region HG3		x
78	HV305	P01766	Ig heavy chain V-III region BRO		x
79	HVM21	P01790	Ig heavy chain V region M511		x
80	IDH1	O75874	Isocitrate dehydrogenase [NADP] cytoplasmic	x	
81	IGHA1	P01876	Ig alpha-1 chain C region	x	x
82	IGHA2	P01877	Ig alpha-2 chain C region	x	x
83	IGHG1	P01857	Ig gamma-1 chain C region	x	x
84	IGHG2	P01859	Ig gamma-2 chain C region	x	
85	IGHG4	P01861	Ig gamma-4 chain C region	x	
86	IGHM	P01871	Ig mu chain C region	x	x
87	IGJ	P01591	Immunoglobulin J chain	x	x
88	IGKC	P01834	Ig kappa chain C region	x	x
89	IGKV1-5	P01602	Ig kappa chain V-I region HK102	x	
90	IGKV4-1	P01625	Ig kappa chain V-IV region Len	x	x
91	IGLC3	P0CG06	Ig lambda-3 chain C regions	x	x
92	IGLL5	B9A064	Immunoglobulin lambda-like polypeptide 5	x	x

93	IKZF3	Q9UKT9	Zinc finger protein Aiolos		x
94	IL1RN	P18510	Interleukin-1 receptor antagonist protein	x	
95	ITIH1	P19827	Inter-alpha-trypsin inhibitor heavy chain H1	x	
96	ITIH2	Q5T985	Inter-alpha-trypsin inhibitor heavy chain H2	x	
97	ITIH4	Q14624	Inter-alpha-trypsin inhibitor heavy chain H4	x	
98	KCNG4	Q8TDN1	Potassium voltage-gated channel subfamily G member 4		x
99	KRT1	P04264	Keratin, type II cytoskeletal 1	x	
100	KRT10	P13645	Keratin, type I cytoskeletal 10	x	x
101	KRT121P	P15241	Keratin-81-like protein KRT121P		x
102	KRT2	P35908	Keratin, type II cytoskeletal 2 epidermal	x	x
103	KRT9	P35527	Keratin, type I cytoskeletal 9	x	
104	KV2A7	P01631	Ig kappa chain V-II region 26-10		x
105	KV307	P04206	Ig kappa chain V-III region GOL		x
106	KYNU	Q16719	Kynureninase	x	
107	LACRT	Q9GZZ8	Extracellular glycoprotein lacritin	x	x
108	LAP3	P28838	Cytosol aminopeptidase	x	
109	LCN1	P31025	Lipocalin-1	x	x
110	LCN2	P80188	Neutrophil gelatinase-associated lipocalin	x	x
111	LDHA	P00338	L-lactate dehydrogenase A chain	x	
112	LGALS3	P17931	Galectin-3	x	
113	LGALS3BP	Q08380	Galectin-3-binding protein	x	
114	LPO	P22079	Lactoperoxidase	x	
115	LRG1	P02750	Leucine-rich alpha-2-glycoprotein	x	
116	LTF	P02788	Lactotransferrin	x	x
117	LUZP1	Q86V48	Leucine zipper protein 1	x	
118	LV302	P80748	Ig lambda chain V-III region LOI		x
119	LV403	P01717	Ig lambda chain V-IV region Hil		x
120	LXN	Q9BS40	Latexin	x	
121	LYZ	P61626	Lysozyme C	x	x
122	MDH1	B9A041	Malate dehydrogenase, cytoplasmic	x	
123	MDN1	Q9NU22	Midasin	x	
124	MOV10L1	Q9BXT6	Putative helicase Mov10l1	x	
125	MSLN	Q13421	Mesothelin	x	x
126	Mtmr14	Q8VEL2	Myotubularin-related protein 14		x
127	MTPN	C9JL85	Myotrophin	x	
128	MUC5AC	P98088	Mucin-5AC	x	
129	NME2	P22392	Nucleoside diphosphate kinase	x	
130	NUCB2	P80303	Nucleobindin-2	x	x
131	ORM1	P02763	Alpha-1-acid glycoprotein 1	x	
132	ORM2	P19652	Alpha-1-acid glycoprotein 2	x	
133	P01596	P01596	Ig kappa chain V-I region CAR	x	
134	P01617	P01617	Ig kappa chain V-II region TEW	x	
135	P01623	P01623	Ig kappa chain V-III region WOL	x	
136	P01717	P01717	Ig lambda chain V-IV region Hil	x	
137	P01765	P01765	Ig heavy chain V-III region TIL	x	
138	P01766	P01766	Ig heavy chain V-III region BRO	x	
139	P04208	P04208	Ig lambda chain V-I region WAH	x	
140	P04430	P04430	Ig kappa chain V-I region BAN	x	
141	P06331	P06331	Ig heavy chain V-II region ARH-77	x	

142	P4HB	P07237	Protein disulfide-isomerase	x	
143	P80362	P80362	Ig kappa chain V-I region WAT	x	
144	PAFAH1B2	P68402	Platelet-activating factor acetylhydrolase IB subunit beta	x	
145	PARK7	Q99497	Protein DJ-1	x	
146	PDIA3	P30101	Protein disulfide-isomerase A3	x	
147	PDXK	O00764	Pyridoxal kinase	x	
148	PEBP1	P30086	Phosphatidylethanolamine-binding protein 1	x	
149	PFN1	P07737	Profilin-1	x	
150	PGAM1	P18669	Phosphoglycerate mutase 1	x	
151	PGD	B4DQJ8	6-phosphogluconate dehydrogenase, decarboxylating	x	
152	PGK1	B7Z7A9	Phosphoglycerate kinase	x	
153	PIGR	P01833	Polymeric immunoglobulin receptor	x	x
154	PIP	P12273	Prolactin-inducible protein	x	x
155	PKM	P14618	Pyruvate kinase isozymes M1/M2	x	
156	PLA2G2A	P14555	Phospholipase A2, membrane associated	x	x
157	PPIA	P62937	Peptidyl-prolyl cis-trans isomerase A	x	
158	PPIB	P23284	Peptidyl-prolyl cis-trans isomerase B	x	
159	PPP1CB	P36873	Serine/threonine-protein phosphatase	x	
160	PRDX1	Q06830	Peroxiredoxin-1	x	
161	PRDX5	P30044	Peroxiredoxin-5, mitochondrial	x	
162	PRDX6	P30041	Peroxiredoxin-6	x	
163	PROL1	Q99935	Proline-rich protein 1	x	x
164	PRR4	Q16378	Proline-rich protein 4	x	x
165	PRSS1	P07478	Putative trypsin-6	x	
166	PSMA2	C9JCK5	Proteasome subunit alpha type-2	x	
167	PSMB1	P20618	Proteasome subunit beta type-1	x	
168	PSMB3	P49720	Proteasome subunit beta type-3	x	
169	PSME1	Q06323	Proteasome activator complex subunit 1	x	
170	PSME2	Q9UL46	Proteasome activator complex subunit 2	x	
171	pyrE	Q7U662	Orotate phosphoribosyltransferase		x
172	RBP4	Q5VY30	Retinol-binding protein 4	x	
173	S100A11	P31949	Protein S100-A11	x	
174	S100A12	P80511	Protein S100-A12	x	
175	S100A4	P26447	Protein S100-A4	x	
176	S100A6	P06703	Protein S100-A6	x	
177	S100A8	P05109	Protein S100-A8	x	
178	S100A9	P06702	Protein S100-A9	x	
179	S100P	P25815	Protein S100-P	x	
180	SCGB1D1	O95968	Secretoglobin family 1D member 1	x	x
181	SCGB2A1	O75556	Mammaglobin-B	x	x
182	SCN2A	A8K0U1	Sodium channel protein type 2 subunit alpha	x	
183	SELENBP1	Q13228	Selenium-binding protein 1	x	
184	SEPN1	Q9NZV5	Selenoprotein N	x	
185	SERPINA1	P01009	Alpha-1-antitrypsin	x	
186	SERPINA3	P01011	Alpha-1-antichymotrypsin	x	
187	SERPINB1	P30740	Leukocyte elastase inhibitor	x	
188	SERPINB5	P36952	Serpin B5	x	
189	SERPINC1	P01008	Antithrombin-III	x	
190	SFN	P31947	14-3-3 protein sigma	x	

191	SH3BGRL	O75368	SH3 domain-binding glutamic acid-rich-like protein	x	
192	SLPI	P03973	Antileukoproteinase	x	x
193	SOD1	P00441	Superoxide dismutase [Cu-Zn]	x	
194	SPARCL1	B4E2Z0	SPARC-like protein 1	x	
195	TAGLN2	P37802	Transgelin-2	x	
196	TALDO1	P37837	Transaldolase	x	
197	TCN1	P20061	Transcobalamin-1	x	
198	TF	P02787	Serotransferrin	x	
199	TGM2	B4DIT7	Protein-glutamine gamma-glutamyltransferase 2	x	
200	TMEM198	C9JXI5	Transmembrane protein 198	x	
201	TMEM57	Q8N5G2	Macoilin	x	
202	TPI1	P60174	Triosephosphate isomerase	x	
203	TPM3	Q5VU61	Tropomyosin alpha-4 chain	x	
204	TTR	P02766	Transthyretin	x	
205	TXN	P10599	Thioredoxin	x	
206	TYMP	C9JGI3	Thymidine phosphorylase	x	
207	UBA1	P22314	Ubiquitin-like modifier-activating enzyme 1	x	
208	UBB	P62987	Ubiquitin-60S ribosomal protein L40	x	
209	WFDC11	Q8NEX6	Protein WFDC11		x
210	YWHAB	P31946	14-3-3 protein beta/alpha	x	
211	YWHAE	P62258	14-3-3 protein epsilon	x	
212	YWHAQ	P27348	14-3-3 protein theta	x	
213	YWHAZ	P63104	14-3-3 protein zeta/delta	x	
214	ZG16B	Q96DA0	Zymogen granule protein 16 homolog B	x	x
215	ZNF292	O60281	Zinc finger protein 292	x	